

AN EXPERIMENTAL STUDY OF SOLID PROPELLANT EXTINGUISHMENT BY RAPID DEPRESSURIZATION

Distribution of this report is provided in the interest of information exchange. Responsibility for the contents resides in the author or organization that prepared it.

**FINAL TECHNICAL REPORT
CONTRACT NO. NAS 1-7815
COVERING THE PERIOD
3 JANUARY 1968 TO 3 JANUARY 1969**

Prepared for
NATIONAL AERONAUTICS AND SPACE ADMINISTRATION

UTC 2311-FR
March 1969

AN EXPERIMENTAL STUDY OF SOLID PROPELLANT EXTINGUISHMENT BY RAPID DEPRESSURIZATION

Distribution of this report is provided in the interest of information exchange. Responsibility for the contents resides in the author or organization that prepared it.

**FINAL TECHNICAL REPORT
CONTRACT NO. NAS 1-7815
COVERING THE PERIOD
3 JANUARY 1968 TO 3 JANUARY 1969**

Prepared for
NATIONAL AERONAUTICS AND SPACE ADMINISTRATION

UTC 2311-FR
March 1969

AN EXPERIMENTAL STUDY OF SOLID PROPELLANT EXTINGUISHMENT BY RAPID DEPRESSURIZATION

by By G. E. Jensen

Distribution of this report is provided in the interest of
information exchange. Responsibility for the contents
resides in the author or organization that prepared it.

Prepared under
Contract No. NAS 1-7815

by

United Technology Center



for

NATIONAL AERONAUTICS AND SPACE ADMINISTRATION

ABSTRACT

This report presents results from an experimental study of solid propellant extinguishment by rapid depressurization. Systematic variations in propellant binder, oxidizer loading level, burning rate catalyst, metal loading, and exhaust pressure level were studied. The effects of motor configuration on extinguishment and reignition are discussed. Results indicate that combustion extinguishment requirements are determined by the binder type, percentage of ammonium perchlorate oxidizer, motor geometry, and exhaust pressure level as well as the pressure and depressurization rate.

CONTENTS

	Page
SUMMARY	1
INTRODUCTION	3
EQUIPMENT AND EXPERIMENTAL PROCEDURES	7
Slab Motor	7
Window Motor	10
Swing-Nozzle Motor	13
Propellants	18
Binder/Curative Studies	18
Oxidizer Variation Studies	28
Metal Loading Level Studies	28
Catalyst Studies	30
Thermodynamic Constants	30
EXPERIMENTAL RESULTS	35
Depressurization Studies	35
Binder/Curative Effects	35
Oxidizer Loading Studies	52
Aluminum Loading Studies	52
Catalyst Studies	64
Reignition Studies	70
High-Speed Film Studies	71
DISCUSSION AND ANALYSIS	73
CONCLUSIONS	95
REFERENCES	97

ILLUSTRATIONS

Figure	Page
1 Schematic Diagram of Combustion Termination Apparatus	8
2 Dual-Nozzle Depressurization Motor	9
3 Schematic of Window Motor	11
4 Window Motor with Xenon-arc Lamp	12
5 Schematic Top View of Window Motor and Camera System	14
6 Swing-Nozzle Motor	15
7 Schematic of Swing-Nozzle Motor	16
8 DSC Traces for Binder Samples in Nitrogen, 1 atm	21
9 Strand Burning Rates for PU, CTPB, and CTPIB Nonaluminized Propellants	25
10 CTPB Nonaluminized Propellant Strand Burning Rates	27
11 Strand Burning Rates of CTPIB Propellants as a Function of Coarse to Fine AP Ratio	29
12 CTPB and CTPIB Aluminized Propellant Burning Rates	31
13 CTPB Catalyzed Propellant Burning Rates	32
14 CTPIB Catalyzed Propellant Burning Rates	33
15 Comparison of Window Motor and Slab Motor CTPB/83.8% AP Propellant	36
16 Comparison of Window Motor and Slab Motor CTPIB/83.8% AP Propellant Extinguishment Characteristics	37
17 Comparison of Window Motor and Slab Motor PU/83.8% AP Propellant Extinguishment	38
18 Combustion Extinguishment Characteristics of UTX 10642 and UTX 10691 (CTPB/83.8% AP) as a Function of Exhaust Pressure	40

ILLUSTRATIONS (Continued)

Figure	Page
19	Combustion Extinguishment Characteristics of UTX 10645 (CTPIB/83.8% AP) as a Function of Exhaust Pressure 41
20	Combustion Extinguishment Characteristics of UTX 10661 (PU/83.8% AP) as a Function of Exhaust Pressure 42
21	Combustion Extinguishment Characteristics of a CTPB-Epoxy Curative Propellant (UTX 11339) 44
22	Effects of Grain Geometry Upon the Extinguishment Characteristics of UTX 10645 (CTPIB/83.8% AP) 46
23	Swing-Nozzle Motor (5-in. Grain) Extinguishment Data for CTPB/AP (UTX 10691) and CTPIB/AP (UTX 10645) Propellants 47
24	Swing-Nozzle Motor (15-in. Grain) Extinguishment Data for CTPB/AP (UTX 10691) and CTPIB/AP (UTX 10645) Propellants 48
25	Combustion Extinguishment Characteristics of Sterilizable CTPIB/AP Propellants 50
26	Combustion Extinguishment Characteristics of Chlorinated CTPIB/AP Propellants 51
27	Combustion Extinguishment Characteristics of Polyepichlorohydrin/AP Propellant 53
28	Combustion Extinguishment Characteristics of CTPB/80% AP Propellant (UTX 11327) as a Function of Exhaust Level 54
29	Combustion Extinguishment Characteristics of CTPIB/83.8% AP, 35 to 65 Coarse to Fine Ratio Propellant (UTX 11336) 55
30	Combustion Extinguishment Characteristics of CTPB/AP/4% Aluminum Propellant (UTX 11317) 56
31	Combustion Extinguishment Characteristics of CTPB/AP/16% Aluminum Propellant (UTX 11325) 57

ILLUSTRATIONS (Continued)

Figure	Page
32 Combustion Extinguishment Characteristics of CTPIB/AP/4% Aluminum Propellant (UTX 11316)	59
33 Combustion Extinguishment Characteristics of CTPIB/AP/16% Aluminum Propellant (UTX 11454)	60
34 Swing-Nozzle Motor Extinguishment Data for CTPB/AP/16% Aluminum Propellant (UTX 11325)	61
35 Swing-Nozzle Motor (5-in. Grain) Extinguishment Data for CTPIB/AP/16% Aluminum Propellant (UTX 11454)	62
36 Swing-Nozzle Motor (5-in. Grain) Extinguishment Data for Mixed Polymer CTPB/CTPIB/16% Aluminum Propellant (UTX 11337)	63
37 Combustion Extinguishment Characteristics of 0.15% Iron Oxide Catalyzed CTPB/AP Propellant (UTX 11326)	65
38 Combustion Extinguishment Characteristics of 0.25% Organo-Iron Catalyzed CTPB/AP Propellant (UTX 11329)	66
39 Combustion Extinguishment Characteristics of HYCAT Catalyzed CTPB/AP/16% Aluminum Propellants	67
40 Combustion Extinguishment Characteristics of 0.25% Organo-Iron Catalyzed CTPIB/AP Propellant (UTX 11333)	68
41 Combustion Extinguishment Characteristics of HYCAT Catalyzed CTPIB/AP/16% Aluminum Propellant (UTX 11342)	69
42 Window Motor Data Trace for CTPB/AP/16% Aluminum Propellant (UTX 11325) Test No. 2	74
43 Window Motor Data Trace for CTPB/AP/16% Aluminum Propellant (UTX 11325) Test No. 2	75
44 Window Motor Data Trace for CTPB/80% AP Propellant (UTX 11327)	76

ILLUSTRATIONS (Continued)

Figure	Page
45	Scanning Electron Micrographs of Terminated Propellant Surface-CTPIB/16% Aluminum 77
46	Swing Nozzles Motor Data Trace for CTPB/83.8% AP Propellant (UTX 10691) 79
47	Comparison of Calculated and Experimental Extinguishment Requirements for CTPB/83.8% AP Propellant (UTX 10691) 80
48	Comparison of Calculated and Experimental Extinguishment Requirements for CTPB/83.8% AP Propellants (UTX 10645). 81
49	Comparison of Calculated and Experimental Extinguishment Requirements for PU/83.8% AP Propellant (UTX 10661) 82
50	Comparison of Calculated and Experimental Extinguishment Requirements for CTPB/80% AP Propellant (UTX 11327) 83
51	Comparison of Calculated and Experimental Extinguishment Requirements for CTPIB/83.8% AP (36:35) Propellant (UTX 11336) 84
52	Comparison of Calculated and Experimental Extinguishment for CTPB/AP/0.25% Organo-Iron Propellant (UTX 11329) 85
53	Comparison of Calculated and Experimental Extinguishment Requirements for CTPIB/AP/0.25% Organo-Iron Propellant 86
54	Comparison of Calculated and Experimental Extinguishment Requirements for CTPB/AP/16% Aluminum Propellant (UTX 11325) 87
55	Comparison of Calculated Experimental Extinguishment for CTPIB/AP/16% Aluminum Propellant (UTX 11454) 88
56	Comparison of Calculated and Experimental Extinguishment Requirements for CTPB/AP/16% Aluminum/1% HYCAT Propellant (UTX 11341) 89
57	Comparison of Calculated and Experimental Extinguishment Requirements for CTPIB/AP/16% Aluminum/1% HYCAT Propellant (UTX 11342) 90

TABLES

Table		Page
I	Motor Parameters	17
II	Binder/Curative Formulations	19
III	Coarse AP Screen Analysis	20
IV	Polymer Decomposition - DSC Tests	22
V	Polymer Decomposition - DSC Tests	23
VI	DSC Polymer Decomposition	24
VII	Propellant Thermodynamic Constants	34

ABBREVIATIONS AND SYMBOLS

A_B	grain surface area
AP	ammonium perchlorate
atm	atmosphere
BKNO ₃	boron pottassium nitrate
b.out	grain burned out
C_1	constant
C_2	constant
CTPB	carboxy-terminated polybutadiene
CTPIB	carboxy-terminated polyisobutylene
c^*	characteristic gas velocity
$\frac{dP}{dt}$	rate of depressurization
DSC	differential scanning calorimeter
HYCAT	UTC proprietary high burning rate catalyst
L^*	chamber volume/nozzle throat area
MAPO	aziridinyI curative
n	burning rate exponent
O/F	oxidizer to fuel
P	pressure
\dot{P}	rapid depressurization, rate of depressurization
P_c	chamber pressure
PBAN	polybutadiene-acrylic acid-acrylonitrile
PIB	polyisobutylene
PU	polyurethane
\dot{r}	burning rate
\bar{r}	steady-state burning rate
Reig	grain reignited
t	time
UTC	United Technology Center
α	propellant thermal diffusivity
λ	constant
ω	window motor
ω_v	window motor vacuum exhaust

SUMMARY

This final technical report is submitted in accordance with the requirements of Contract No. NAS 1-7815. The principal objective of the studies conducted under this contract was to experimentally investigate solid propellant combustion extinguishment by P. The following four goals were included within the scope of this program:

- A. Determination of the specific conditions of propellant combustion extinguishment
- B. Investigation of the influence of propellant formulation differences upon extinguishment behavior
- C. Establishment of the effect of exhaust pressure level upon extinguishment and tendency for reignition
- D. Determination of the effect of motor differences upon extinguishment requirements.

The experimental studies were conducted using three different depressurization motors with a selected series of propellants and motor operating conditions. Systematic variations of the propellant binder, oxidizer loading, catalyst content, metal loading, and exhaust pressure level were evaluated.

The results obtained in the course of this program showed that the requirements for combustion extinguishment are determined by the propellant formulation, the motor geometry, and, under certain conditions, the exhaust pressure level. The pressure and depressurization rate limits for extinguishment can be altered by formulation differences, variation of the motor geometry, and changing the exhaust atmosphere. A number of trends concerning the effect of formulation differences were established in the course of this program:

- A. The substitution of aluminum for AP in either CTPB or CTPIB propellants decreased the termination requirements, although the tendency for reignition was increased.
- B. The addition of burning rate catalysts to a propellant had little or no effect upon the termination requirements in the large-volume small-grain area motors used in this program. However, the addition of HYCAT catalyst in aluminized CTPB and CTPIB propellants caused consistent reignition under atmospheric exhaust conditions.
- C. The addition of halogens at low concentrations in CTPIB propellants had no effect upon extinguishment limits.
- D. Increasing the endothermicity of the propellant surface, either by the use of propellants (CTPIB) showing lower thermal decomposition temperature or by using higher binder levels, resulted in moderate decreases of the extinguishment requirements.

The motor geometry influenced the pressure and depressurization rate at extinguishment. Individually increasing the grain area, decreasing the motor volume, or increasing the termination nozzle throat area of a particular motor will increase the extinguishment pressure and extinguishment depressurization rate. Extinguishment in any particular motor is dependent upon the depressurization path.

The exhaust pressure can influence extinguishment and reignition behavior. When the motor geometry was such that extinguishment occurred below the dechoking pressure, the exhaust pressure influenced the extinguishment limits. Unless the exhaust pressure is below the propellant minimum ignition pressure, reignition may occur, particularly with aluminized propellants.

The Von Elbe type of combustion extinguishment model provided a rough guideline for motor development work. The effects of formulation differences and motor geometry can be adequately considered for preliminary design studies. The effect of exhaust pressure, particularly in regard to reignition behavior, cannot be adequately treated.

INTRODUCTION

During the past few years, significant effort has been directed to evaluations in the field of \dot{P} and L^* induced combustion extinguishment of solid propellants. The majority of these studies have been directed toward establishment of the depressurization rates required for extinguishment of different propellants. In general, these studies^{(1,2,3)*} have not provided the necessary insight into the mechanisms of combustion termination nor a sound basis for engineering correlations to permit the design of reliable, controllable solid propellant motors. Data have been particularly lacking for a quantitative description of transient combustion phenomena, the predictability of the actual point of combustion extinguishment, the mechanisms of the extinguishment processes, and the factors which control possible reignition of the grain.

Theoretical efforts to describe transient combustion and extinguishment phenomena have shown the complexity of the process. One major impediment in describing transient combustion behavior is the lack of basic information in the description of propellant-ingredient decomposition mechanisms, gas-phase mixing of decomposition products, and gas-phase combustion kinetics under both steady-state and transient combustion conditions. Simple transient combustion models^(4,5,6) shown in general form in equation 1, are based on a simple surface energy balance, the assumption of a constant surface temperature, and the use of an empirical description of steady-state combustion behavior

$$\dot{r} = \bar{r} \left(1 + \frac{1}{\lambda} \frac{n\alpha}{r^2} \frac{1}{P} \frac{dP}{dt} \right) \quad (1)$$

\dot{r} = transient burning rate

\bar{r} = steady-state burning rate at P

n = burning rate exponent

α = thermal diffusivity

λ = constant

As predicted by the Von Elbe-type model, the transient burning rate is always less than the steady-state burning rate at any pressure during transient combustion. The conditions required for extinguishment are determined by equating \dot{r} to zero.

The aforementioned model has been partially successful in describing extinguishment; however, studies conducted under Contract No. NAS 1-6601⁽⁷⁾ and Marxman⁽⁸⁾ have shown it to be inadequate for the description of propellant differences. Also, the utility of the model for apriori design studies has not been well proven.

*Parenthetical superscript numbers denote references appearing on page 97.

More complex transient combustion models,^(7,8,9) which are based on the assumption of an Arrhenius-type regression rate expression, have been considered. The initial transient surface regression rate is predicted to be greater than the steady-state rate. However, if the depressurization rate is large enough or the solid-phase kinetics are sufficiently slow, the gas-phase flame will extinguish, and the surface regression rate will drop rapidly with subsequent extinguishment. These models are probably more realistic and have a greater potentiality for describing the effects of propellant formulation differences; but in their present form they are of limited usefulness, primarily due to a lack of propellant kinetics understanding.

The complex combustion models based on an Arrhenius law for description of binder and oxidizer decomposition are limited by the paucity of quantitative decomposition data. Kinetic parameters based on hotplate regression rate studies must be extrapolated for use under postulated combustion conditions. Because Cantrel⁽¹⁰⁾ and Nachbar and Williams⁽¹¹⁾ have shown that measured hotplate temperatures are different from the actual surface temperature of the sample, the validity of using the extrapolated data is questionable. Porous plate experiments developed by Coates⁽¹²⁾ have a greater potential for yielding representative results, but even this technique is less readily adaptable to the study of polymers than to oxidizers.

The use of an Arrhenius-type pyrolysis law is open to question. Thermal decomposition studies conducted by Ryan⁽¹³⁾ have indicated that the decomposition of polybutadiene acrylic-acid copolymers may be an equilibrium vaporization process. Other binder polymers with lower molecular weights (less than 3,000) and which have well-defined melting and boiling points are also quite likely to be controlled by equilibrium vaporization. The presence of oxidative species could modify this process by oxidative bond scission or by polymerization effects which yield products with higher molecular weights.

While bulk thermal degradation data generally are not directly applicable to propellant combustion phenomena (because of the differences in sample heatup time and environmental composition), they do provide a guide to understanding combustion mechanisms. In general, it has been shown that thermal decomposition of polymers consists of a series of complex degradation mechanisms, each of which can be influenced by the temperature, the heat rate, the pressure, the presence of catalysts and solid oxidizers within the sample, the composition of the gaseous environment, and the molecular structure of the polymer.^(13,14) Binder changes (the addition of burning rate catalysts or other perturbations in a propellant system) may radically alter the decomposition mechanisms of the propellant. Hence, any model of steady-state or transient combustion based on a single binder (or oxidizer) decomposition mechanism has limited value. The major differences among state-of-the-art binder systems lies in the melting and boiling behavior, the extent of thermal depolymerization in the presence of oxidizing gaseous species, the effect of catalysts, and the molecular weight and distribution of the decomposition species. Once these factors have been determined, the possibility of an adequate model of combustion phenomena is conceivable. Present studies, using high-heating-rate techniques such as flash pyrolysis with both pure and mixed propellant ingredients, should provide much necessary information. The reverse procedure of trying to infer combustion kinetics parameters from contrived combustion models or experiments must be viewed as being far less satisfactory.

In addition to the lack of quantitative decomposition information, there is considerable uncertainty in the mechanisms of gas-phase mixing and combustion. Reaction zones of 100μ to 800μ ^(15,16,17) above the combusting surface have been measured experimentally at moderate pressures. The inconsistency of these results makes it difficult to accurately represent the contribution of either gas-phase heat feedback to the combustion process or the possible contributions of exothermic oxidizer decomposition and oxidative degradation of the binder. There is also evidence⁽¹⁸⁾ to indicate that the gas-phase combustion process is a mixing and diffusion problem not representable by premixed gas-flame analysis. Until realistic ingredient decomposition and gas-phase combustion mechanisms are available for the development of transient combustion models, design information must be obtained from experimental investigations.

Particularly lacking for design purposes are experimental data which specify: (1) the conditions of propellant extinguishment (the pressure and depressurization rate at extinguishment), (2) the effect of propellant differences upon extinguishment condition, (3) the perturbing influence of exhaust pressure upon extinguishment and permanence of extinguishment, and (4) the effect of motor differences upon extinguishment behavior. The following sections of this report are the result of an experimental program to elucidate these four areas. It should be noted that an objective of this program, which is an outgrowth of Contract No. NAS 1-6601, was to extend the work of the previous program and extend the program to a wider variety of propellant systems. The propellant systems studied and the experimental procedures of these studies are described in the following text.

EQUIPMENT AND EXPERIMENTAL PROCEDURES

Depressurization studies were conducted using three \dot{P} motors. A dual-nozzle window motor was used for high-speed film studies, propellant formulation evaluation, and for the study of environmental effects. A larger volume dual-nozzle slab motor and a tubular grain single-nozzle motor were used for the study of motor differences. Details of these motors, the experimental techniques associated with their usage, and the experimental results obtained are presented in the following sections.

Slab Motor

The slab motor used for \dot{P} characterization is shown schematically in figure 1 and pictorially in figure 2. The basic element is a small motor containing propellant slabs (1-lb) with a dual-nozzle assembly located at the motor centerline. The smaller nozzle assembly is the steady-state nozzle used during the entire testing period, and the large assembly is the depressurization nozzle. The depressurization nozzle used for this motor consists of a double-burst disc assembly with a pressurization port located between the discs. The motor was designed so that a liner may be attached to all of the internal motor surfaces, if desired. Though the test apparatus may be attached to a surge tank (as illustrated in figure 1) to simulate various exhaust conditions, the motor was exhausted to the atmosphere (14.7 psia) in all the studies reported herein.

The motor had an internal volume of 110 in.³ and used a neutral-burning flat grain 2-1/4-in. wide by 5-in. long which was placed on the underside of the top cover plate. The test grains were ignited by initiation of a bag of BKNO₃ pellets placed adjacent to the sample surface.

Depressurization was accomplished by bursting the downstream disc of the double-burst disc assembly with a momentary overpressure in the chamber between the burst discs. Upon rupture of the downstream disc, a large pressure difference was developed across the upstream disc causing it to burst and open the termination nozzle. If correctly sized, the combination of the two nozzles results in a depressurization rate sufficient to terminate combustion.

The testing cycle was a programmed operation. At t_0 , the fire switch activated the recorder. After a short time delay, t_1 , which assured that the recorder attained the proper chart speed, the igniter was initiated. Following another delay, t_2 , which allowed sufficient time for the motor to reach steady-state conditions, the termination solenoid was activated, causing overpressure of the downstream disc. The remaining delay, t_3 , allowed sufficient time for the actual termination period before recorder shutdown.

Instrumentation for these tests consisted of two Texas Instrument LS-223 photovoltaic light cells, a Statham 0- to 750-psia strain gage pressure transducer and a Taber 0- to 1,000-psig strain gage transducer. Data were recorded at 40 in./sec, using a CEC oscillograph recorder.

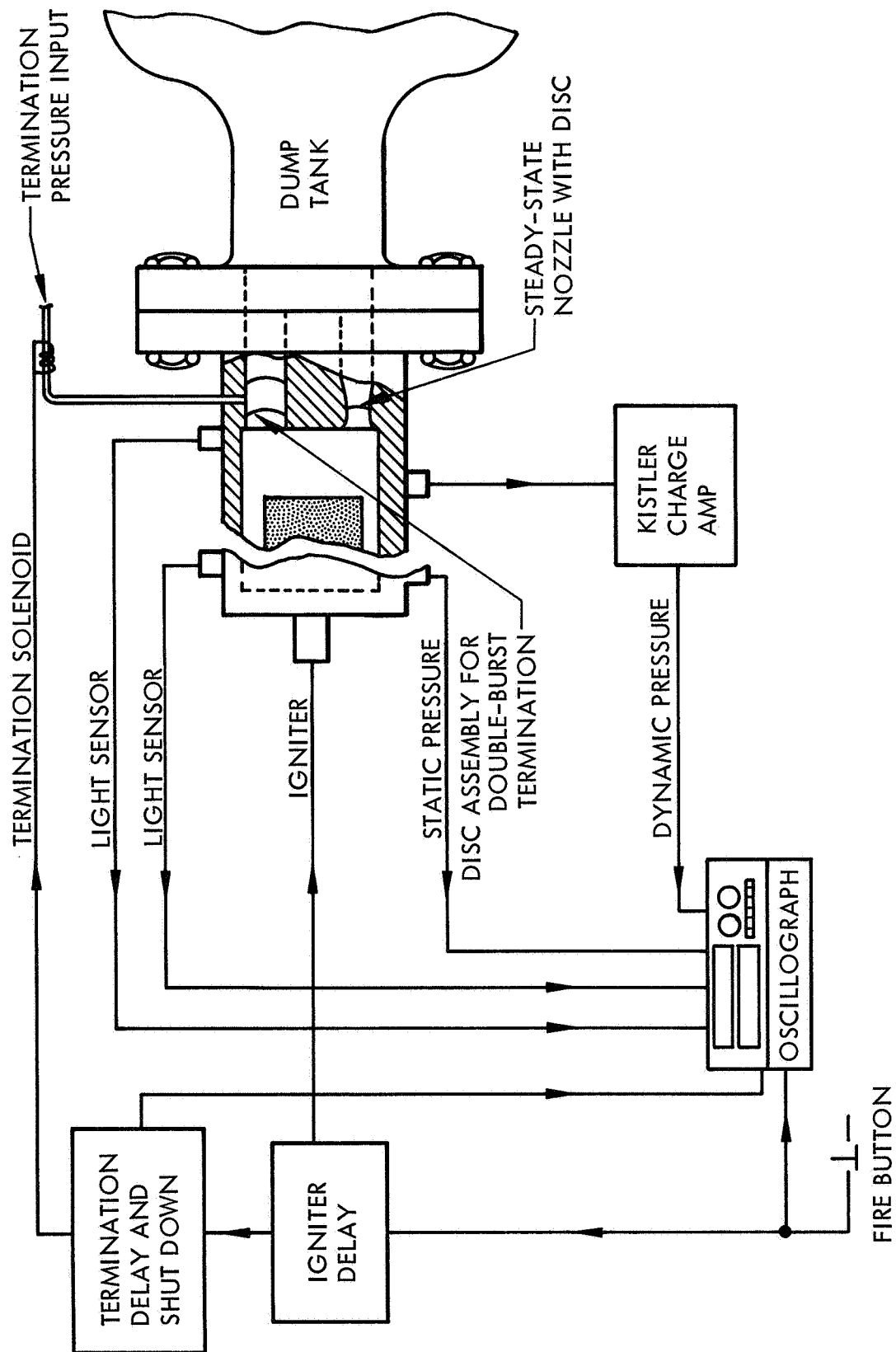


Figure 1. Schematic Diagram of Combustion Termination Apparatus

90465

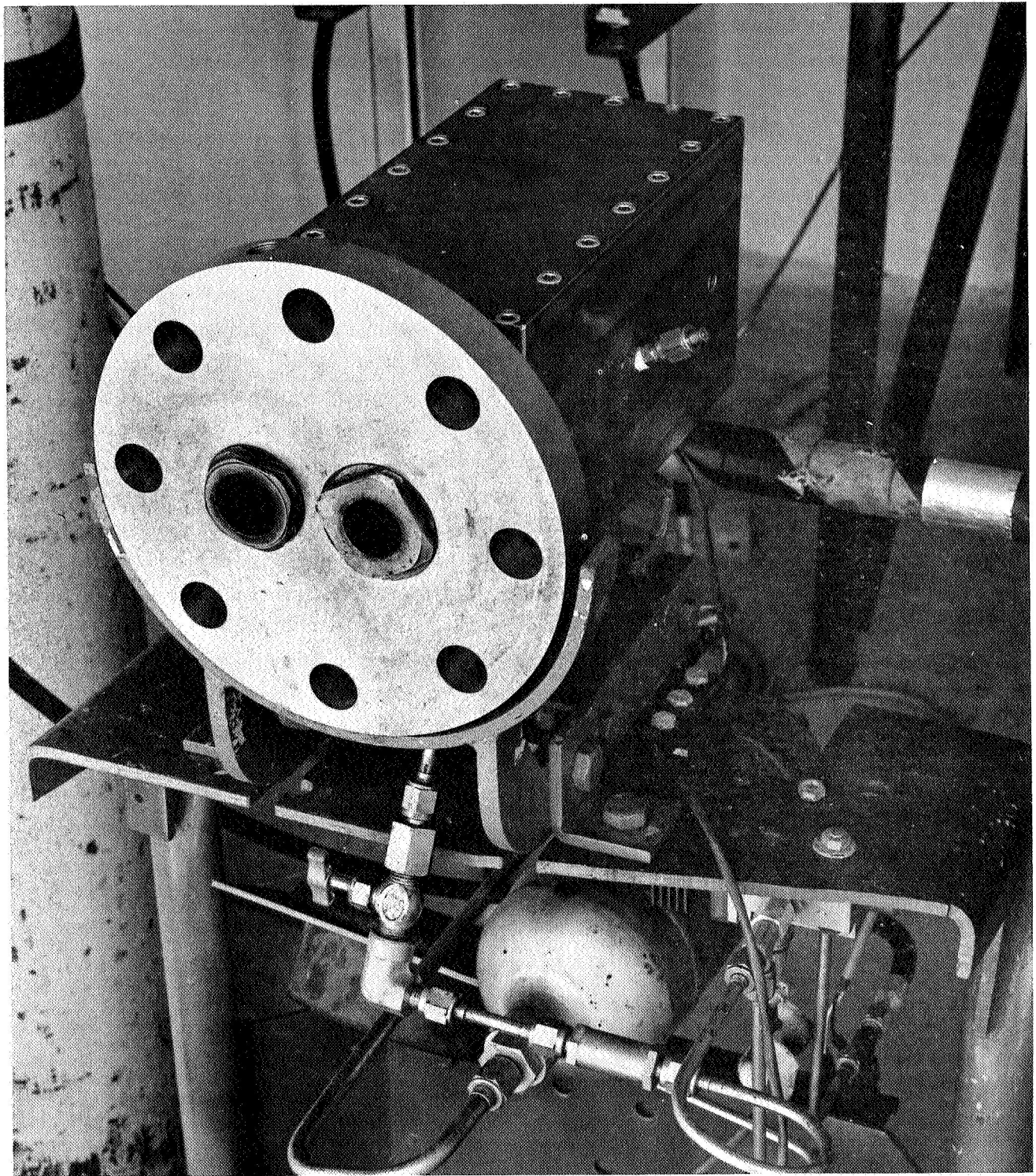


Figure 2. Dual-Nozzle Depressurization Motor

90466

Window Motor

The windowed depressurization motor, shown schematically in figure 3 and pictorially in figure 4, was designed and constructed under Contract No. NAS 1-6601 for both \dot{P} and L^* extinguishment studies. The motor has a dual-nozzle system with a top-mounted nozzle for steady-state operation and a nozzle at the aft end for either depressurization of the motor or L^* operation. In conducting L^* tests, the upper nozzle is plugged and the termination nozzle serves as a steady-state nozzle. Both the \dot{P} and L^* propellant grains can be viewed through the 1-in.-thick tempered Pyrex windows mounted on the sides of the motor.

Depressurization in the initial atmospheric pressure tests was achieved by use of a single brass disc which was burst by driving a spike into it. Figure 4 shows the motor with the solenoid driver and the spike mounted at the aft end of the motor. This method of depressurizing the motor was satisfactory for the atmospheric exhaust tests. When conducting subatmospheric depressurization studies with the window motor, both the steady-state and termination nozzle assemblies were attached to a 1,000-liter vacuum tank. To permit testing under these conditions, it was necessary to discard the solenoid system and devise a double-burst disc assembly mounted between the termination nozzle and the vacuum tank. Initially, an offset pressure between the two discs was used to contain the motor gases at pressures higher than the burst pressure of the upstream disc. After a specified burn period the offset pressure was increased, resulting in bursting of the downstream disc. After some experience was gained with this system, it was noted that the sudden increase of the offset pressure flexed the upstream disc inward, thus reducing the motor volume and causing a moderate pressure pulse. To eliminate this perturbation, a modified double-disc system was developed and used for all subsequent tests. This system employed a composite disc of brass and 0.015-in.-thick Mylar; the brass was exposed to the combustion chamber. The composite disc assembly was flange-mounted on the aft end of the motor downstream of the termination nozzle. A nichrome heater wire was then placed around the unrestrained periphery of the Mylar disc and connected to a voltage supply. With suitable selection of the thickness of the brass disc, this disc and the Mylar contained the pressures developed in the motor. Electrical heating of the nichrome wire then caused the Mylar disc to fail and the brass disc to burst, depressurizing the motor. Excellent results were obtained with this system at both atmospheric and vacuum exhaust pressures, and the system was used exclusively for the remainder of the program.

The motor, with steel plugs in place of the windows on the sides, has a 22-in.³ internal volume. To reduce the motor volume to 22 in.³ the plugs were used for all tests except the high-speed film tests.

Two types of propellant grains were used in this motor. Cylindrical end-burning grains (1.75-in. diameter, 0.5-in. deep) were used for the high-speed film studies, while rectangular neutral-burning grains (1-in. wide, 5-in. long) were used for the propellant characterization studies. The small, end-burning grains were most satisfactory for the film tests because of viewing restrictions; however, the larger rectangular grains used for the characterization studies permitted better control of the motor pressure by allowing the use of larger diameter steady-state nozzles which were less subject to fouling. Both types of grains were cast into stainless-steel sample dishes. The end-burning

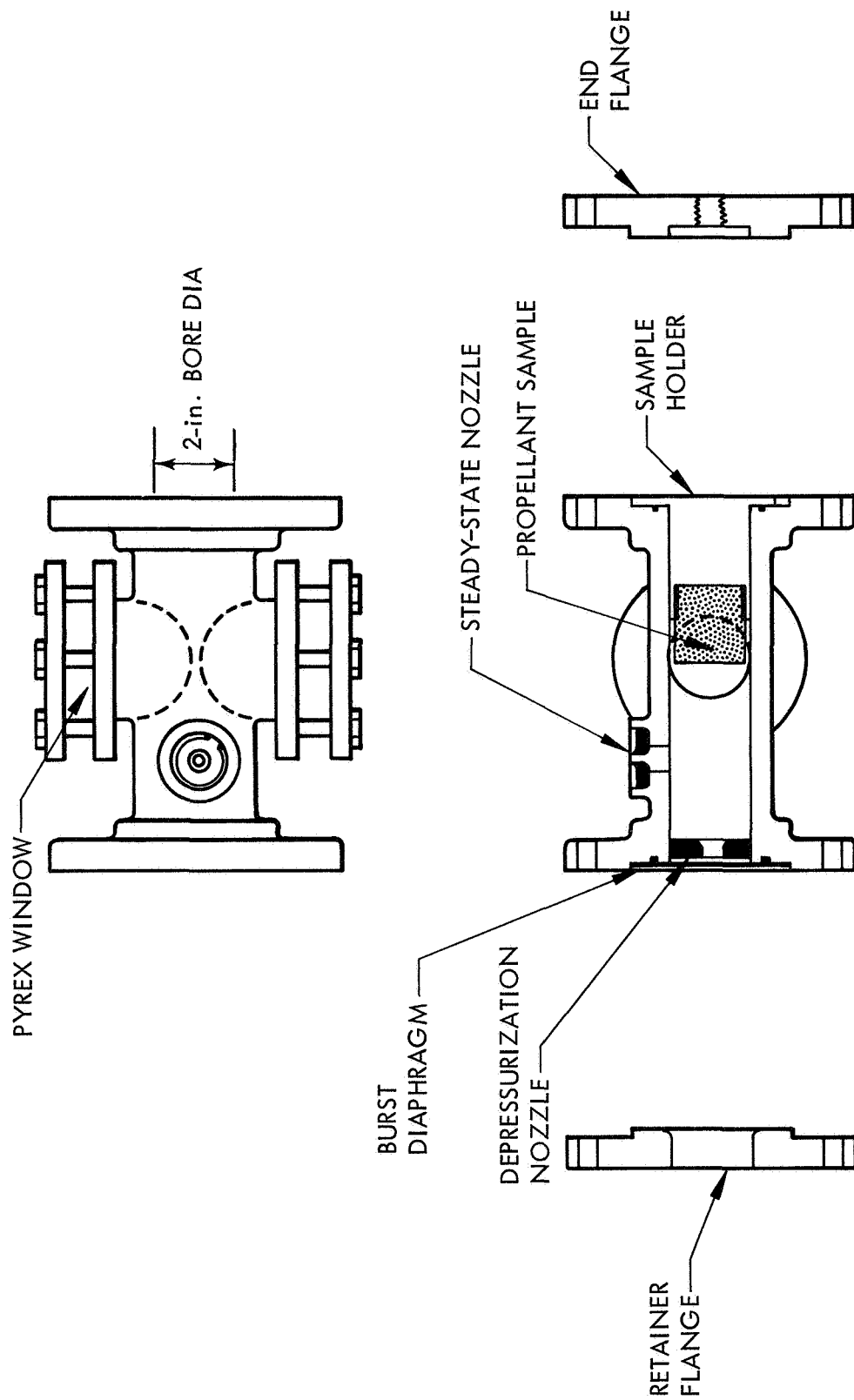


Figure 3. Schematic of Window Motor

90467

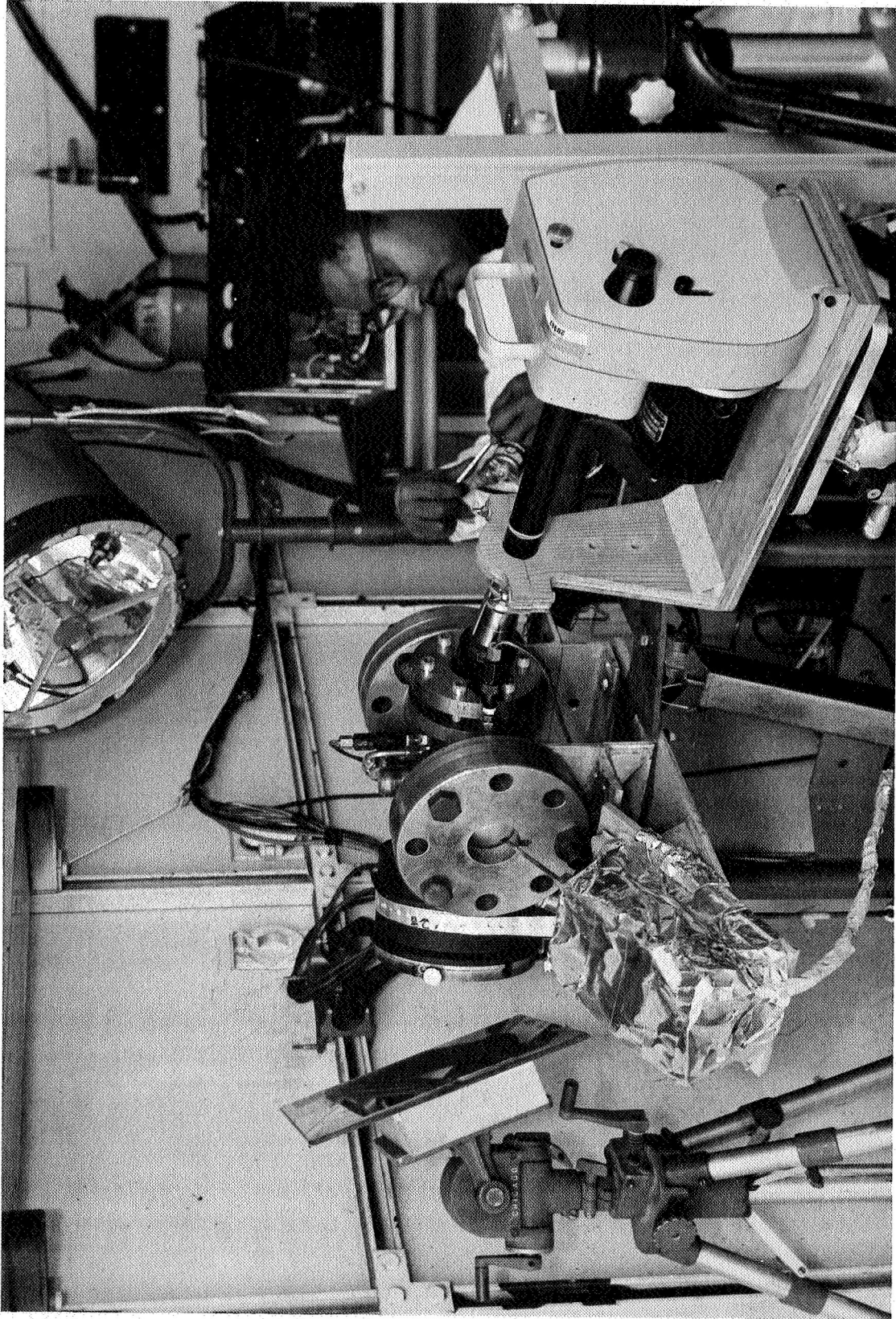


Figure 4. Window Motor with Xenon-arc Lamp

90468

round grains were ignited with a nichrome heater wire attached to the roughened propellant surface; the flat samples were ignited using a methane/oxygen hot gas igniter firing for 0.4 sec.

Instrumentation for both the film tests and the characterization tests consisted of two Texas Instrument LS-223 photovoltaic light sensors and two strain-gage pressure transducers. Signals from these instruments were recorded on a CEC 124 oscillograph using 7-319 galvanometers and a recording chart speed of 64 in./sec.

The bulk of the high-speed film tests were performed using a 500 to 1,000 frame/sec 16-mm camera and a light system similar to that shown in figure 5. With the camera aligned approximately 30° to the combusting face of the sample, filming was initiated immediately prior to ignition of the sample and stopped 500 to 1,000 msec after chamber depressurization. An ASA 125 color film was used with a 1/2,500-sec shutter speed and an aperture stop of about 8.0, depending on the expected luminosity.

Earlier photographic tests performed under Contract No. NAS 1-6601 were made using relatively slow framing rates, little magnification, and low f number apertures. To obtain higher framing speeds, greater magnification, and better resolution, it was necessary to use lighting levels higher than those provided by the flash lamp used previously. During the early portion of this program, an evaluation was made of the utility of a Fastax WF360 Xenon arc lamp. The greater light intensities provided by the lamp improved the photographic results and the radiant flux output from the lamp (measured using a black body calorimeter) was $25 \text{ cal/cm}^2\text{-sec}$. This flux caused rapid ignition of the propellant and also served as a perturbing influence upon the combustion processes. The arc lamp was replaced by a General Electric Marc-300 projection lamp system which was used for the remainder of the program. This system did not provide sufficient light to overpower the flame at higher pressures; but it did permit clear viewing as the pressure fell below 100 psi during depressurization and the flame intensity correspondingly decreased.

Swing-Nozzle Motor

The motor shown in figures 6 and 7 was utilized to achieve \dot{P} data during the program. As shown, internal-burning grains used in the motor can either be restricted on the ends of the grain or left unrestricted, giving a moderately progressive burning trace. The grains had an initial port diameter of 0.5 in. and a final port diameter of 1.5 in. and thus, provide up to 2 sec of burn time. Two grain lengths of 5-in. and 15-in. grains were used for the swing-nozzle motor tests. The 5-in.-long grains had a burnout volume of 10 in.^3 , and the 15-in.-long grains had a burnout volume at 27.7 in.^3 . In general, the volumes at termination were 4 in.^3 and 9.1 in.^3 , respectively. The tie rods, as shown in figure 6, were used to restrain the motor and allow motor pressures up to 2,000 psi.

The motor was ignited using a methane/oxygen hot-gas igniter firing for 0.5 sec. After ignition and a burn time of 0.7 to 1.0 sec, the motor was depressurized by releasing the graphite steady-state nozzle assembly. Figure 6 shows the swing-nozzle assembly in the open position next to the catch used to stop the door's swing. The assembly

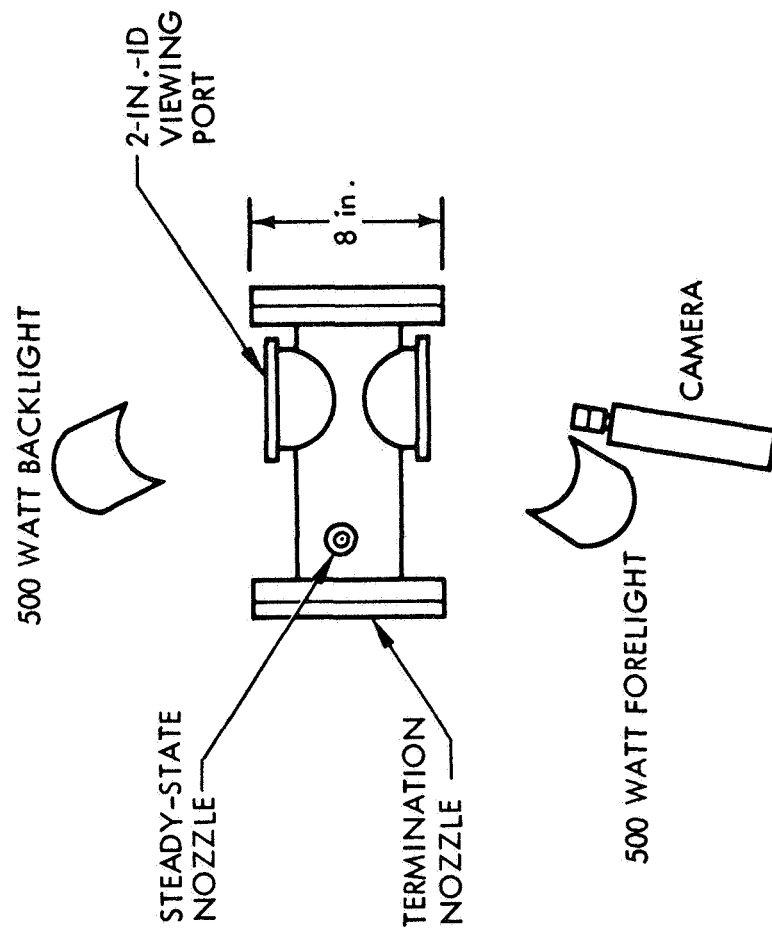


Figure 5. Schematic Top View of Window Motor and Camera System



Figure 6. Swing-Nozzle Motor

90470

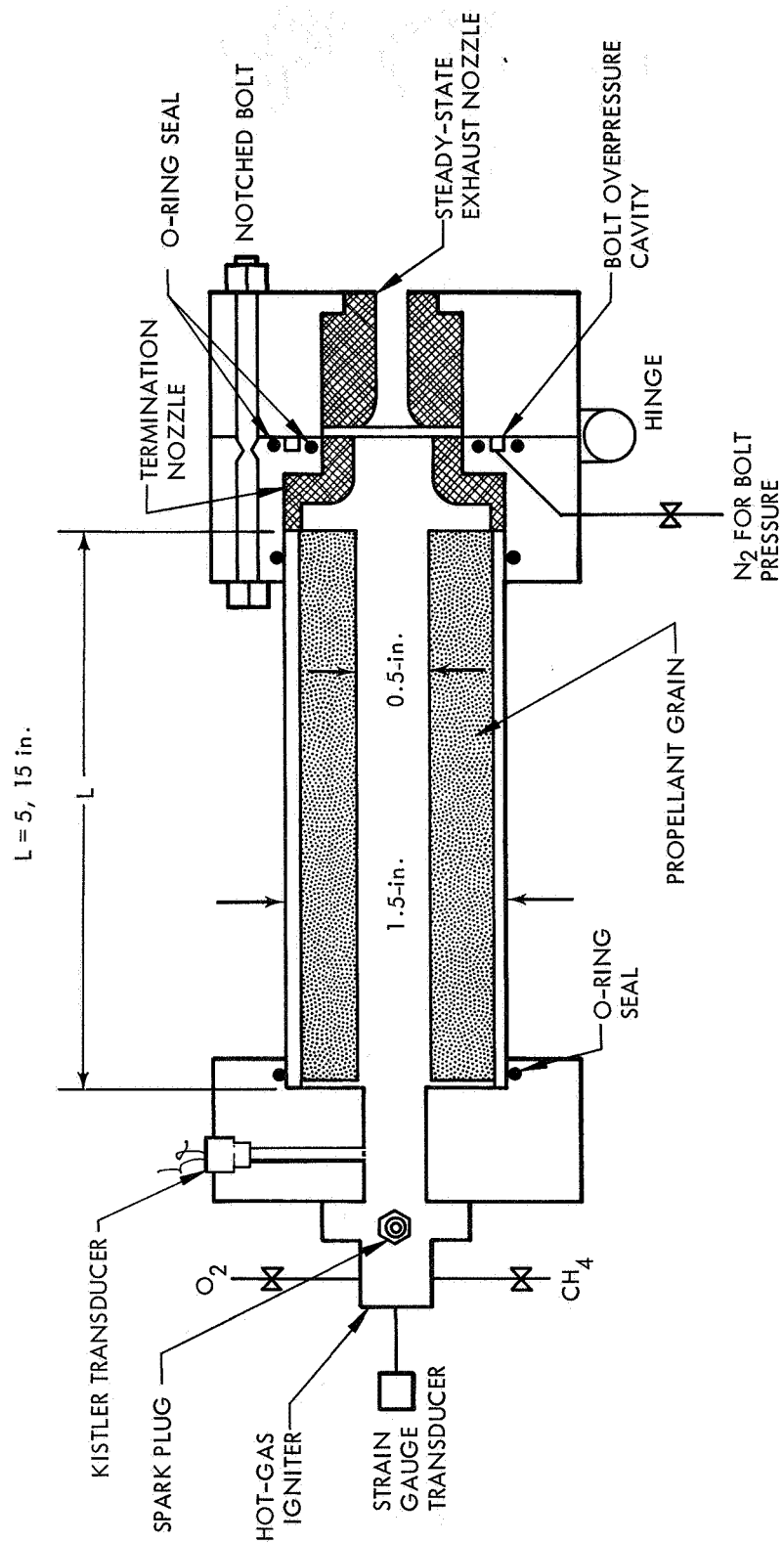


Figure 7. Schematic of Swing-Nozzle Motor

90471

was released upon command by exceeding the tensile strength of the single, notched bolt used to restrain the assembly during steady-state operation. This was accomplished by pressurizing the space between two O-rings mounted on the aft face of the motor between the nozzle assembly and the motor body. The restraining bolt was sized to fail when the force caused by pressurization was equal to that force exerted on the door by the motor gases.

The rate of depressurization of the motor was controlled by a large-diameter nozzle assembly mounted at the aft end of the grain. As shown in figure 6, this assembly consisted of a copper nozzle retainer and a graphite nozzle. The nozzle was mounted close to but not touching the aft end of the grain to minimize reignition problems.

Instrumentation for this motor consisted of a Kistler 601-A quartz pressure transducer, a Statham strain-gage pressure transducer, and a Solar Systems 300-2 light sensor. The pressure transducers were mounted at the head end of the motor, and the light sensor viewed a zone between the steady-state nozzle and the termination nozzle at the aft end of the motor. Data were recorded at 80.0 in./sec on a CEC oscillograph using a 7-326 galvanometer for recording the Kistler transducer signal and 7-342 galvanometers for the other transducer signals. A conventional sequence unit was used for control of the entire firing and depressurization cycle.

Table I summarizes the major parameters of the three motor systems. The operational commonality of these three motor systems is that each motor was fired for 0.7 to 1.0 sec before depressurization. Because of the progressive nature of the swing-nozzle motor grains and the differences in burning rates of the tested propellants, there was a slight variation of both motor free volume and grain area at the moment of depressurization. Some tests were conducted with once-terminated grains so that, at the time of the second depressurization test, the grain area and the motor volume were greater than shown in table I. Tests conducted with such grains have been noted in following text. In general, the swing-nozzle grains burned from a 0.5-in. internal diameter to 0.8-in. diameter at first extinguishment and to 1.15-in. diameter at second extinguishment.

TABLE I
MOTOR PARAMETERS

	<u>1-lb Slab Motor</u>	<u>Window Motor</u>	<u>Swing-Nozzle Motor</u>	
			<u>5-in. grain</u>	<u>15-in. grain</u>
Grain area, in. ²	11.25	5.0	≈13.50	≈38.00
Motor volume, in. ³	110.00	22.0	≈4.00	≈9.10
Length of motor, in.	8.25	7.5	5.25	15.25

Propellants

Four basic formulation variables were evaluated in the course of the program: (1) binder-polymer-curative variations, (2) AP loading level and size distribution, (3) aluminum loading level, and (4) catalyst content. Previous studies conducted under Contract No. NAS 1-6601 were primarily concerned with the perturbing influence of formulation variables upon the extinguishment behavior of propellants formulated with the saturated polymer, CTPIB. The efforts of this program were directed toward a better understanding of basic combustion extinguishment phenomena by means of more extensive studies; however, emphasis was also placed on the study of other binder systems, in particular the unsaturated binder, CTPB. The formulation studies with CTPB paralleled the earlier CTPIB studies in that the effects of oxidizer loading level, metal loading level, and catalyst content upon extinguishment behavior were studied. In addition, the earlier studies with the CTPIB polymer were extended by studies with chlorinated CTPIB binders, sterilized systems, other catalysts, and catalyst/metal loadings.

Binder/Curative Studies - The propellants used for the study of binder and curative variations all contained 83.8% AP with 65:35 coarse to fine ratio, 0.2% carbon black, and were nonaluminized. As indicated in table II, the effect of binder polymer structure upon termination behavior was studied with the CTPIB system and its chlorinated variations, CTPB, polyurethane, and polyepichlorhydrin.

All the propellants were plasticized with dioctyl adipate to permit the 84% solids loading level. Screen analysis data of the coarse AP used throughout the program is shown in table III. Screening of the ground (or fine) AP showed 10% of the material to be less than 2μ in diameter, 50% to be less than 6.3μ in diameter and 90% to be less than 10.4μ in diameter.

The CTPIB, CTPB, and polyurethane propellants were selected for study because of the diverse thermal and oxidative degradation characteristics of the binder polymers. Limited studies^(13,19,20) indicate that the more easily terminated polyurethane and CTPIB formulations are less subject to exothermic oxidative degradation of the binder and are more easily degraded by endothermic thermal decomposition. The CTPB polymer shows greater susceptibility to oxidative degradation, is less subject to thermal degradation, and has a higher flame temperature which may contribute to greater heat feedback from gas-phase combustion.

DSC studies conducted during this program, along with concurrent studies by Shannon⁽²¹⁾ demonstrate the differences of the thermal decomposition of the three binders. The DSC traces for the three reference binders and two PBAN binders in nitrogen are shown in figure 8. At a heating rate of 10° per minute and a 3.1 mg sample of CTPB binder in nitrogen, first decomposition (endothermic) was noted at 303°C , and sample darkening was observed at 390°C . Bubble formation within the sample occurred at 450°C , followed by rapid fume-off at 470°C . Decomposition was complete at 491°C with a 0.05-mg residue remaining.

Under similar conditions polyurethane was observed to melt at 215°C and decomposition was complete at 397°C . Decomposition of CTPIB first resulted in droplet formation on the viewport at 153°C . The sample melted

TABLE II
BINDER/CURATIVE FORMULATIONS

<u>Propellant-UTX No.</u>	<u>Binder</u>	<u>Curing Agent(s)</u>	<u>Binder Equivalent/ Curative Equivalent</u>
10642	CTPB	Epoxy/Aziridinyl/ MAPO	1.0/0.4:0.9 ^a
10691	CTPB	Epoxy/Aziridinyl/ MAPO	1.0/0.4:0.9
11339	CTPB	Epoxy	1.0/0.5:1.25
10661	PU	Isocyanate	0.4/1.0
10645	CTPIB	Aziridinyl	1.0/1.2
11314	CTPIB	Aziridinyl	1.0/1.5
10698 (chlorinated)	CTPIB	Aziridinyl	1.0/1.2
11306 (chlorinated)	CTPIB	Aziridinyl	1.0/1.2
11315 (chlorinated)	CTPIB	Aziridinyl	1.0/1.2
10720 (sterilized)	CTPIB	Aziridinyl	1.0/1.2
11402 (sterilized, aluminum)	CTPIB	Aziridinyl	1.0/1.2
11318	Polyepichloro- hydrin	Isocyanate	1.0/1.1

a. 0.4 equivalent of epoxy, 0.9 equivalent aziridinyl (MAPO).

TABLE III
COARSE AP SCREEN ANALYSIS

<u>Sieve No. (Tyler)</u>	<u>Cumulative Retained, %</u>	
	<u>Minimum</u>	<u>Maximum</u>
16 (1,000)	0	0
48 (297)	4	12
65 (210)	30	50
100 (149)	62	80
200 (74)	95	99
325 (44)	98	100

Mean particle diameter - 190

between the range of 240^o to 269^oC. Bubble formation began at 280^oC, and rapid fume-off occurred from 300^o to 350^oC. Decomposition was complete at 419^oC.

As noted in tables IV, V, and VI, the gaseous environment has a significant influence upon binder decomposition. The presence of oxygen lowers the entire temperature zone of decomposition and apparently alters the decomposition mechanisms. It is likely that the oxidizer-rich combustion zone of a solid propellant would have a more dramatic effect upon degradation behavior. These data, while limited in scope, indicate the problems of modeling combustion phenomena without a clear description of the decomposition and kinetic mechanisms. Any major alteration of the propellant binder or oxidizer system and pressure can markedly alter the combustion processes.

The measured-strand burning rates of propellants prepared from the three basic binders used in this program—CTPB, polyurethane, and CTPIB—are shown in figure 9. With the exception of the CTPB propellant, the burning rates cannot be adequately described by a simple power-law expression at pressures less than 100 to 200 psia. Though strand data for the CTPIB propellant could not be obtained for pressures above 750 psia, motor tests were conducted easily at much higher pressures, indicating the upper deflagration limit is peculiar to the strand data.

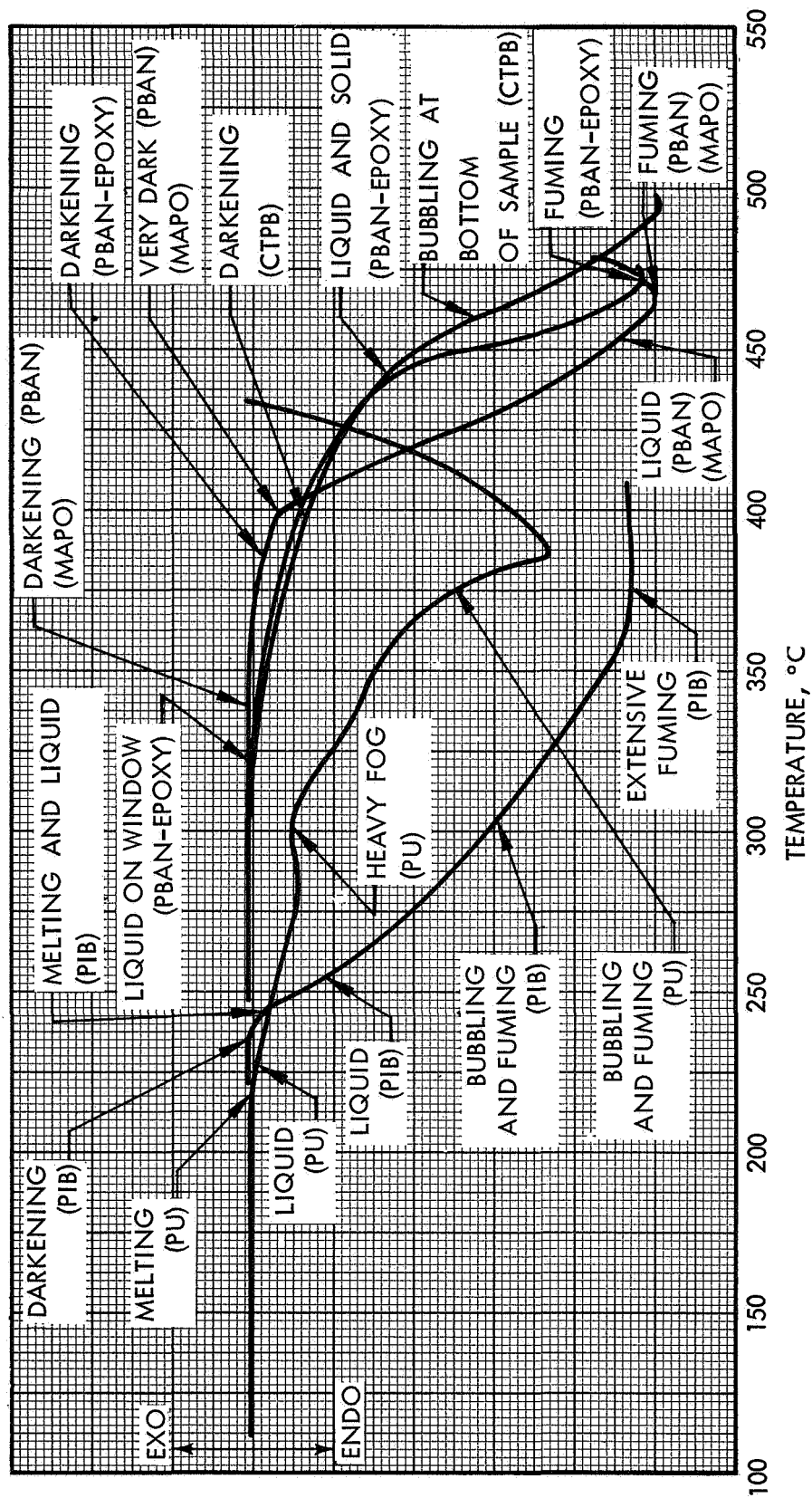


Figure 8. DSC Traces for Binder Samples in Nitrogen, 1 atm

TABLE IV

POLYMER DECOMPOSITION - DSC TESTS

N₂ - 1 atm.

<u>Polymer</u>	200° to 250°C	250° to 300°C	300° to 350°C	350° to 400°C	400° to 500°C
PIB	Darkening, 225°C Melting, 240°C	Bubbling and fuming	Extensive fuming		
PU	Melting, 215°C	Limited fuming	Bubbling and fuming		
PBAN- EPOXY			Condensate on viewing window	Darkening, 375°C	Liquid and solid. Bubbling in liquid layer. Fuming at 475°C.
PBAN- MAPO			Darkening, 325°C	Extensive darkening	Liquid and solid. Fuming at 470°C.
CTPB				Darkening, 390°C	Liquid and solid. Bubbling at bottom of sample at 470°C.

TABLE V
POLYMER DECOMPOSITION - DSC TESTS

Air - 1 atm				
Polymer	200° to 250°C	250° to 300°C	300° to 350°C	350° to 400°C
PIB	Darkening, 225°C Melting, 240°C	Bubbling and fuming	Extensive fuming	
PU	Melting, 215°C	Limited fuming	Bubbling and condensation	
PBAN- EPOXY	Condensation and darkening, 200° to 220°C	Sample is black at 250°C	Condensation	Limited decomposition ^a
PBAN- MAPO	Condensation and darkening, 200° to 225°C	Increased condensation	Sample is black at 300°C	Limited decomposition ^a
CTPB	Darkening, 204°C		Sample is black at 350°C	Condensation and decomposition, 400°C ^a

^a At completion of run, sample had original shape but was black and charred. Residue was hard and brittle.

TABLE VI
DSC POLYMER DECOMPOSITION
1 atm O₂

Polymer	<u>175° to 250°C</u>	<u>250° to 300°C</u>	<u>300° to 350°C</u>	<u>350° to 400°C</u>	<u>400° to 500°C</u>
PIB	Condensation on viewing window, 190°C Melting, 221°C	Liquid becomes red-brown, 267°C. Bubbling and fuming	Extensive fuming	Carbon residue is formed on sides of pan	Partial decomposition of residue ^a
PU	Condensation on viewing window, 190°C Limited melting, 210°C	Sample has soft, waxy appearance and has become discolored	Sample has appearance of thick gel. Dark in color	Carbon residue is formed on bottom of pan	Partial decomposition of residue ^a
PBAN-EPOXY	Condensation on viewing window, 200°C Sample darkening, 205°C	Increased condensation	Extensive fuming	Sample begins to swell and form char, 400°C	Partial decomposition of residue ^a
PBAN-MAPO	Condensation on viewing window, 200°C Sample darkening, 200°C	Increased condensation	Fuming	Sample begins to form char	Partial decomposition of residue ^a
CTPB	Sample darkening, 190°C Condensation on viewing window, 200°C		Sample is black at 300°C	Sample begins to form char	Partial decomposition of residue ^a

^a Runs were terminated at 500°C. A residue remained in each test. In the case of the CTPIB and polyurethane polymers, this residue weighed 8 to 10% of the initial sample. In the case of PBAN and CTPB polymers, the residue weighed approximately 30% of the initial sample.

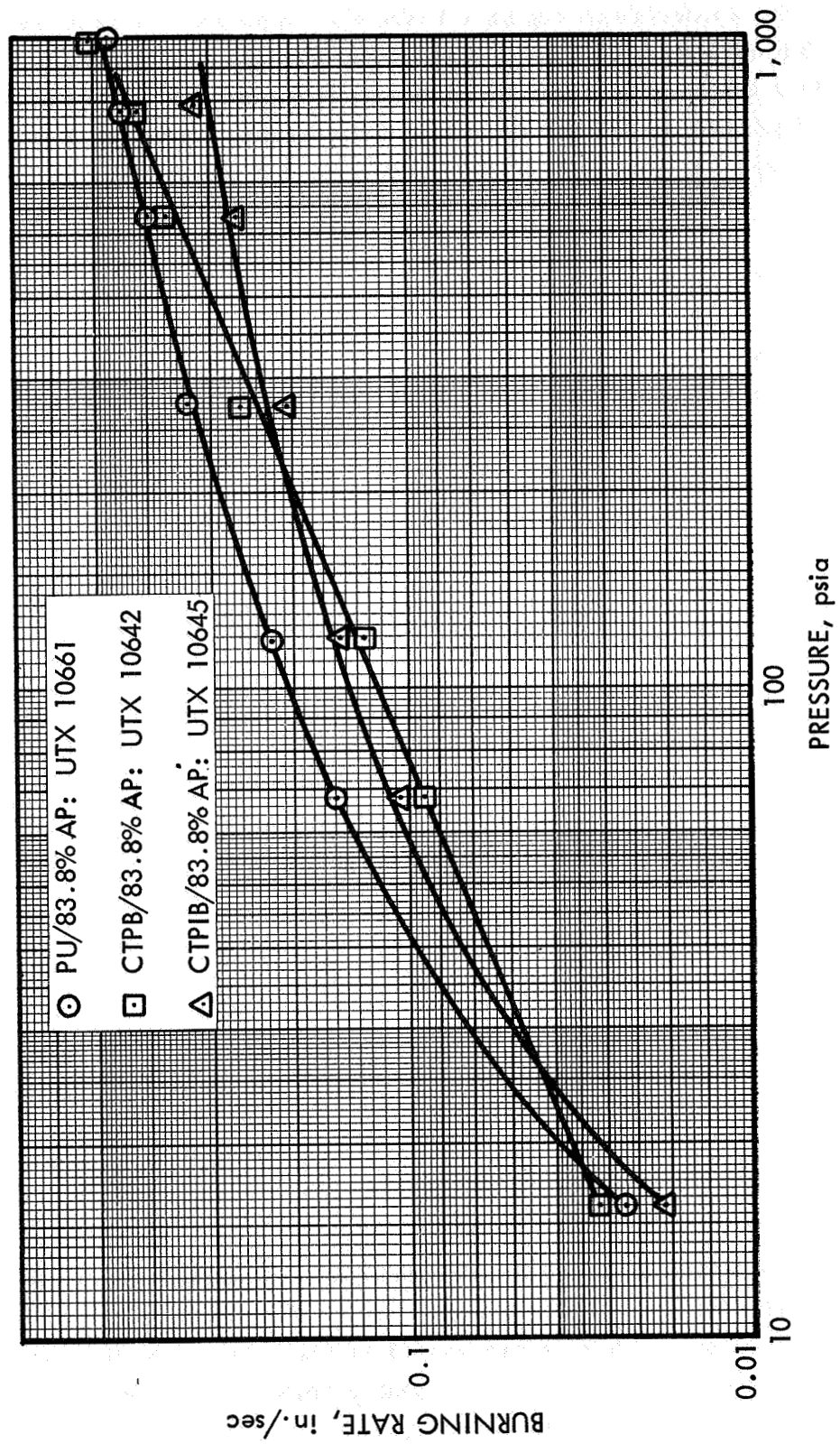


Figure 9. Strand Burning Rates for PU, CTPB, and CTPIB Nonaluminized Propellants

90473

The CTPB propellant (UTX 10642) used for initial testing was poorly cured and had a plastic consistency not representative of state-of-the-art propellants. To determine the possible influence of these characteristics upon termination behavior, a second CTPB system (UTX 10691), which had a more representative physical behavior, was prepared with a different epoxide resin. Termination results obtained with the two formulations were nearly identical, thus indicating that (1) the binder polymer is the dominant factor influencing \dot{P} behavior and (2) the physical properties of the propellant have little or no influence upon termination behavior. In this instance, the use of the new epoxy resin also had no appreciable effect upon the burning rate of the basic formulation. An additional variation had only marginal effects upon both the burning rate and termination behavior. (The strand burning rate data for the three CTPB systems are shown in figure 10.)

It is possible that curative variations which modify the combustion behavior, i.e., burning rate, of the propellant will also modify the \dot{P} behavior. However, the film studies of this program and the compositional studies of Contract No. NAS 1-6601⁽⁷⁾ showed that the \dot{P} and burning rate modifications are not influenced by changes in physical properties of the propellant. The film studies did not show any of the propellant surface tearing away during depressurization, an aspect which might be influenced by the binder physical properties, nor did the compositional studies of Contract No. NAS 1-6601 indicate that extreme changes of the binder physical properties have any measurable influence upon \dot{P} behavior. Prior to initiation of this program, it was postulated that the propellant physical properties might influence \dot{P} behavior, and physical property tests were planned in the course of this program. Considering the evidence that gross changes in physical properties showed no effect on \dot{P} behavior, characterization of the physical properties of the propellants used in this program was not pursued.

The effect of polymer to curative ratio upon \dot{P} behavior was explored with the CTPIB formulation which contained 1.5 equivalents of MAPO curative (UTX 11314), rather than the 1.2 equivalents used for the base CTPIB formulation (UTX 10645). The results of these studies parallel the findings obtained with the CTPB propellants. It was found that for the CTPIB system the curative-to-polymer equivalence ratio has little or no effect upon termination behavior or burning rate.

The use of chlorinated CTPIB binders was investigated using three chlorine concentrations—1.2%, 3.4%, and 14.5% of the binder polymer. Because the propellant was composed of 12.55 wt-% binder, the actual chlorine concentrations were 0.15%, 0.43%, and 1.82% of the propellant. All three chloropolyisobutylene binders were prepared by chlorination with chlorine gas at 60°C in a carbon tetrachloride-polymer solution. The extent of chlorination was controlled by varying the reaction time from 1 to 5 hr and by varying the rate of introduction of chlorine into the reactor.

The purpose of these additions was to determine whether such halogens would reduce the \dot{P} termination requirements of saturated binder systems and whether any possible reduction could be related to gas-phase flame inhibition or to modification of the thermal decomposition behavior of the binder. Halogenated hydrocarbons and halide salts are demonstrated gas flame suppressants which are widely used to reduce the flammability of organic

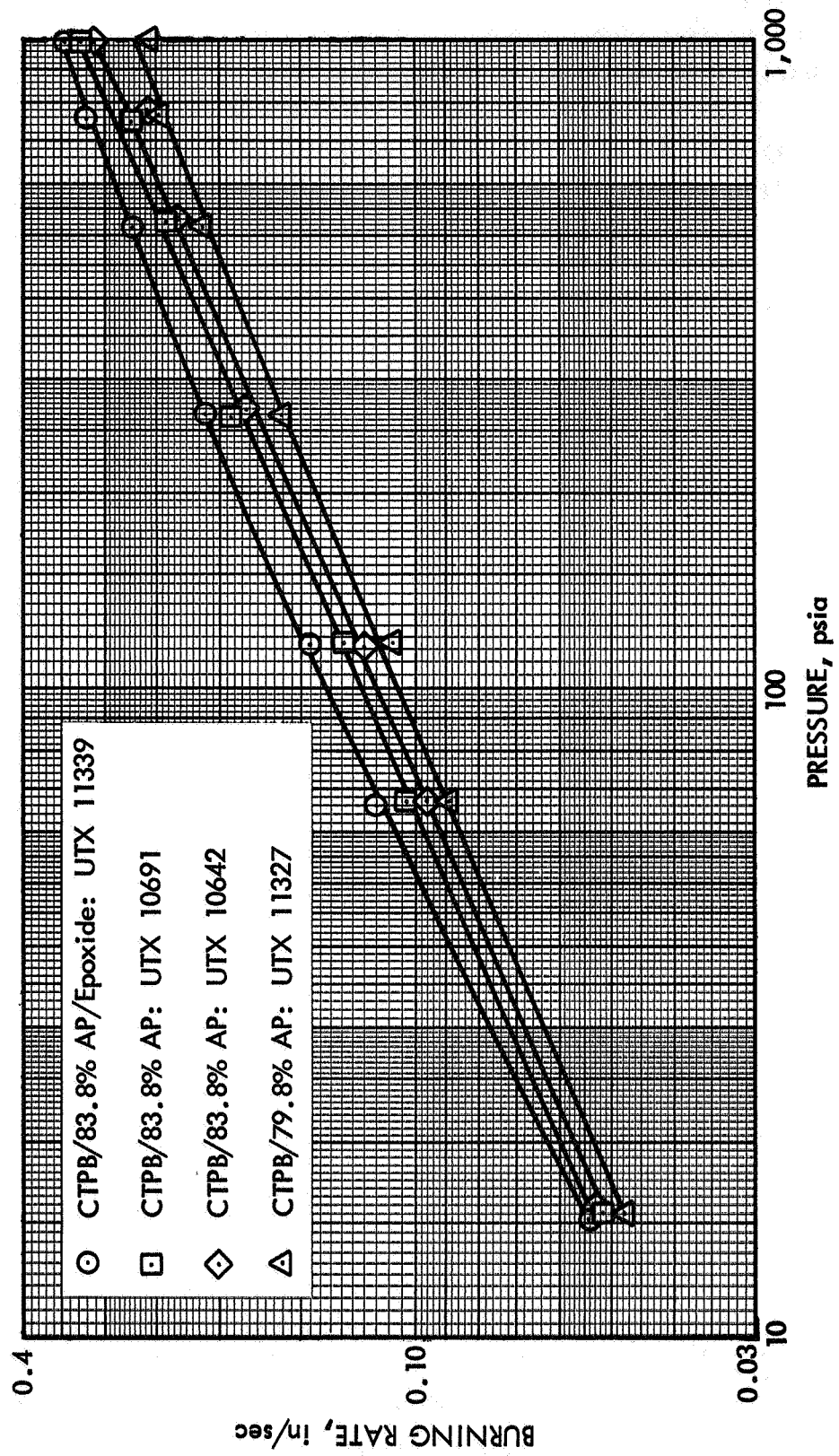


Figure 10. CTPB Nonaluminized Propellant Strand Burning Rates

90474

polymers. Introduction of the halogen molecule into the binder should also reduce the decomposition temperature of the binder, thereby making combustion termination less difficult. The burning rates of the chlorinated systems were not measurably different than those of the nonchlorinated system.

In addition to the chlorinated CTPIB studies, limited characterization tests were conducted with two sterilizable CTPIB propellants. The first formulation (UTX 10726) contained 84% AP and no aluminum, while the second propellant (UTX 11402) contained 68% AP and 16% aluminum. The primary purpose for these studies was to determine what effect the sterilization process might have upon termination behavior. Though burning rates were not measured for these propellants, other studies have shown the sterilization process to have little or no effect upon burning rate behavior.

The polymer, polyepichlorohydrin, was tested as having potential for an easily terminated propellant system. This work was done on the basis that polyepichlorohydrin, which contains 37.5% chlorine, should show low temperature, low molecular weight species thermal decomposition behavior. These factors, when incorporated into a propellant system, should realize low depressurization-extinguishment requirements. Because of the limited amount of polymer available, no strand data were obtained for this system and only limited termination studies, described in a later section, were performed.

Oxidizer Variation Studies - The effect of oxidizer loading level upon the combustion extinguishment behavior of the CTPB system was investigated using a formulation containing 79.8% AP (UTX 11327), rather than the 83.8% AP level used in the base CTPB system (UTX 10691). A comparison of the strand burning rates of the two systems is shown in figure 10. Over the range of pressures tested, the lower oxidizer loading level reduced the burning rate and the burning rate exponent only slightly.

To evaluate the effect of oxidizer particle size on termination behavior, attempts were made to prepare a CTPIB propellant using unimodal AP. Because of processing restrictions at oxidizer loadings representative of comparative propellants, this approach was not pursued. Alternatively, the effect of oxidizer coarse-to-fine ratio in the CTPIB system was explored using a 35 to 65 coarse-to-fine ratio rather than the 65 to 35 ratio used for the other propellants.

The strand burning rate data for the UTX 11336 propellant and the previously referenced UTX 10645 CTPIB system are shown in figure 11. The burning rate characteristics were much the same and, although upper deflagration limits were found at 420 psi to 520 psi for strands, both propellants were successfully fired at motor pressures up to 1,000 psi.

Metal Loading Level Studies - Four metallized noncatalyzed formulations were characterized in the course of the program: (1) a CTPB formulation containing 4% aluminum (UTX 11317), (2) a CTPB formulation containing 16% aluminum (UTX 11325), (3) a CTPIB formulation containing 4% aluminum (UTX 11316), and (4) a CTPIB

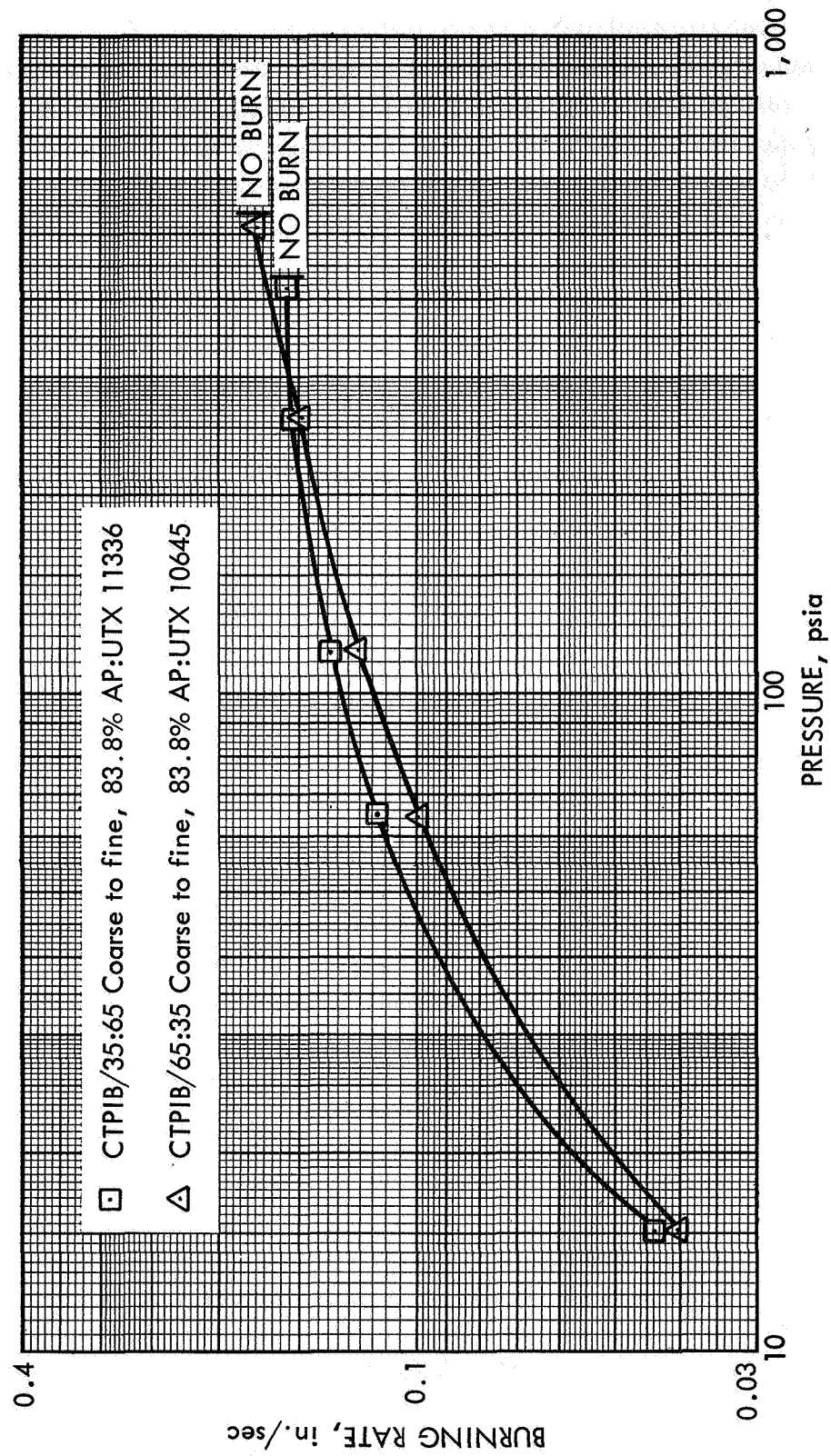


Figure 11. Strand Burning Rates of CTPIB Propellants as a Function of Coarse to Fine AP Ratio

formulation containing 16% aluminum (UTX 11454). While the CTPIB systems were characterized under Contract No. NAS 1-6601,⁽⁷⁾ they were reevaluated to provide comparison data for the CTPB system and to provide a reference for the exhaust level studies described later in this report. All four formulations contained a total solids loading of 84% and contained a bimodal AP oxidizer blend. The burning rate characteristics of these propellants are shown in figure 12 along with the strand burning rates of the nonaluminized base propellants. When aluminum was substituted for AP, both the CTPB and CTPIB systems showed a slight reduction of the burning rate. The CTPB system showed the greatest decrease when 16% aluminum was added.

Catalyst Studies - The effect of the burning rate catalyst upon the termination behavior of the CTPB system was studied with two nonmetallized propellants and two aluminized propellants. The two nonmetallized CTPB propellants, UTX 11326 and UTX 11329, were formulated respectively with 0.25% iron oxide and 0.25% organo-iron burning rate catalyst and contained 83.8% AP. The two aluminized CTPB systems, UTX 11473 and UTX 11341, contained 16% aluminum and 3% and 1% HYCAT, respectively, with a total solids loading of 84%.

Inclusion of 0.25% iron oxide burning rate catalyst in the CTPB nonaluminized system, as shown in figure 13, increased the propellant strand burning rate at higher pressure levels, but did not affect the burning rate at 15 psia. At 1,000 psia the noncatalyzed base propellant had a burning rate of 0.32 in./sec, while the catalyzed UTX 11326 formulation burned at 0.39 in./sec. At 15 psia both propellants have a strand burning rate of 0.05 in./sec. The organo-iron catalyst increased the strand burning rate over the entire pressure range without significantly changing the burning rate exponent.

The aluminized CTPB propellants with 1% and 3% HYCAT showed significantly higher burning rates at all pressure levels and the 3% HYCAT formulation showed the greatest increase; however, the strand data of figure 13 show little change of the burning rate exponent at pressures above 200 psi.

The effect of burning rate catalyst addition to the CTPIB system was studied with UTX 11333 containing 0.25 organo-iron catalyst and 83.8% AP. Also studied was UTX 11342 containing 1% HYCAT, 16% aluminum and 68% AP. The strand burning rates for these propellants are shown in figure 14 with the strand data for the base CTPIB nonaluminized propellant (UTX 10645) and the 16% aluminum CTPIB formulation (UTX 11454). The addition of 0.25% organo-iron catalyst to the CTPIB system moderately increased the burning rate at pressures above 15 psia. The addition of 1% HYCAT and 16% aluminum markedly increased the burning rate at all pressure levels.

Thermodynamic Constants - The calculated c^* and flame temperatures for the majority of propellants tested are shown as a function of pressure (see table VII). As noted in table VII, the introduction of 14.5% chlorine into the CTPIB binder (UTX 11315) did not significantly affect the flame temperature or c^* ; therefore, these quantities were not calculated for the lower chlorine concentration formulations.

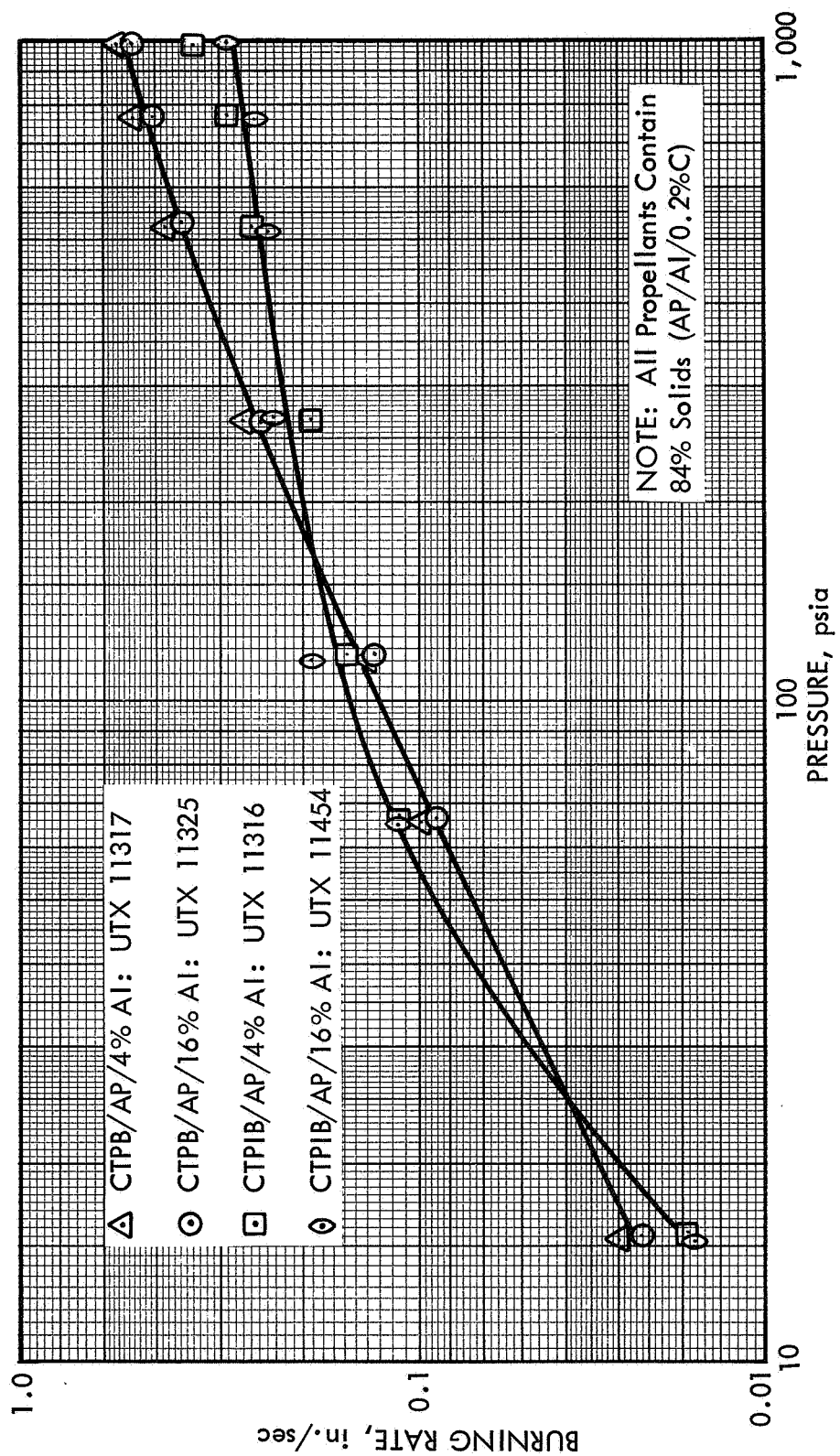


Figure 12. CTPB and CTPIB Aluminized Propellant Burning Rates

90476

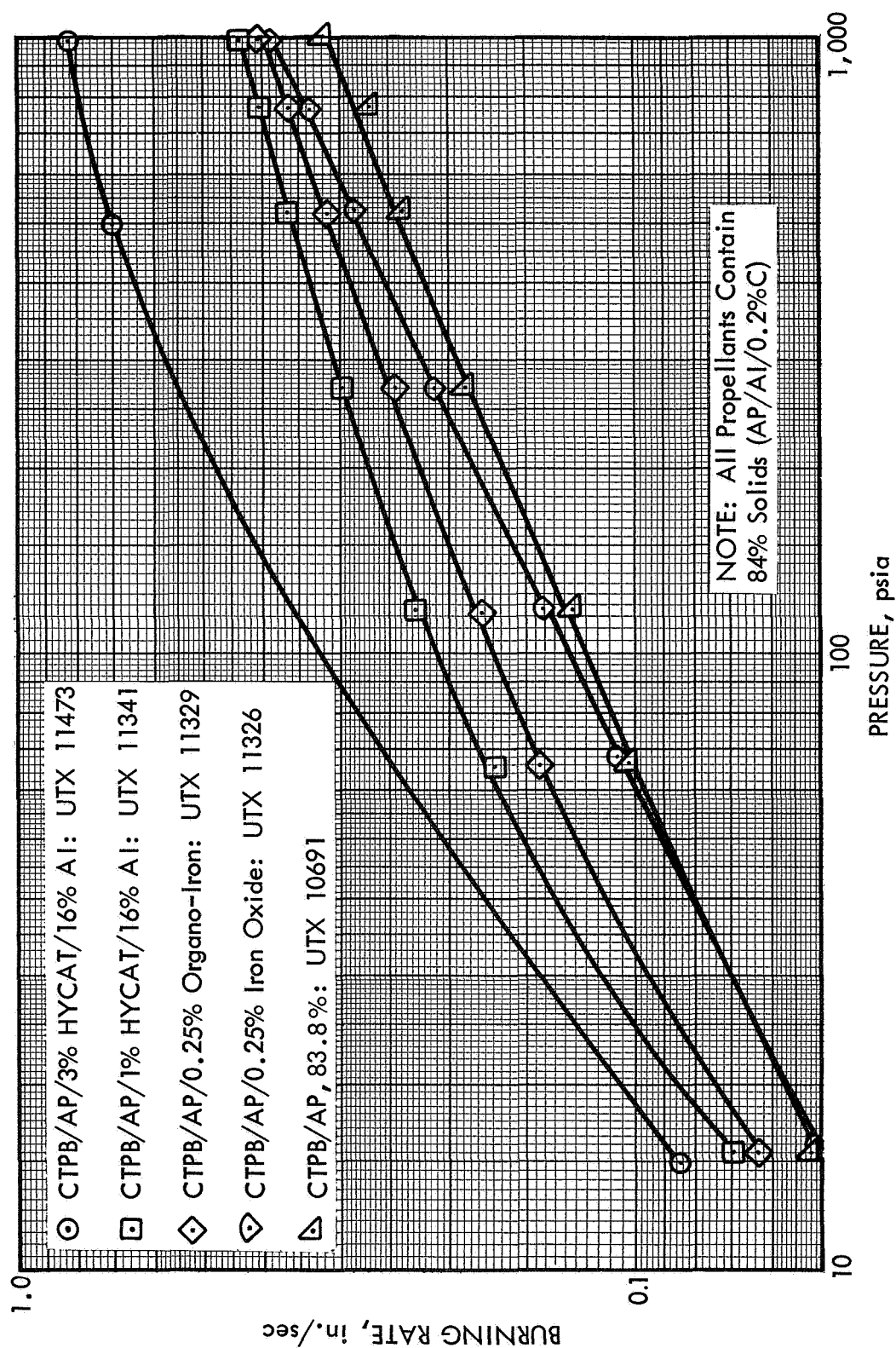


Figure 13. CTPB Catalyzed Propellant Burning Rates

90477

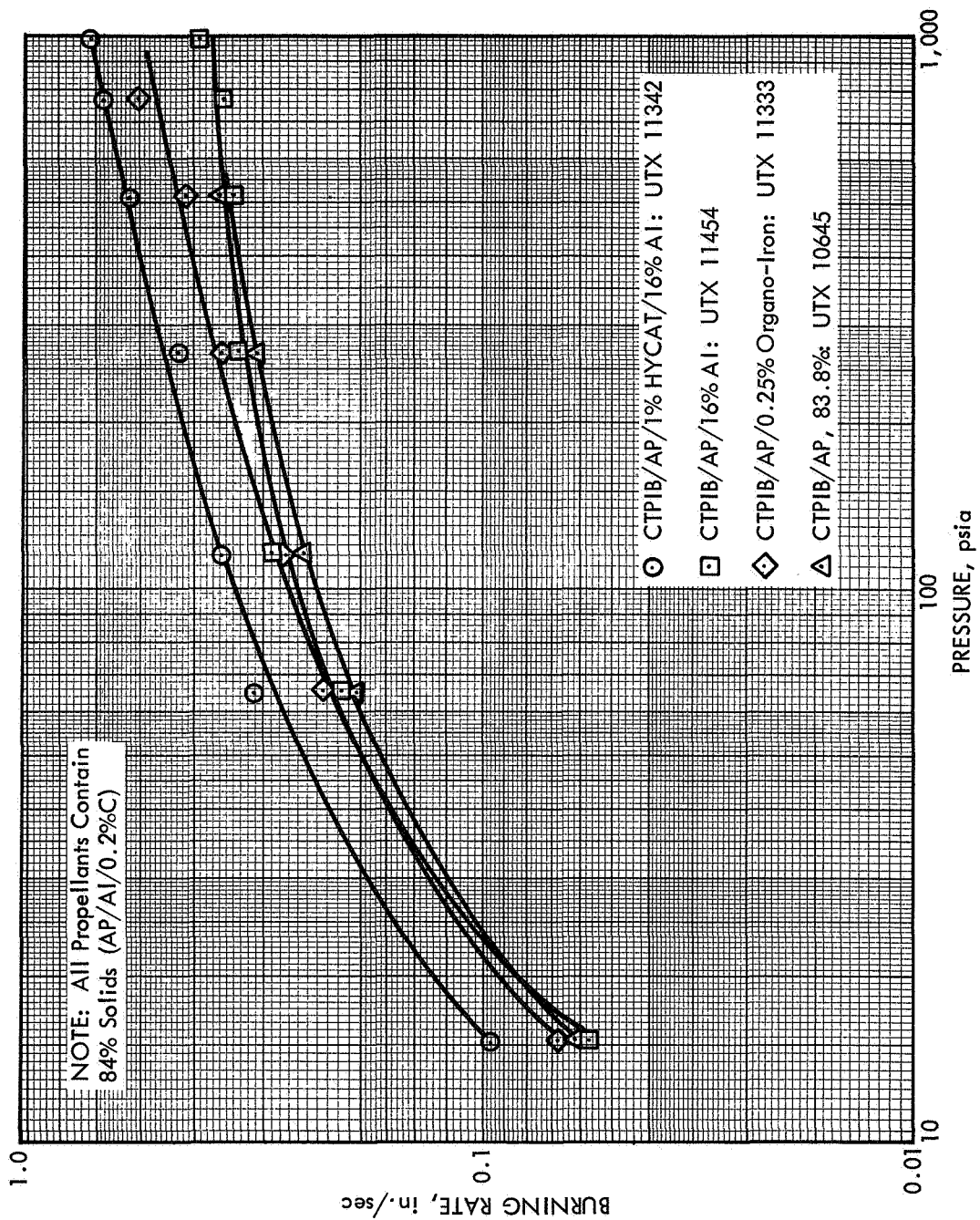


Figure 14. CTPIB Catalyzed Propellant Burning Rates

TABLE VII
PROPELLANT THERMODYNAMIC CONSTANTS

Formulation	1,000 psia		100 psia		14.7 psia	
	<u>c*</u> , ft/sec	<u>T_f</u> , °K	<u>c*</u>	<u>T_f</u>	<u>c*</u>	<u>T_f</u>
CTPB/83.8% AP (10691)	4,965	2,799	4,949	2,723	4,916	2,624
CTPB/80% AP (11327)	4,780	2,438	4,778	2,419	4,775	2,383
CTPB/4% Aluminum (11317)	5,042	2,931	5,016	2,833	4,970	2,715
CTPB/16% Aluminum (11325)	5,209	3,266	5,145	3,096	5,067	2,927
PU/83.3% AP (10661)	4,974	2,936	4,927	2,803	4,863	2,667
CTPIB/83.8% AP (10645)	4,844	2,596	4,839	2,558	4,828	2,497
CTPIB (14.5% Cl/83.8% AP (11315))	4,888	2,714	4,877	2,653	4,852	2,569
CTPIB/4% Aluminum (11316)	4,934	2,732	4,924	2,676	4,900	2,595
CTPIB/16% Aluminum (11454)	5,148	3,107	5,103	2,977	5,040	2,835

EXPERIMENTAL RESULTS

For the purpose of presentation, the experimental results of this program have been divided into three categories: (1) a summary of the experimental \dot{P} characterization tests of the different propellants, (2) the results of a series of reignition studies, and (3) a discussion of the high-speed film studies. Included in the \dot{P} studies summary are the results obtained with each of the three types of motors.

Depressurization Studies

Binder/Curative Effects - The combustion termination characteristics of the three reference propellants, which correspond to the three binder systems, were evaluated during this program using the 1-lb slab motor described in an earlier section of this report. These formulations were equivalent to the propellants which were characterized under Contract No. NAS 1-6601 with the exception that 0.2% carbon was included in the new formulations in place of the same quantity of AP. This evaluation permitted comparison of the \dot{P} results with motors of different geometries; and it eliminated the uncertainty in comparison of results from addition of the carbon black and the use of different lots of binder polymer which might influence termination behavior. The combustion termination characteristics of the three propellants are depicted in figures 15, 16, and 17, wherein the initial rate of depressurization is shown as a function of the initial or steady-state motor pressure. The lines represent the critical conditions, in that depressurization rates above the line result in combustion termination, while rates below the critical line represent nontermination or reignition.

In addition to the slab motor data, the results obtained using the window motor are shown. This motor has approximately one-fifth the motor volume of the larger slab motor. The results obtained with the two motors agree within the experimental error associated with either system, thus demonstrating a lack of motor volume effect between these relatively large-volume, small grain motors. Also shown are several data points obtained when, as a result of mechanical failures, the initial pressurization of the motor caused the burst disc to rupture and the motor to be exhausted early. In these instances (designated short runs in the figures), the resulting rate of depressurization, though normally sufficient for termination, failed to cause combustion extinguishment. This is interpreted to be the result of grain heat soak during ignition which normally would not be of importance. These data do indicate the possibility of marginal operation if a multiple start-restart motor were to be pulsed rapidly. Both short burn times and short times between pulsing could increase the depressurization requirements for propellant termination.

As may be noted, the CTPB propellant was most difficult to terminate, the polyurethane propellant was intermediate, and the CTPIB propellant had the lowest termination requirements. In addition to having different termination limits, qualitative physical differences were evident. The polyurethane propellant exhibited poor interfacial bonding between the fuel and AP crystals, and any cutting or machining of the propellant resulted in loss of crystals from the cut surface. The CTPB propellant had a plastic consistency, while the polyurethane and CTPIB propellants were much harder.

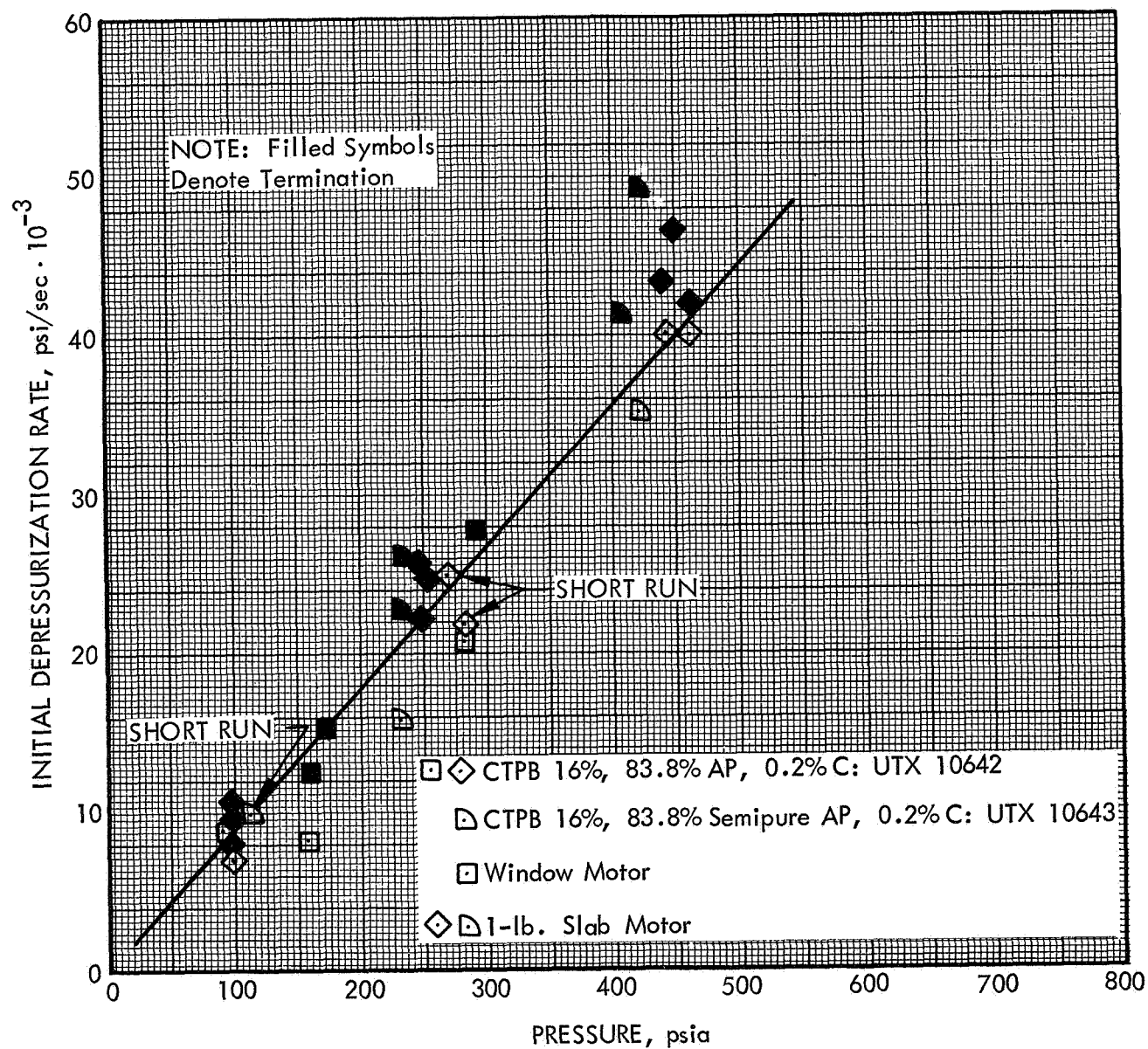


Figure 15. Comparison of Window Motor and Slab Motor
CTPB/83.8% AP Propellant

90479

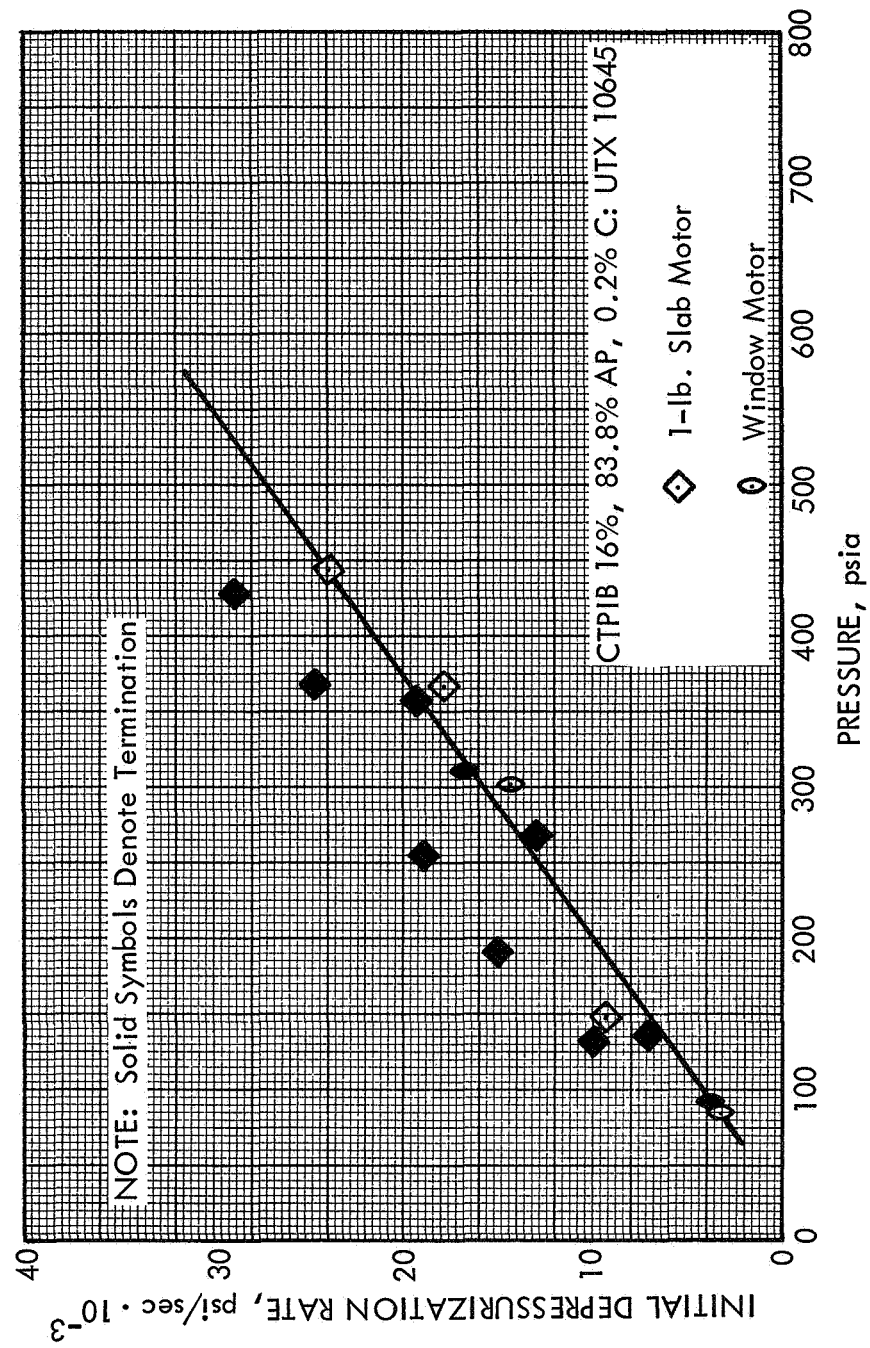


Figure 16. Comparison of Window Motor and Slab Motor
CTPIB/83.8% AP Propellant Extinguishment Characteristics

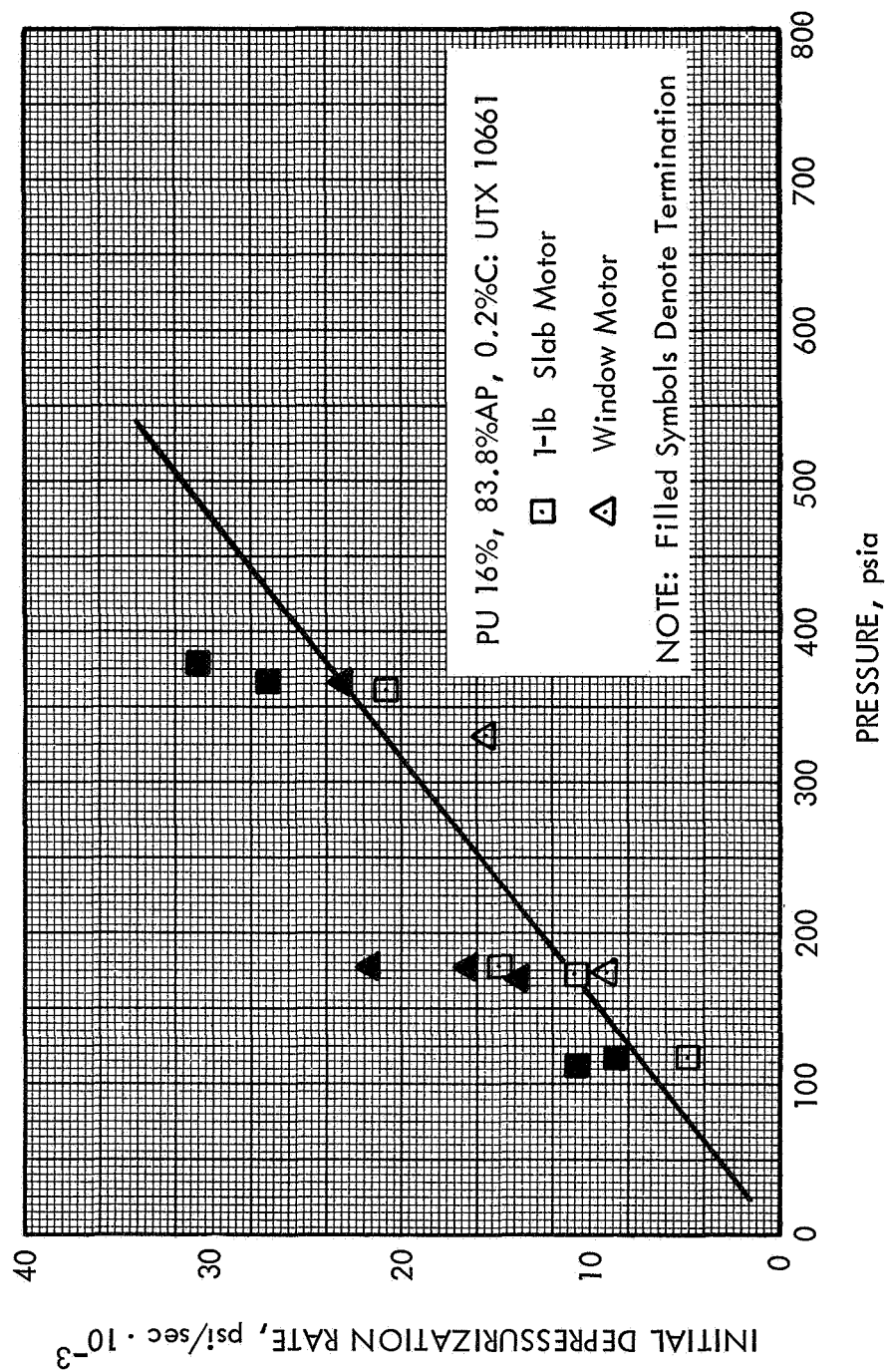


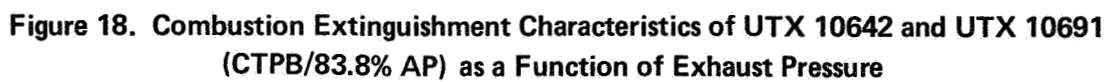
Figure 17. Comparison of Window Motor and Slab Motor
PU/83.8% AP Propellant Extinguishment

Photomicrographs of several terminated propellant surfaces also revealed differences in the decomposition and combustion behavior of the propellants. The CTPB propellant surfaces had a glassy appearance in the areas around the large-particle AP crystals. In these areas the polymer appeared to have either melted or thermally polymerized, producing a smooth glossy surface. Neither the polyurethane or CTPIB propellant surfaces had this appearance. A distinctive characteristic of the CTPIB propellant surfaces was the presence of round balls of once-molten tricalcium phosphate. (The AP used for these studies contained 0.2% TCP (mp 1,620°C) which is added to prevent caking and agglomeration of the AP crystals.) No TCP balls were in evidence on the CTPB- and polyurethane-terminated grain surfaces. The presence of the TCP balls on the CTPIB surface may be the result of the lower burning rate of the CTPIB propellant, or more likely, an indicator of combustion differences between the three types of propellants. It is difficult to assess whether or not the molten TCP balls have a perturbing effect upon combustion behavior. The \dot{P} results obtained with a CTPB formulation containing no TCP (UTX 10643) are shown in figure 15. By comparison, it can be seen that the presence of TCP did not affect the combustion termination characteristics of the basic propellant.

Upon completion of the 1-lb slab motor and window motor comparison studies, the basic propellants and the other propellants described previously were characterized with the window motor as a function of exhaust pressure level. Motor firings at both atmospheric and vacuum exhaust levels were conducted. The test results of the three basic formulations — UTX 10691 and its equivalent, UTX 10642 (CTPB/AP); UTX 10645 (CTPIB/AP); and UTX 10661 (polyurethane/AP) — are shown in figures 18, 19, and 20. (The numbers beside the data points are the ratio of final throat area to initial throat area). The CTPIB formulation UTX 10691 is the same as UTX 10642 with the only exception being the epoxy polymer used for crosslinking. In order to improve the propellant physical properties, UTX 10642 was formulated with a different polymer. As shown in figure 18, the epoxide polymer has little effect upon termination behavior.

The results shown in figures 18 and 19 indicate that there is a marked influence of exhaust pressure level upon the ease of extinguishment of the CTPB system, but that exhaust pressure level has little influence upon the extinguishment requirements of the CTPIB system. A number of data points shown in figure 19 do indicate that there was a greater potential for reignition of the CTPB grains, if the grains were terminated under atmospheric exhaust conditions rather than under vacuum exhaust conditions. However, this is to be expected on the basis that exhaust levels below the minimum ignition pressure will prevent reignition. Possible reasons for the difference in behavior of the two propellant systems are discussed in a later analysis section of this report.

At 100-psi initial pressure and 14.7-psia exhaust pressure, a number of the CTPB (UTX 10642) grains reignited even though the termination nozzles used were large enough to cause termination at higher initial pressures. The data recordings indicate that a chuffing-type phenomenon may have been established in the motor. It is also possible that hot combustion residue was retained on the horizontal grains, thus causing reignition. However, the reason reignition occurred following termination from 100 psia and not at higher initial pressures is not clearly defined at this time. It is possible that a vacuum exhaust pressure would have resulted in successful terminations. If



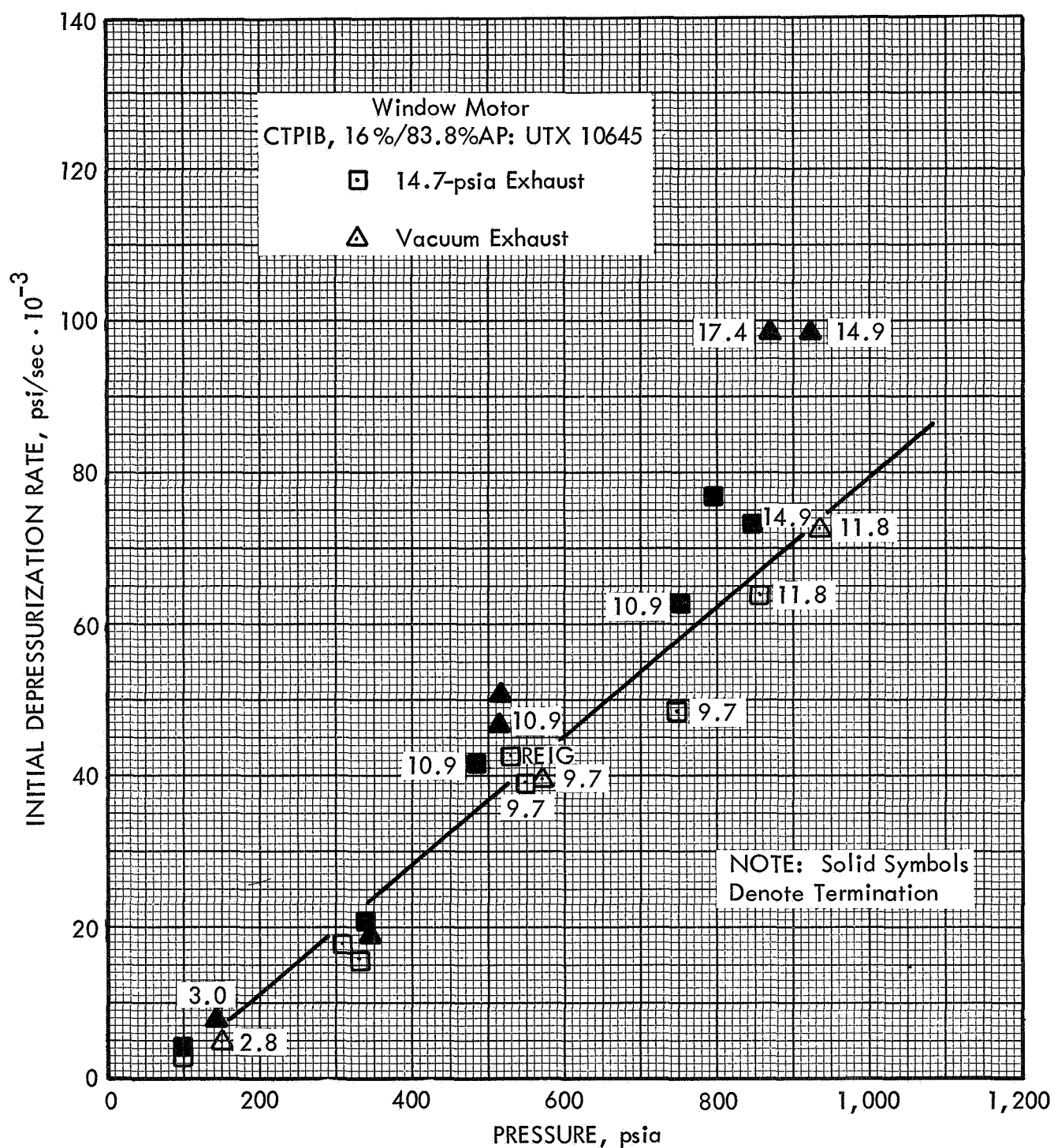


Figure 19. Combustion Extinguishment Characteristics of UTX 10645 (CTPIB/83.8% AP) as a Function of Exhaust Pressure

90483

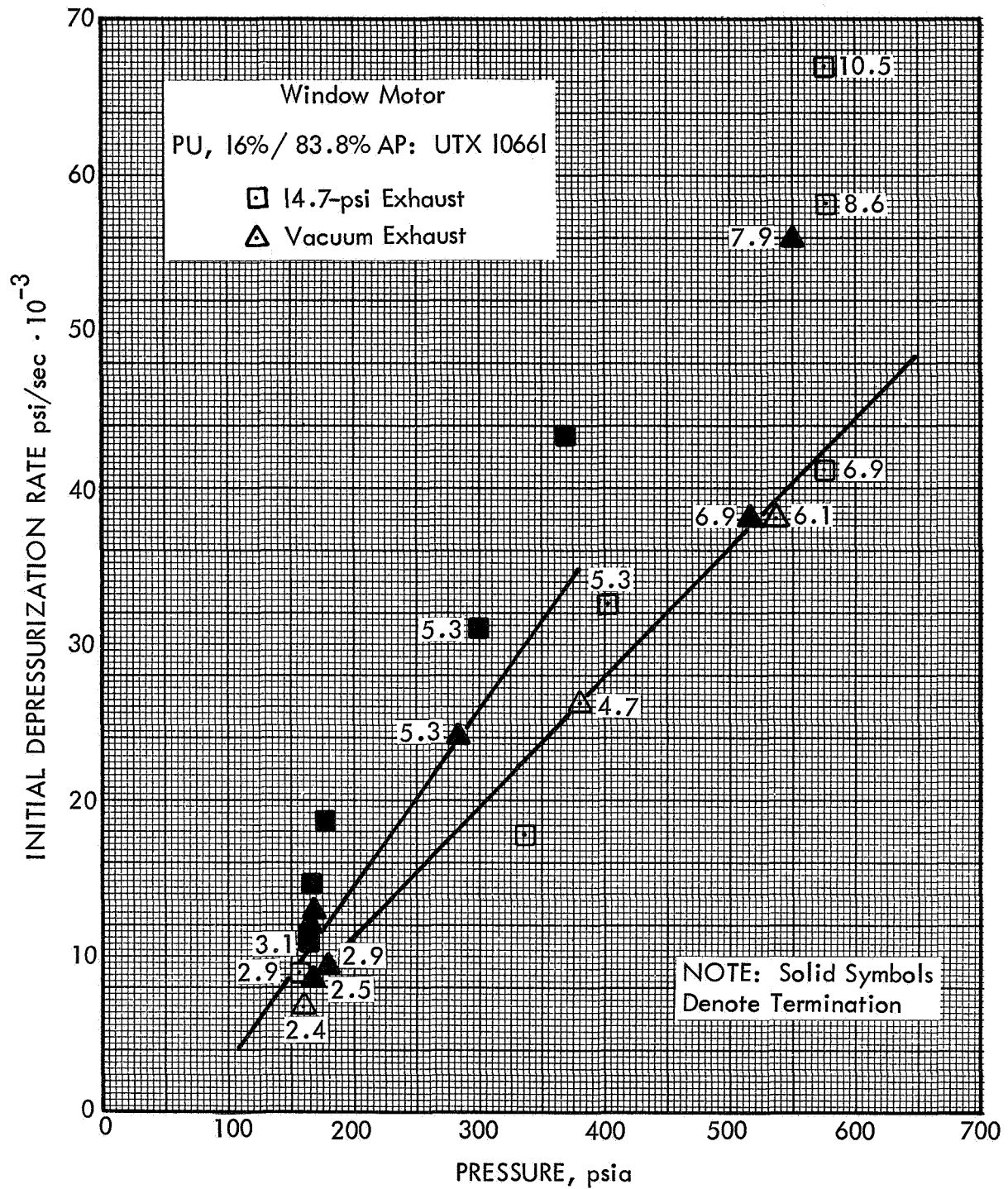


Figure 20. Combustion Extinguishment Characteristics of UTX 10661 (PU/83.8% AP) as a Function of Exhaust Pressure

90484

the motor pressure drops below the minimum ignition pressure after the grain has terminated, there is little possibility that the grain will ignite.

In the case of the polyurethane formulation, UTX 10661, the vacuum exhaust condition resulted in a small reduction of the termination requirements at 200-psi initial pressure and a large reduction at 500-to 600-psi initial pressures. While it is conceivable that nontermination could be due to reignition, the data traces did not support this possibility. Under atmospheric exhaust conditions it is possible that hot, terminated grains gasify sufficiently to permit reignition of the grain when oxygen from the air enters the motor after depressurization. However, examination of the data traces showed no interruption in burning after depressurization, such as would be necessary to permit air to enter the motor. In all instances the grains burned out at pressures above the exhaust pressure.

Traces obtained from the vacuum tests, using the polyurethane formulation and also using the CTPB and CTPIB formulations, showed that termination often occurred long after the motor pressure had fallen to the new, low value consistent with the increased nozzle area. Termination thus occurred 0.5 to 1.0 sec after depressurization by an L^* or P_{dl} type process rather than as a result of the depressurization process. At atmospheric exhaust conditions the motor pressure decayed to 1 atm and the grain continued to burn out because the L^* process could not be initiated or because the motor pressure was higher than the minimum deflagration pressure.

The possible perturbing influence of the curative system upon the termination behavior was explored by evaluation of a CTPB propellant with an all-epoxide curative (UTX 11339, a 16% CTPB, 83.8% AP system) rather than the aziridinyI curative used with the reference CTPB formulation (UTX 10691). The results obtained with the all-epoxy cured propellant are shown in figure 21. As with the reference CTPB system (UTX 10691) the exhaust pressure level had a marked influence upon ease of extinguishment. Though the termination behavior of this propellant was not well-defined at 1-atm exhaust, reducing the exhaust level from 14.7 psia to vacuum decreased the critical depressurization rate by approximately 36%. In addition to the effect of exhaust pressure, the termination requirements shown in figure 21 are nearly the same as those found for the reference propellant. Both these data and the similarity of the burning rate behavior indicate that the curative system had little effect upon extinguishment behavior.

The influence of the binder polymer to curative equivalents ratio on termination behavior was explored with the CTPIB system. A new CTPIB formulation (UTX 11314), containing 1.5 equivalents of aziridinyI curative to 1.0 equivalent of CTPIB prepolymer, was tested for comparison with the reference CTPIB system (UTX 10645) which contained an aziridinyI curative to prepolymer equivalents ratio of 1.2. Both the \dot{P} characteristics and burning rate behavior of the high equivalence formulation (UTX 11314) coincided with that observed for the base propellant system. These results, in conjunction with results of earlier studies, have shown that only those formulation variables which modify the burning rate in the pressure region of combustion extinguishment have any real effect upon combustion extinguishment behavior.

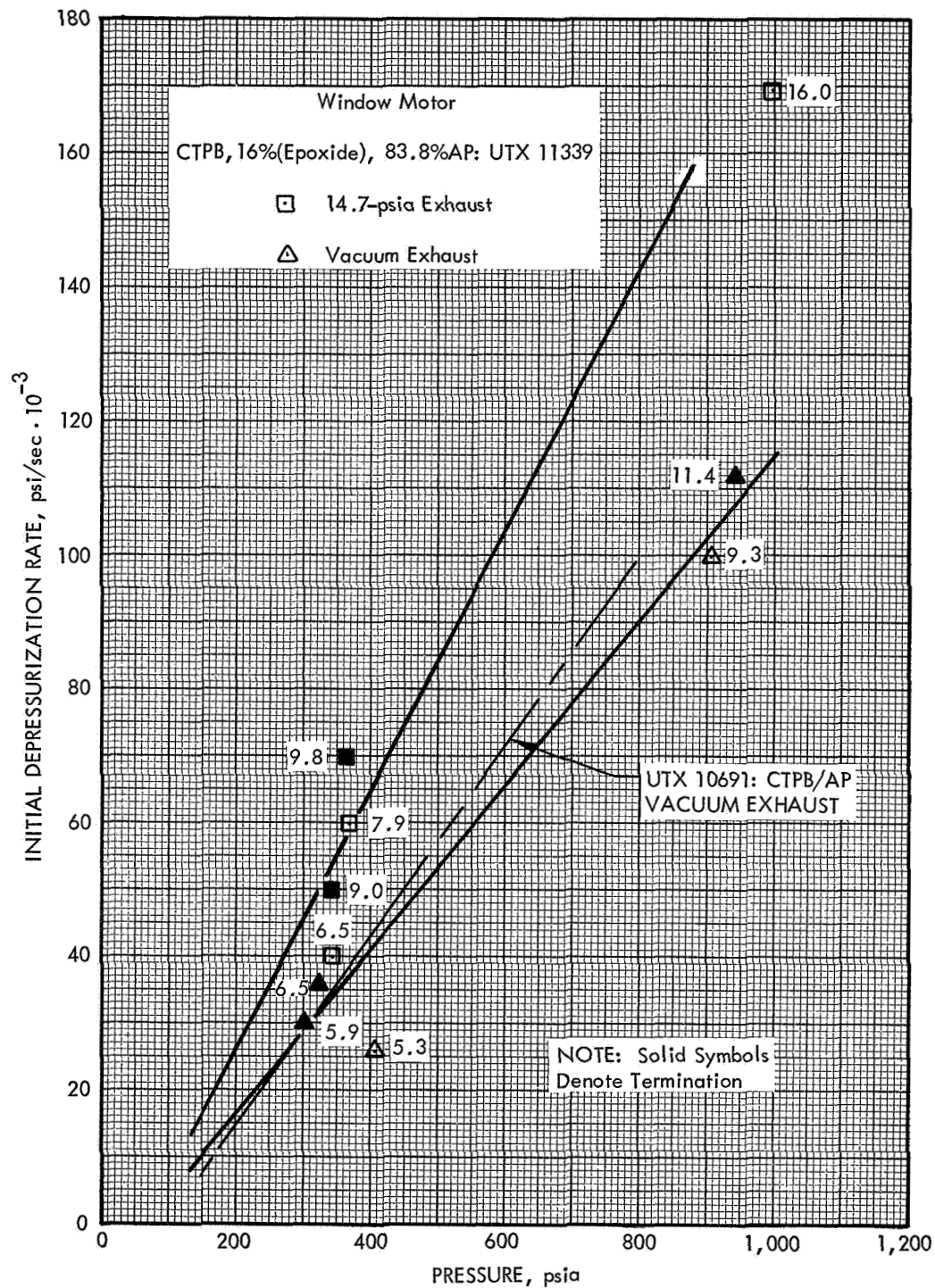


Figure 21. Combustion Extinguishment Characteristics of a CTPB-Epoxy Curative Propellant (UTX 11339)

90485

The propellant characterization and exhaust-pressure studies were all performed using single, neutral-burning slab grains 1-in. wide and 5-in. long. In order to determine what effect motor geometry might have upon termination behavior, a number of tests were conducted with the base CTPIB propellant (UTX 10645) using two opposed slab grains 5/32 in. apart. As with the single grains, the double grains were ignited with an oxygen/methane hot gas igniter firing for 0.4 sec. Results of the tests conducted at 1 atm of pressure are shown in figure 22, where it can be seen that the two parallel grain configurations resulted in a significant increase in the termination requirements. Because the initial depressurization rate in any particular motor is independent of grain area and the depressurization path is a function of grain area, different critical initial depressurization rates were found for the two grain orientations. After initial depressurization in the motor with two parallel grains, the larger burning area reduced the rate of depressurization at any pressure when compared with the rates achieved in the single grain tests. Thus, in order to achieve the pressure(s) and depressurization rate(s) required for combustion extinguishment, much larger termination nozzles and consequently much higher initial depressurization rates were required for extinguishment when two parallel grains were used.

The results obtained using 1.75-in.-diameter end-burning grains are also shown in figure 22. Though these grains had one-half the surface area of single slab grains, a large number of grains reignited at initial depressurization rates high enough to ensure complete quenching of the large slab grains. While these results may indicate a geometry effect, it is likely that reignition was caused by the residue from the hot-wire igniter system used for ignition of the end-burning grains. Photographic studies indicated that reignition was often caused by the hot-igniter leads or igniter lead insulation charred by the firing.

The effect of grain geometry was explored further using the swing-nozzle motor described previously. Both the base CTPIB (UTX 10645) and CTPB (UTX 10691) formulations were characterized, using 5- and 15-in.-long grains in the swing-nozzle motor which was fired into the atmosphere. The steady-state nozzles were sized to yield nominal motor pressures of 500 and 1,000 psi at the time of depressurization which was programmed to occur after a burn time of about 0.8 sec. The results of these tests are shown in figures 23 and 24 in the form of initial depressurization rate plotted versus steady-state motor pressure at the time of depressurization. The numbers beside the data points are the ratios of termination nozzle area to steady-state nozzle area. Comparison of these data with those shown in figures 18 and 19 shows the initial depressurization rates required for termination to be greater than those found for the window motor. There was also relatively little difference between the initial depressurization rates required to terminate the two types of propellants (CTPB and CTPIB) in the swing-nozzle motor, which was in contrast to the data obtained with the window motor. Comparison of the 5- and 15-in. grain length data also shows little difference in combustion extinguishment requirements for this difference in grain length.

The difference of critical depressurization rates for the swing-nozzle and window motor was paralleled by a difference of extinguishment conditions at the point of extinguishment in the two motors. Analysis of the data traces showed that extinguishment occurred at lower depressurization rates and lower pressures in the window motor than in the swing-nozzle motor. While extinguishment in the swing-nozzle motor occurred at 100 to 200 psi,

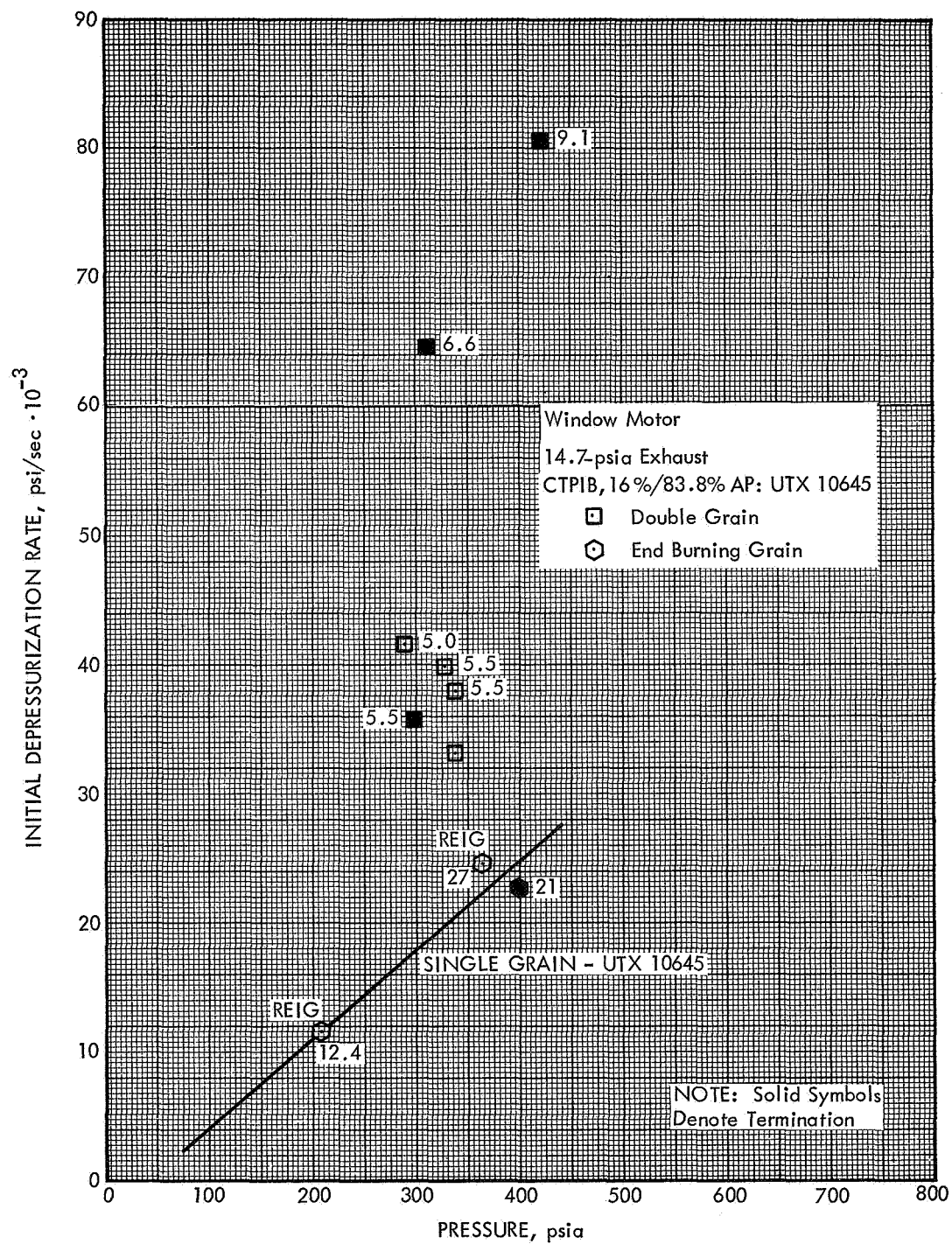


Figure 22. Effects of Grain Geometry Upon the Extinguishment Characteristics of UTX 10645 (CTPIB/83.8% AP)

90486

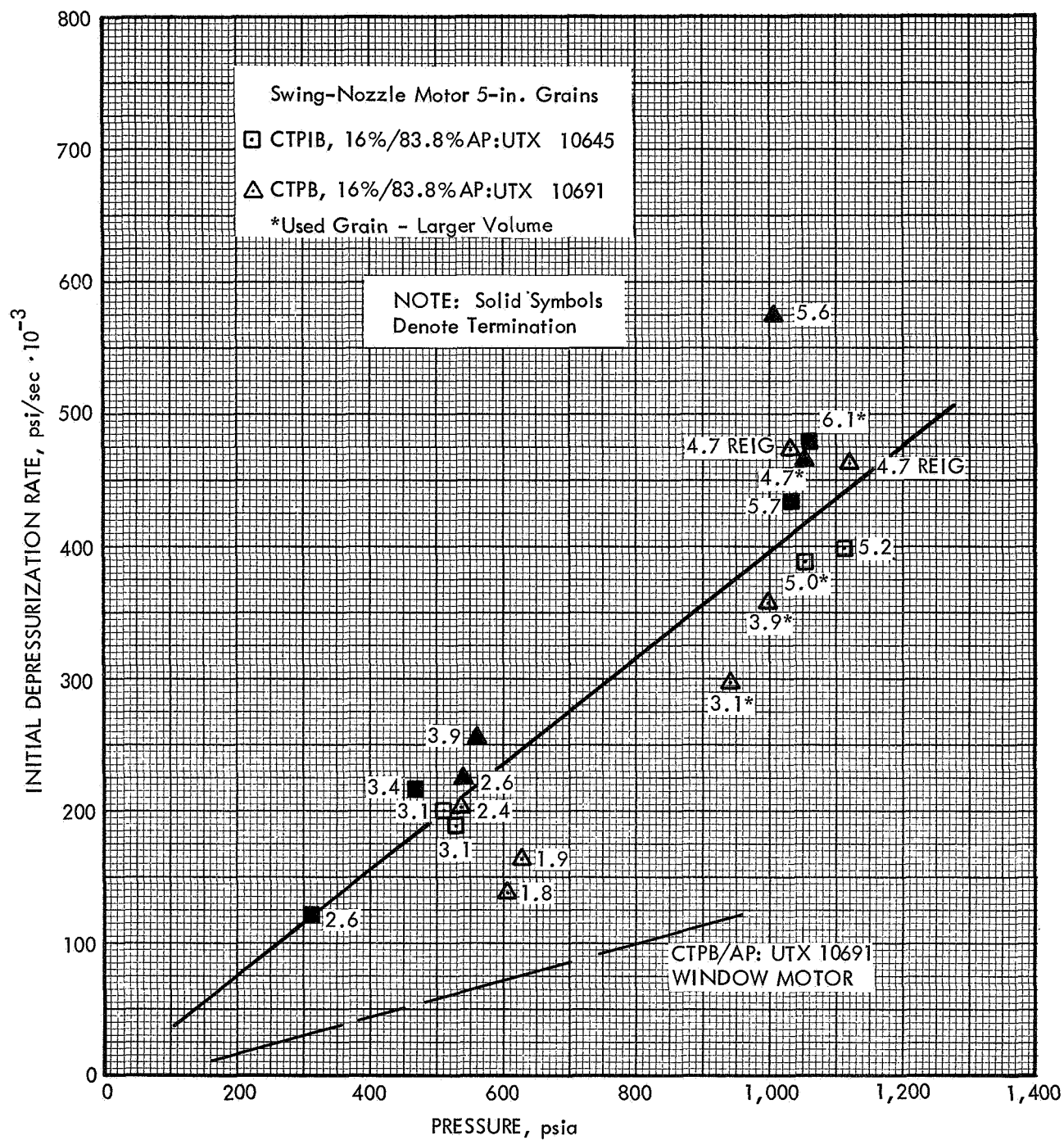


Figure 23. Swing-Nozzle Motor (5-in. Grain) Extinguishment Data for CTPB/AP (UTX 10691) and CTPIB/AP (UTX 10645) Propellants

90487

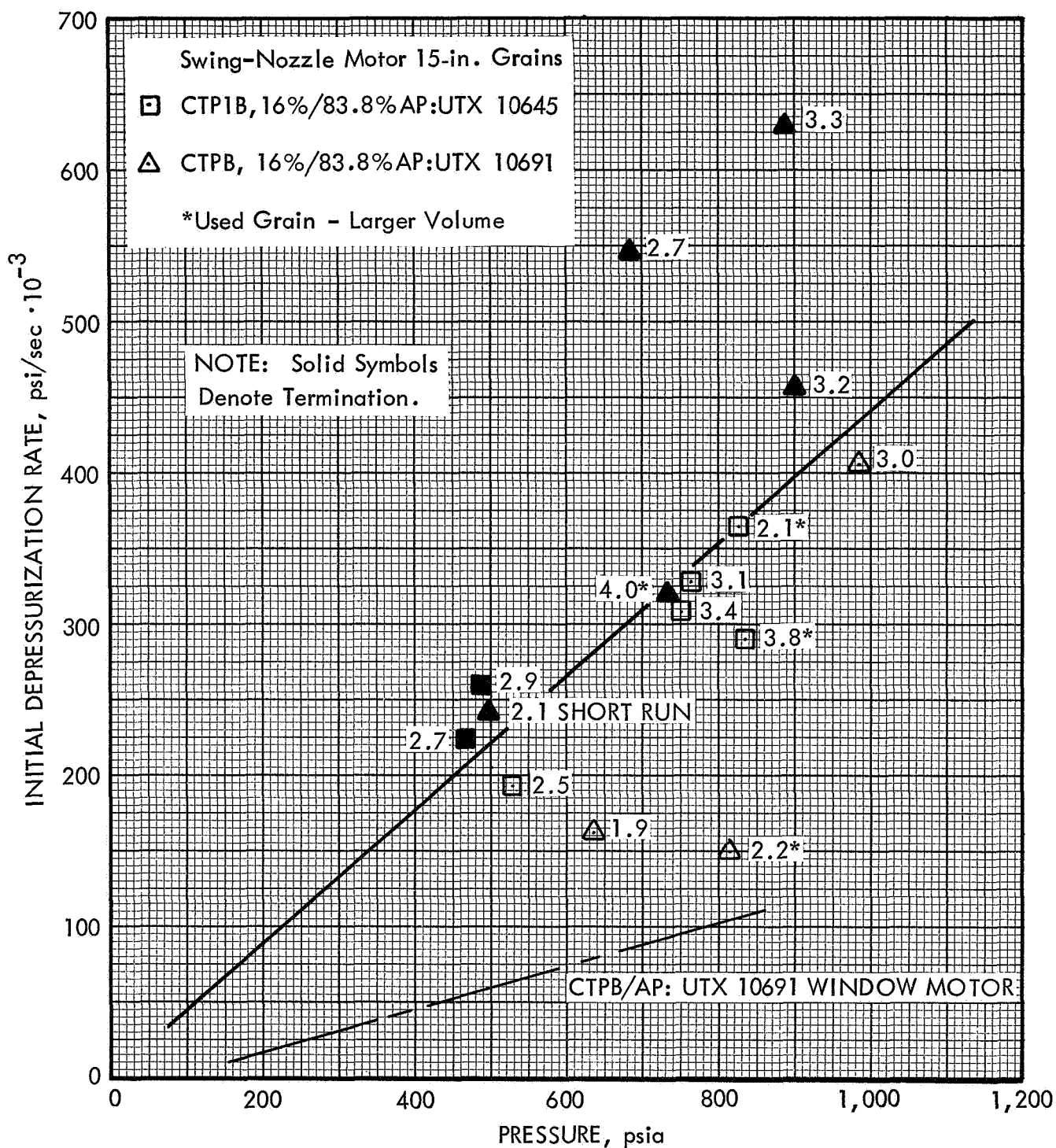


Figure 24. Swing-Nozzle Motor (15-in. Grain) Extinguishment Data for CTPB/AP (UTX 10691) and CTP1B/AP (UTX 10645) Propellants

90488

extinguishment in the window motor occurred at pressures of the order of 15 to 25 psia. The possible significance of these results are discussed in a later section.

As indicated earlier, a number of propellant variations based on the CTPIB binder were characterized in the course of the program. Two sterilizable systems, both based on the CTPIB system were investigated. The first formulation contained no aluminum but did contain 84% AP. The second formulation contained 68% AP and 16% aluminum. Both formulations were sterilized over a 2-week period by heating the grains at 275°F for six periods of 53 hr each. Results obtained using these formulations are shown in figure 25. The \dot{P} requirements for the nonaluminized formulation were determined both prior to and following the sterilization procedure, while the \dot{P} requirements for the aluminized formulation were only determined after sterilization.

Prior to sterilization, the \dot{P} requirements of the nonaluminized propellant (UTX 10720) were essentially equivalent to those of the reference CTPIB formulation (UTX 10645). After sterilization the \dot{P} requirements were found to be double those determined previously. A possible explanation for the increase is a loss of low molecular weight material during the sterilization procedure, which would cause an increase in the effective binder decomposition temperature and possibly reduce the endothermic heat of decomposition and increase the O/F ratio of the propellant. Any of these factors might result in an increase of the termination requirements.

While less well defined, the \dot{P} requirements of the sterilized aluminized system were essentially the same as those of the nonaluminized formulation after sterilization. Pressure-time traces were not obtained for the two tests depicted by the underlined points shown on figure 25, but on the basis of the nozzle sizes, estimates of the results were made. Based on previous studies⁽⁷⁾ the termination requirements of the aluminized system prior to sterilization should be about the same as those of the nonaluminized, nonsterilized formulation. While an increase of the extinguishment requirements is indicated, the lack of data for the aluminized propellant prior to sterilization and the limited data after sterilization make it difficult to define the effect of the sterilization process.

The effect of the binder chlorine content on termination susceptibility was evaluated using the chlorinated CTPIB binder-based propellants described earlier. As shown in figure 26, the termination requirements were not reduced markedly by this binder modification and only minor differences were noted in termination behavior. At the two lower concentration levels there was a slight reduction of the termination requirements. A 0.312-in.-diameter nozzle was sufficient for termination of the chlorinated grains, and a 0.332-in.-diameter nozzle was the smallest nozzle which caused consistent termination of the nonchlorinated CTPIB propellant (UTX 10645). Introduction of the higher chlorine concentration increased the termination requirements. At the highest level, it is possible that the chlorine effectively increased the O/F ratio of the propellant through a replacement of hydrogen atoms, thereby increasing the termination requirements. As an adjunct to another program⁽²¹⁾ the ignition characteristics of the three formulations were determined using an arc-image furnace. It was found that the ignition behavior of the chlorinated and nonchlorinated systems were nearly identical.

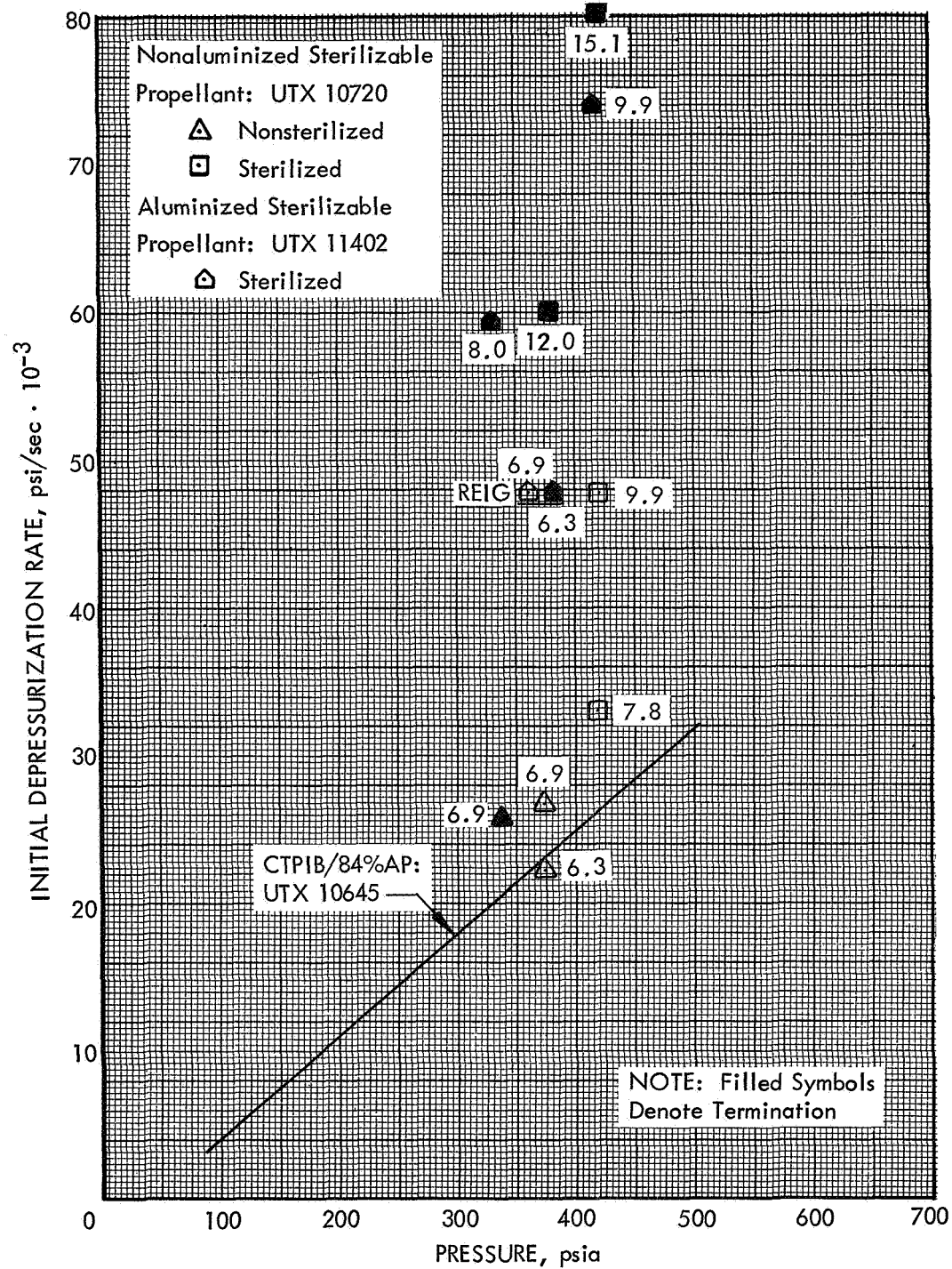


Figure 25. Combustion Extinguishment Characteristics of Sterilizable CTPIB/AP Propellants

90489

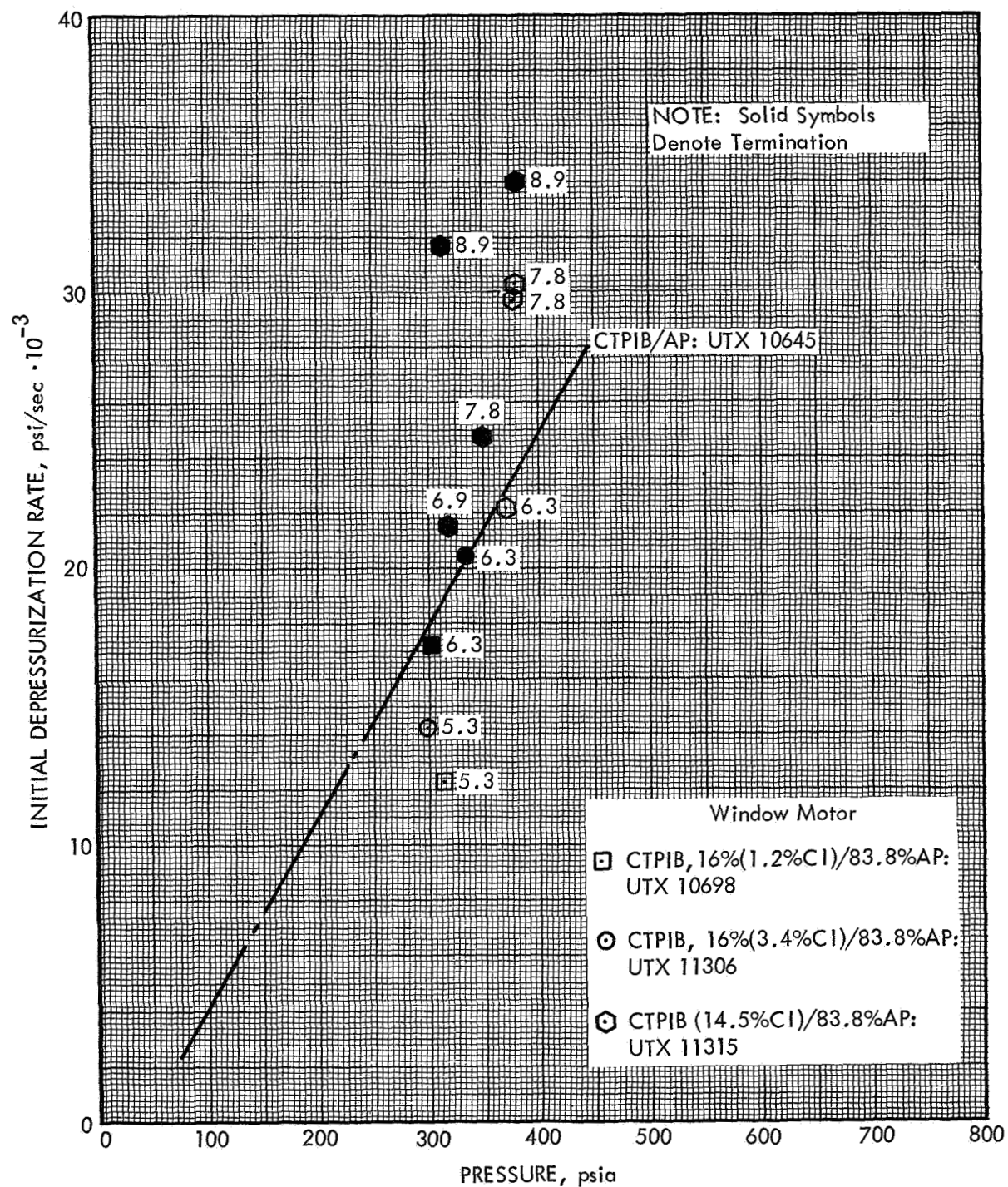


Figure 26. Combustion Extinguishment Characteristics of Chlorinated CTPIB/AP Propellants

90490

The polyepichlorohydrin system, which has a higher chlorine content than the chlorinated CTPIB propellants, failed to demonstrate reduced termination requirements. Limited tests, using this system, resulted in termination requirements significantly greater than those found for the CTPIB propellant system; this is shown by the data of figure 27. Depressurization rates which caused termination of the CTPIB propellant UTX 10645 (represented by the solid line in figure 27) were not sufficient to cause termination of the polyepichlorohydrin grains. On the basis of these results, this path of investigation was not pursued further.

Oxidizer Loading Studies - Reduction in the burning rate of the 79.8% AP/CTPB formulation (UTX 11327), as discussed earlier, was also reflected by a reduction of the critical depressurization limits with reduced AP loading from 83.8% to 79.8% AP at both atmospheric and vacuum exhaust pressure levels. The data of figure 28, when compared with that of the base system, show a reduction of the critical depressurization rate of approximately 30% at an initial motor pressure of 800 psi. While this reduction is significant, it is less than that found for the CTPIB system in the course of studies conducted under Contract No. NAS 1-6601. Reducing the oxidizer level from 84% to 80% in the CTPIB system reduced the termination requirements by 50%. The data of figure 28 also show that a reduction in the exhaust level from atmospheric (14.7 psi) to vacuum conditions (≈ 0.003 atm) reduced the critical depressurization limits by about 30% at an initial motor pressure of 800 psi.

Reversing the coarse-to-fine oxidizer ratio in the CTPIB system from 65:35 to 35:65 resulted in a slight increase of the termination requirements at both atmospheric and vacuum exhaust conditions. As shown in figure 29, the increased fines concentration in the CTPIB, 83.8% AP propellant (UTX 11336), increased the termination requirements. However, it did not alter the general behavior of the CTPIB system because, in both the UTX 11336 and the reference CTPIB propellant (UTX 10645), termination requirements were unaffected by exhaust pressure level.

Aluminum Loading Studies - The \dot{P} characteristics of the four aluminized, noncatalyzed propellants were evaluated at both atmospheric and vacuum exhaust conditions. Examination of the results obtained with the two CTPB formulations, as shown in figures 30 and 31, demonstrates that the substitution of 4% aluminum for AP in the TX 11317 propellant system did not influence the termination requirements (comparison of UTX 11317 with UTX 10691), but the substitution of 16% aluminum (UTX 11325) decreased the termination requirements. Under vacuum exhaust conditions and 800-psi initial pressure, the nonaluminized CTPB propellant (UTX 10691) had a critical depressurization rate of about 1×10^5 psi/sec with a 0.406-in.-diameter termination nozzle required for extinction. Under similar conditions, the CTPB propellant (UTX 11317) containing 4% aluminum also required a depressurization rate of about 1×10^5 psi/sec and a 0.406-in.-diameter termination nozzle for extinction. UTX 11325 containing 16% aluminum required a depressurization rate of approximately 7.5×10^4 psi/sec and termination nozzle of about 0.358 in. in diameter for successful extinction at 800 psi and vacuum exhaust conditions.

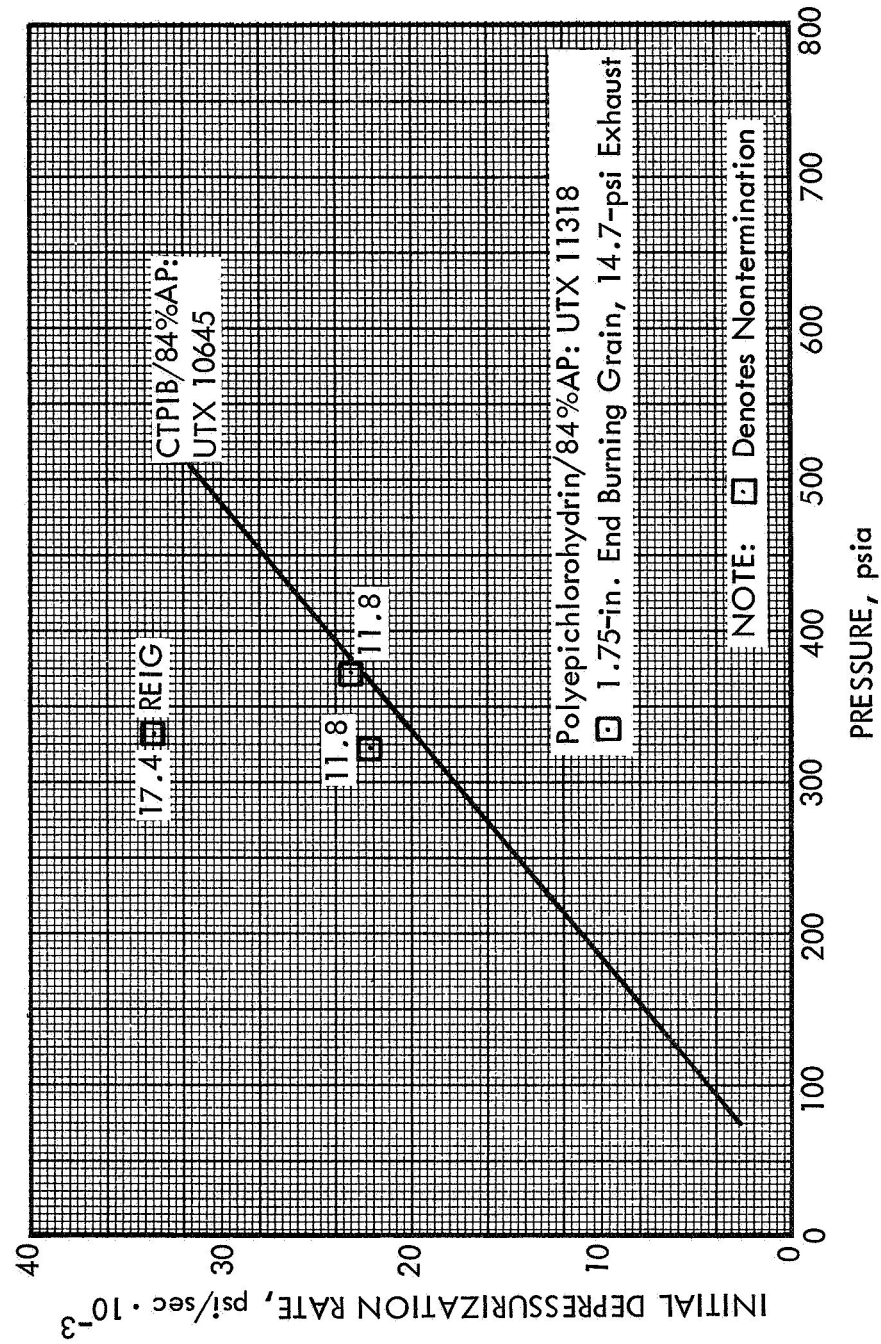


Figure 27. Combustion Extinguishment Characteristics of Polyepichlorohydrin/AP Propellant

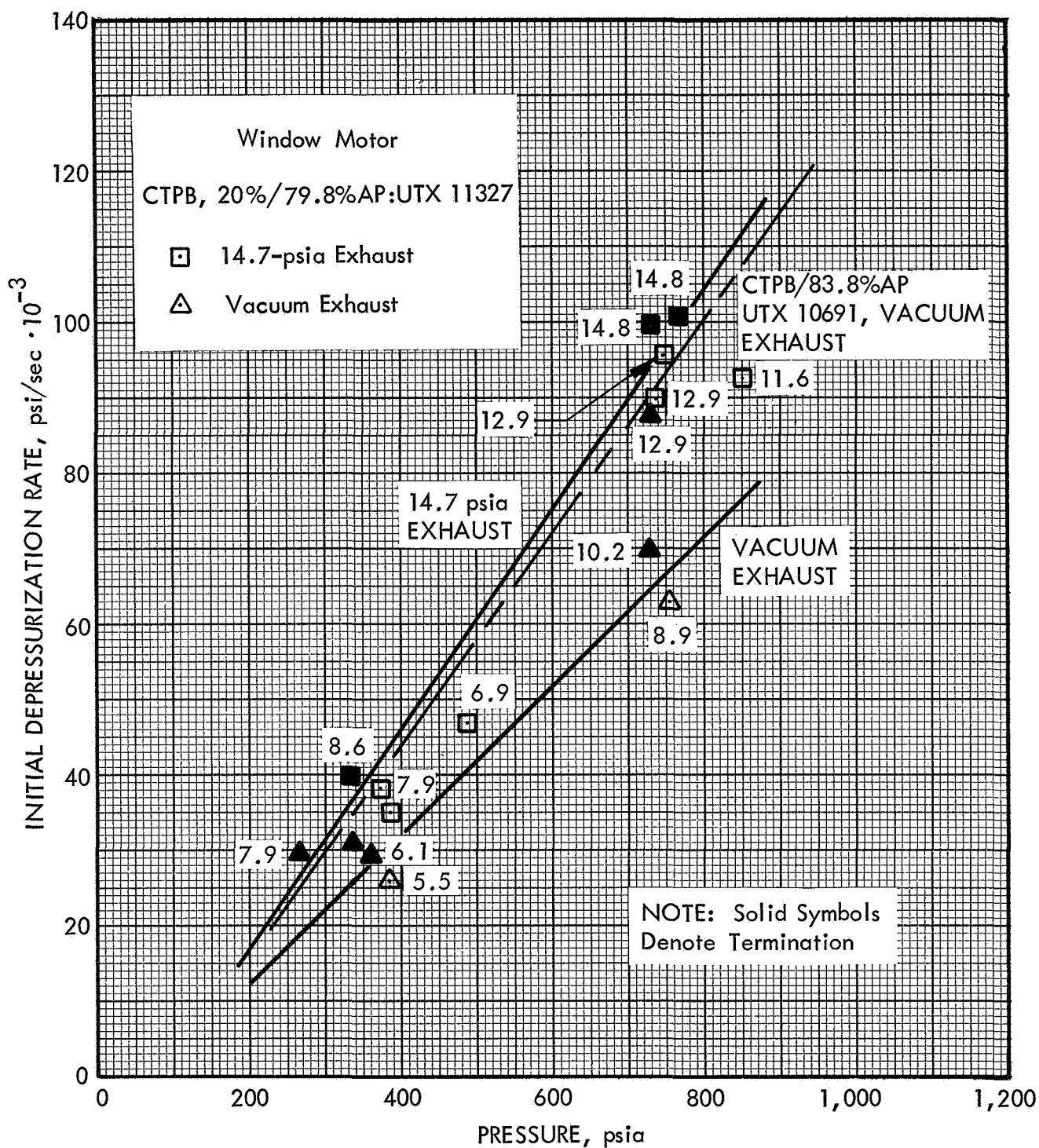


Figure 28. Combustion Extinguishment Characteristics of CTPB/80% AP Propellant (UTX 11327) as a Function of Exhaust Level

90492

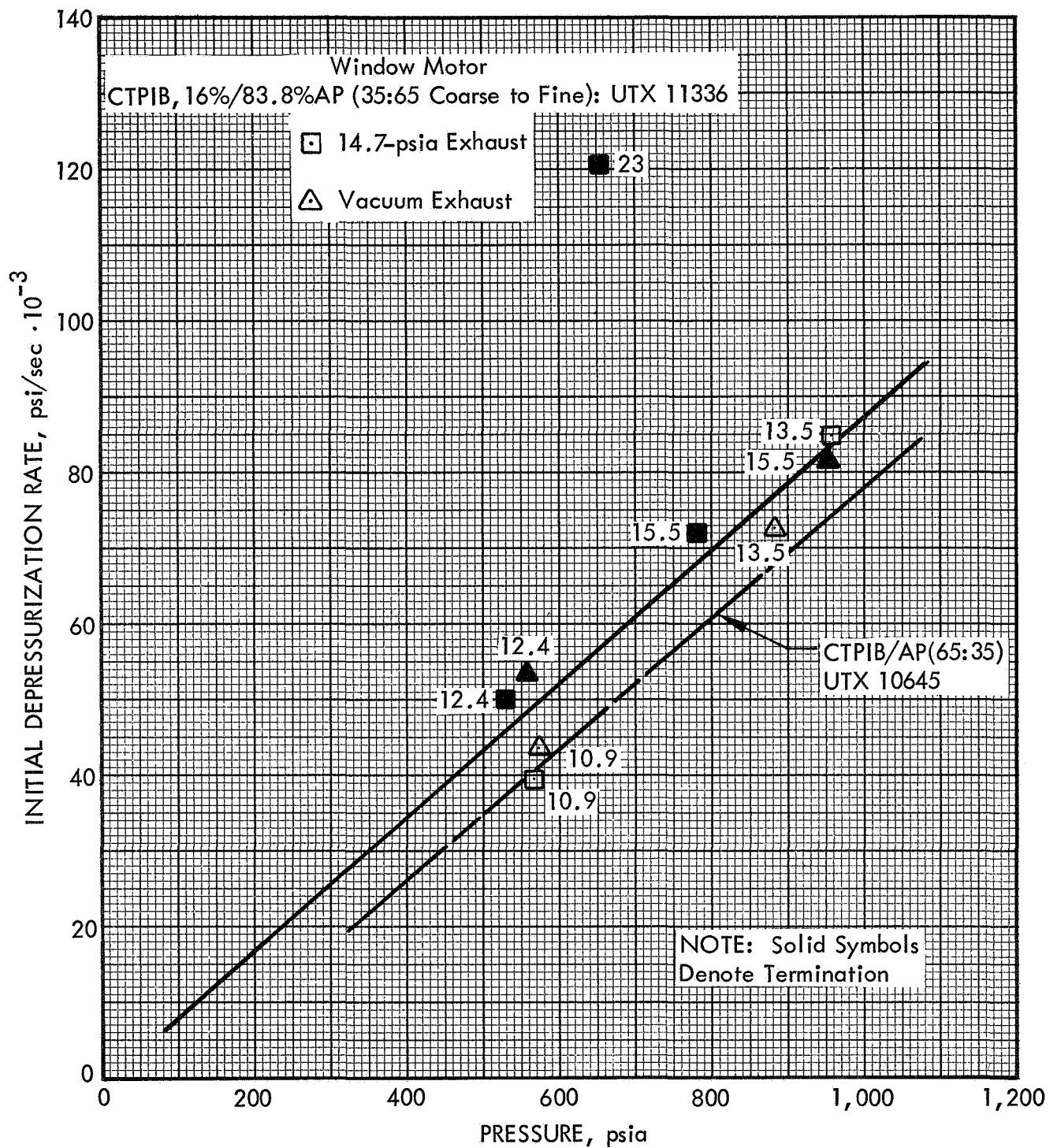


Figure 29. Combustion Extinguishment Characteristics of CTPIB/83.8% AP, 35 to 65 Coarse to Fine Ratio Propellant (UTX 11336)

90493

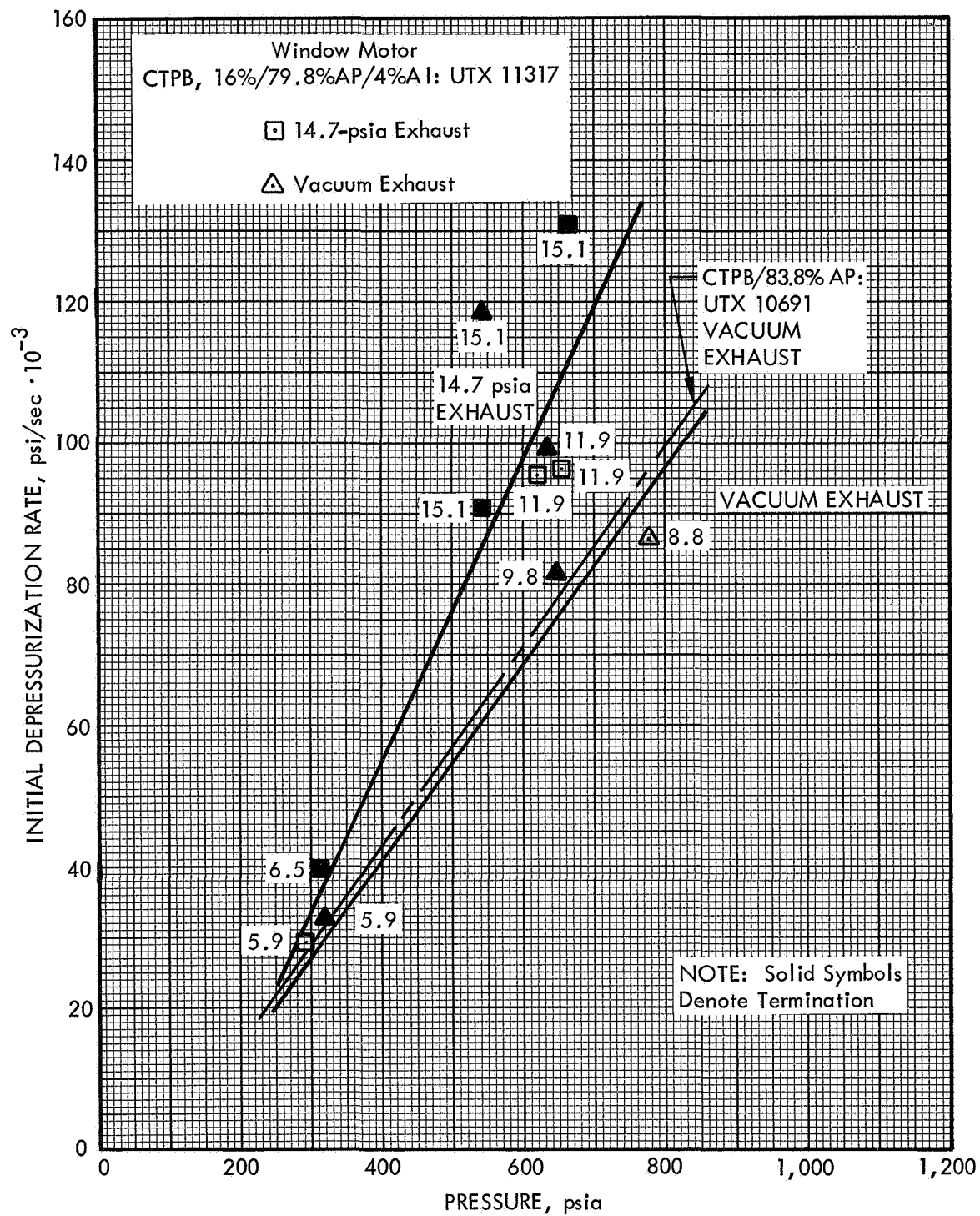


Figure 30. Combustion Extinguishment Characteristics of CTPB/AP/4% Aluminum Propellant (UTX 11317)

90494

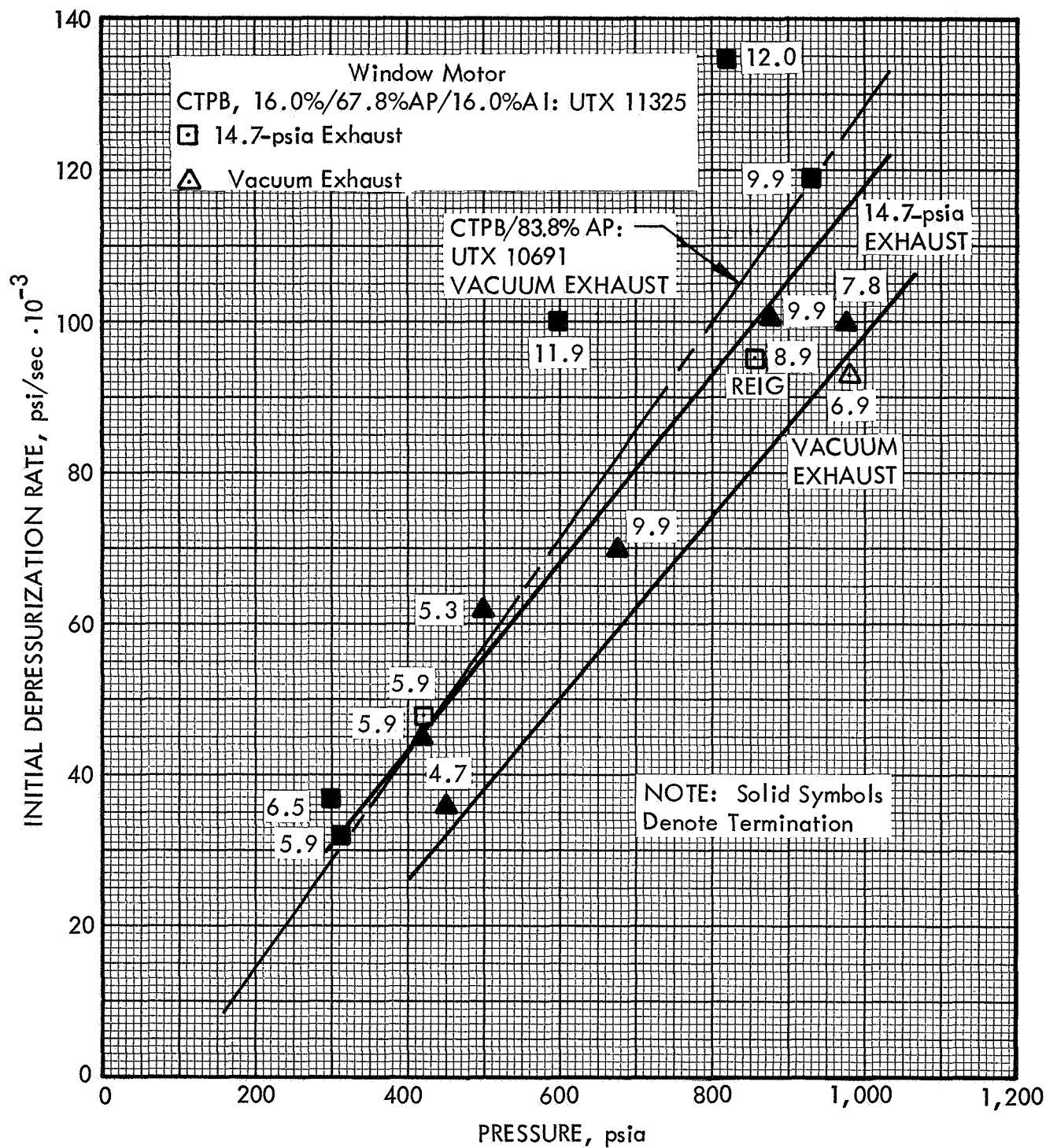


Figure 31. Combustion Extinguishment Characteristics of CTPB/AP/16% Aluminum Propellant (UTX 11325)

90495

The CTPIB system showed a slight reduction of termination requirements with aluminum loading. As shown in figure 32, the data obtained with CTPIB which contained 4% aluminum (UTX 11316) showed critical depressurization rates approximately 15% less than those found for the nonaluminized system. The 4% aluminized CTPIB propellant required a 0.312-in.-diameter termination nozzle at 800-psi initial pressure and vacuum exhaust, while UTX 10645 which contained no aluminum required a termination nozzle of 0.332 in. in diameter. Increasing the aluminum loading level to 16% (UTX 11459) in the CTPIB system decreased the termination requirements even further, as noted in figure 33. The reduction of the termination requirements coincides with a reduction of the propellant burning rate.

The data for both aluminized CTPB formulations indicate that a reduction in the exhaust pressure level also reduced the termination requirements significantly. This was not evidenced with the CTPIB systems. While there were a number of instances of reignition at the 14.7-psia exhaust level with the two CTPIB propellants, the termination requirements for atmospheric and vacuum exhaust conditions were essentially equivalent.

Swing-nozzle motor tests were also conducted with three aluminized propellants. Data obtained using the 16% aluminum/CTPB propellant (UTX 11325) are shown as a function of grain length in figure 34. Initial examination of these data indicate much higher extinguishment requirements for the aluminized system in the swing-nozzle motor in comparison to the swing-nozzle motor data obtained with the nonaluminized propellants. However, the pressure traces for many of these tests showed the exhaust level pressure decrease (14.7 psia) with a distinct pause in the combustion and subsequent reignition and burnout of pressure. High-speed film studies of these tests also revealed a definite interruption of the combustion process prior to reignition. Consequently, the higher or more stringent termination conditions required for extinguishment are not a result of formulation differences per se but are due to a difference of reignition behavior.

The possibility of grain reignition was explored further with the CTPIB/16% aluminum system (UTX 11454) and a mixed binder propellant CTPIB/CTPB/16% aluminum formulation (UTX 11337). The results for these propellants are shown in figures 35 and 36. A nitrogen purge was synchronized with the timing circuit so that the swing-nozzle motor could be purged with a moderate flow of nitrogen if the motor pressure fell below 100 psig during the depressurization cycle. As evidenced in figures 35 and 36, many of the test grains that resulted in reignition without the purge were successfully terminated by use of the purge under equivalent test conditions. The area between the two lines on figure 35 represents a zone of possible reignition. In this intermediate region, reignition will occur without the purge while complete extinguishment will be achieved with a purge. This is contrasted to continued combustion to complete burnout at conditions below the limit where the purge is effective.

The mechanism by which the purge prevented reignition (or snuffed the flame) was not established. Nitrogen flowing through the motor could act by quenching any residual combustion flame, cooling the propellant surface or any hot combustion residue, or preventing atmospheric oxygen from entering the motor after blowdown. The wide reignition zone for this motor indicates potential problems for operational motors depressurized at moderate exhaust pressures. Reignition prevention may require gaseous or liquid purging for reliability.

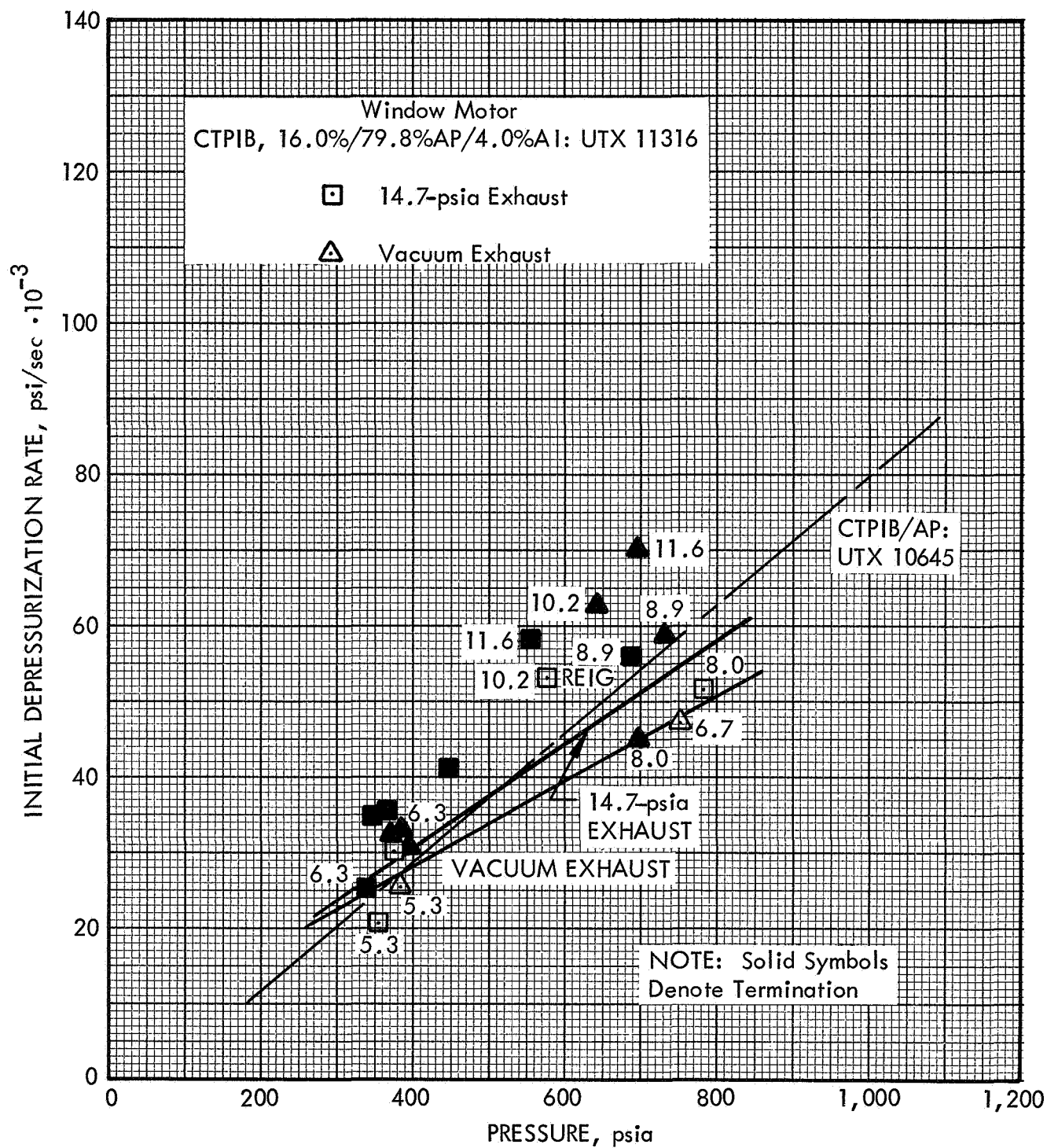


Figure 32. Combustion Extinguishment Characteristics of CTPIB/AP/4% Aluminum Propellant (UTX 11316)

90496

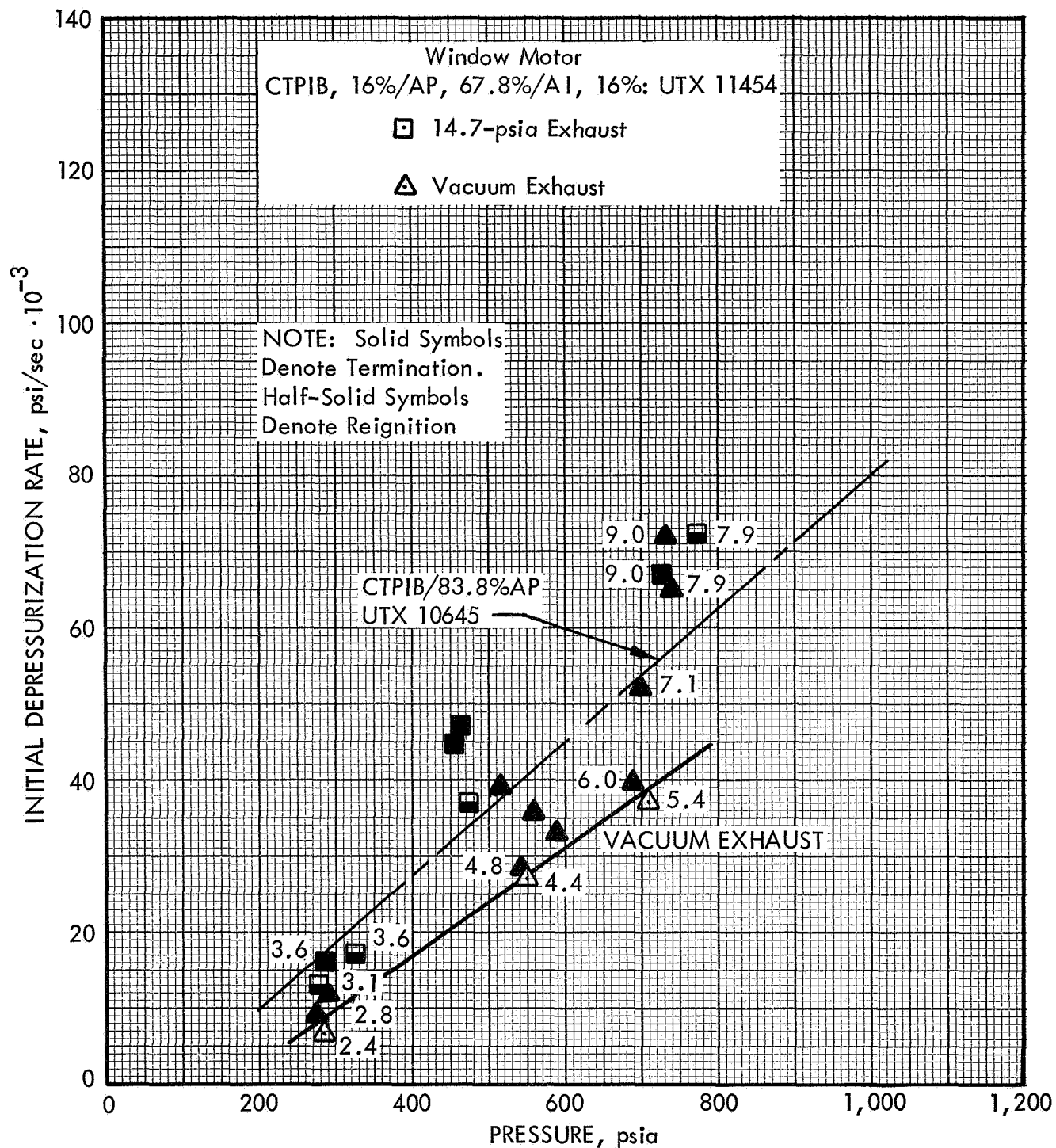


Figure 33. Combustion Extinguishment Characteristics of CTPIB/AP/16% Aluminum Propellant (UTX 11454)

90497

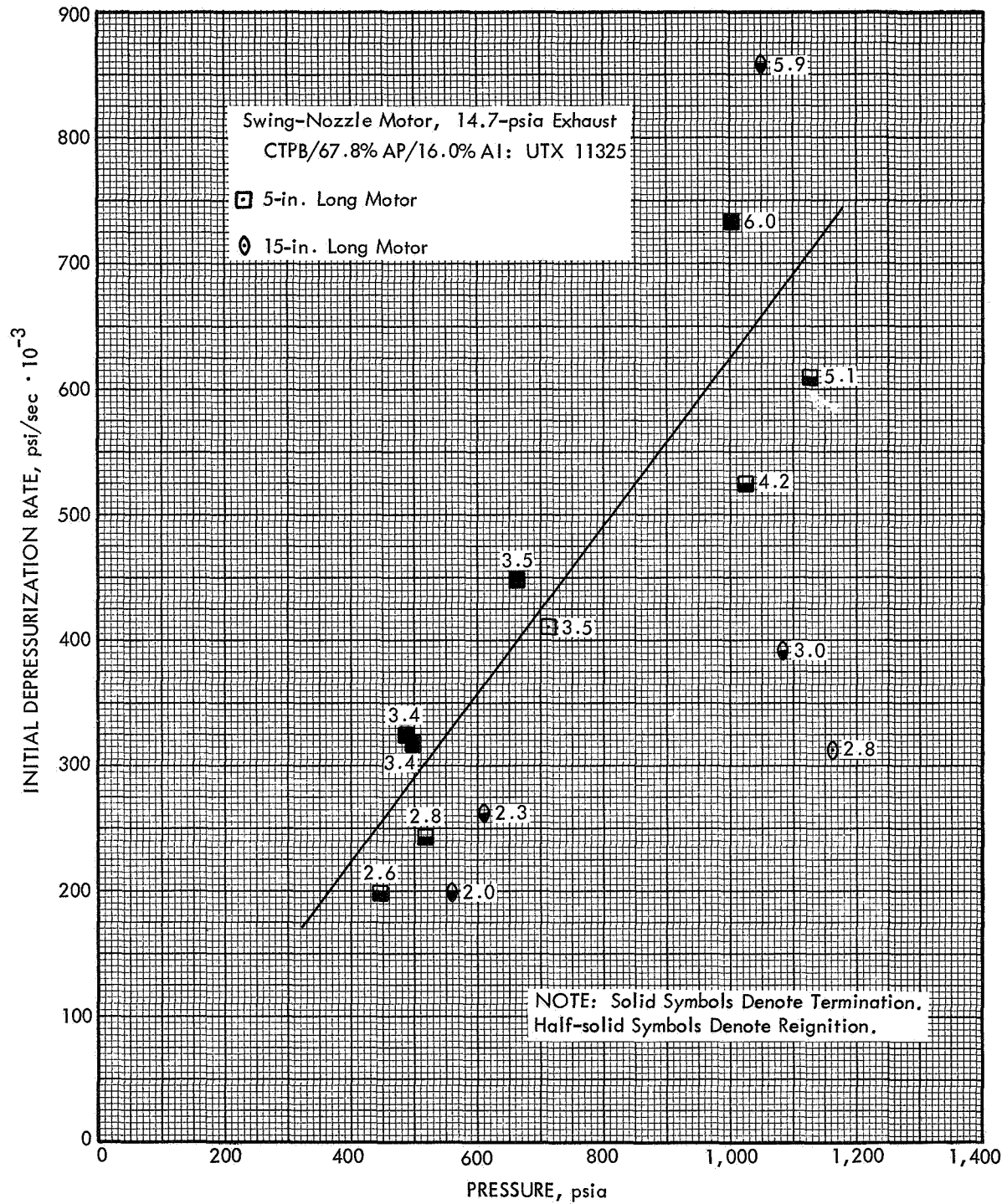


Figure 34. Swing-Nozzle Motor Extinguishment Data
for CTPB/AP/16% Aluminum Propellant (UTX 11325)

90498

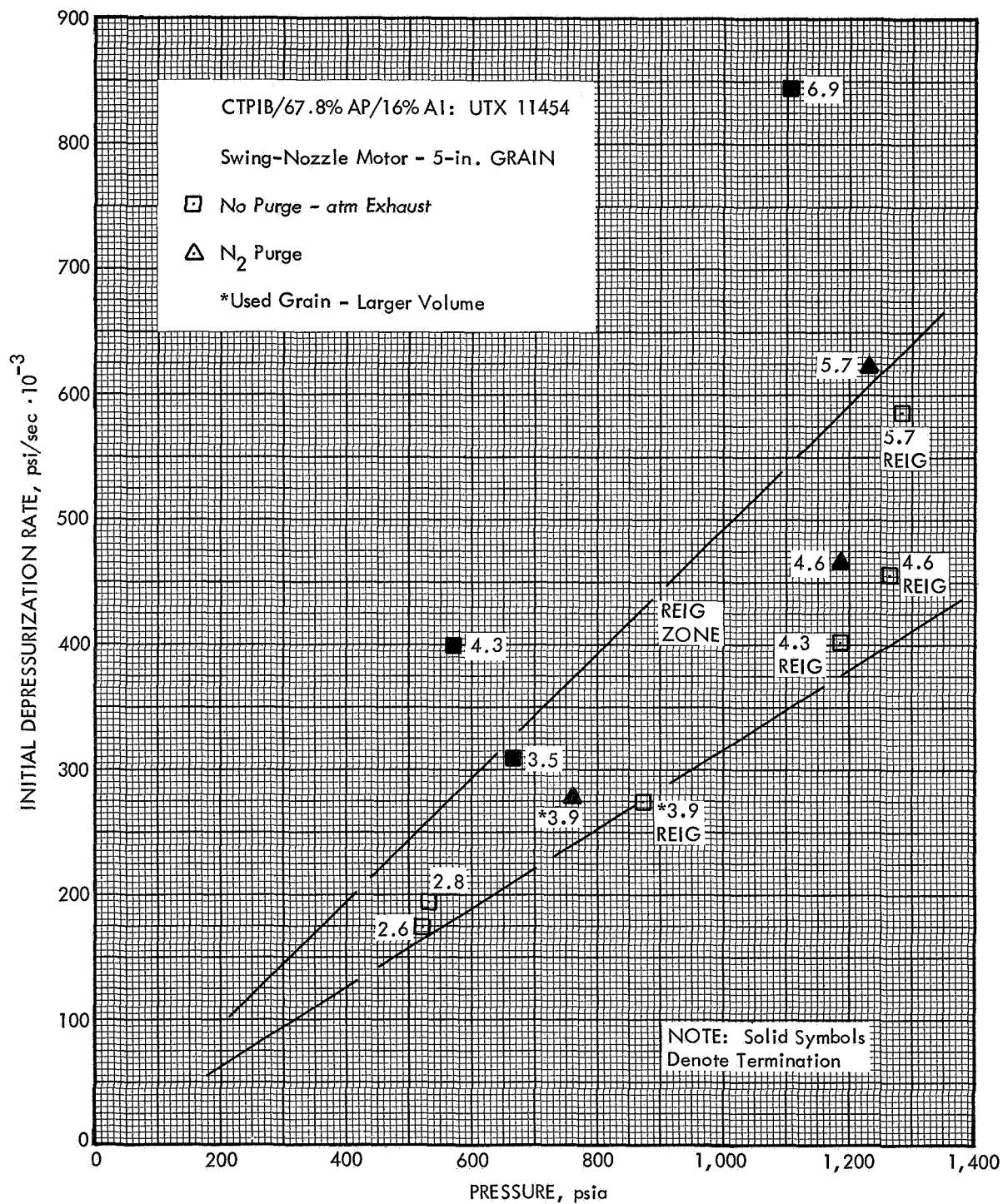
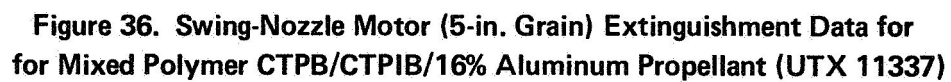


Figure 35. Swing-Nozzle Motor (5-in. Grain) Extinguishment Data for CTPIB/AP/16% Aluminum Propellant (UTX 11454)

90499



Catalyst Studies - The influence of catalyst addition upon the extinguishment behavior of both aluminized and nonaluminized CTPB and CTPIB propellants was explored. The tested compositions consisted of two nonaluminized CTPB propellants (one with 0.25% iron oxide burning rate catalyst, UTX 11326, and the other with 0.25% organo-iron catalyst, UTX 11329, and two CTPB/16% aluminum formulations, UTX 11541 and UTX 11473) catalyzed respectively with 1% and 3% HYCAT. The depressurization results at both atmospheric and vacuum exhaust conditions are shown in figures 37, 38, and 39. Though the burning rates of all the catalyzed systems were greater than the nonaluminized base propellants, particularly at higher pressure levels, the higher burning rates were not reflected in increased extinguishment requirements. Using an 800-psi initial motor pressure and a vacuum exhaust level as a basis of comparison, both the catalyzed and noncatalyzed propellants had approximately a 9×10^4 psi/sec critical depressurization rate and required a termination nozzle of at least 0.406-in. in diameter for successful termination. These data are similar to results obtained with the CTPIB under Contract No. NAS 1-6601. The \dot{P} test results for CTPIB formulated with iron oxide or copper chromite catalysts showed little or no influence of catalyst upon termination behavior, although the burning rates at higher pressure levels were increased markedly.

At 1-atm exhaust there was a much greater probability for reignition of the aluminized CTPB grains containing HYCAT than for the base CTPB/16% aluminum system containing no catalyst. Neither of the two HYCAT-catalyzed propellants were terminated without reignition at 1-atm exhaust. Microscopic examination of the grains terminated under vacuum conditions revealed a thick layer of agglomerated aluminum balls which would serve as a reignition source under atmospheric exhaust conditions but not at pressures below the minimum ignition pressure. A similar, but much thinner layer of agglomerated aluminum balls was found on the surfaces of the noncatalyzed, aluminized propellants.

The introduction of 0.25% organo-iron catalyst into the nonaluminized CTPIB system also had little effect upon the depressurization rates required for extinguishment. The critical depressurization rates and termination nozzles for UTX 11335, which contained 0.25% catalyst, matched those of the noncatalyzed system (UTX 10645). The data shown in figure 40 also indicate that the exhaust pressure level had little effect upon termination requirements.

The termination behavior of the 1% HYCAT catalyzed, 16% aluminum CTPIB system (UTX 11342) was similar to that of the CTPB analog. Under vacuum exhaust conditions the termination requirements were the same as those of the uncatalyzed, 16% aluminum CTPIB propellant. At 1-atm exhaust the grains consistently reignited at initial termination rates at an order of magnitude greater than the critical rates under vacuum exhaust. These data are shown in figure 41. The terminated grain surfaces were covered with a thick layer (0.2 to 0.5 mm) of agglomerated aluminum balls up to 0.25 mm in diameter. It is conceivable that such a layer of hot aluminum would consistently reignite grains terminated at 14.7 psia.

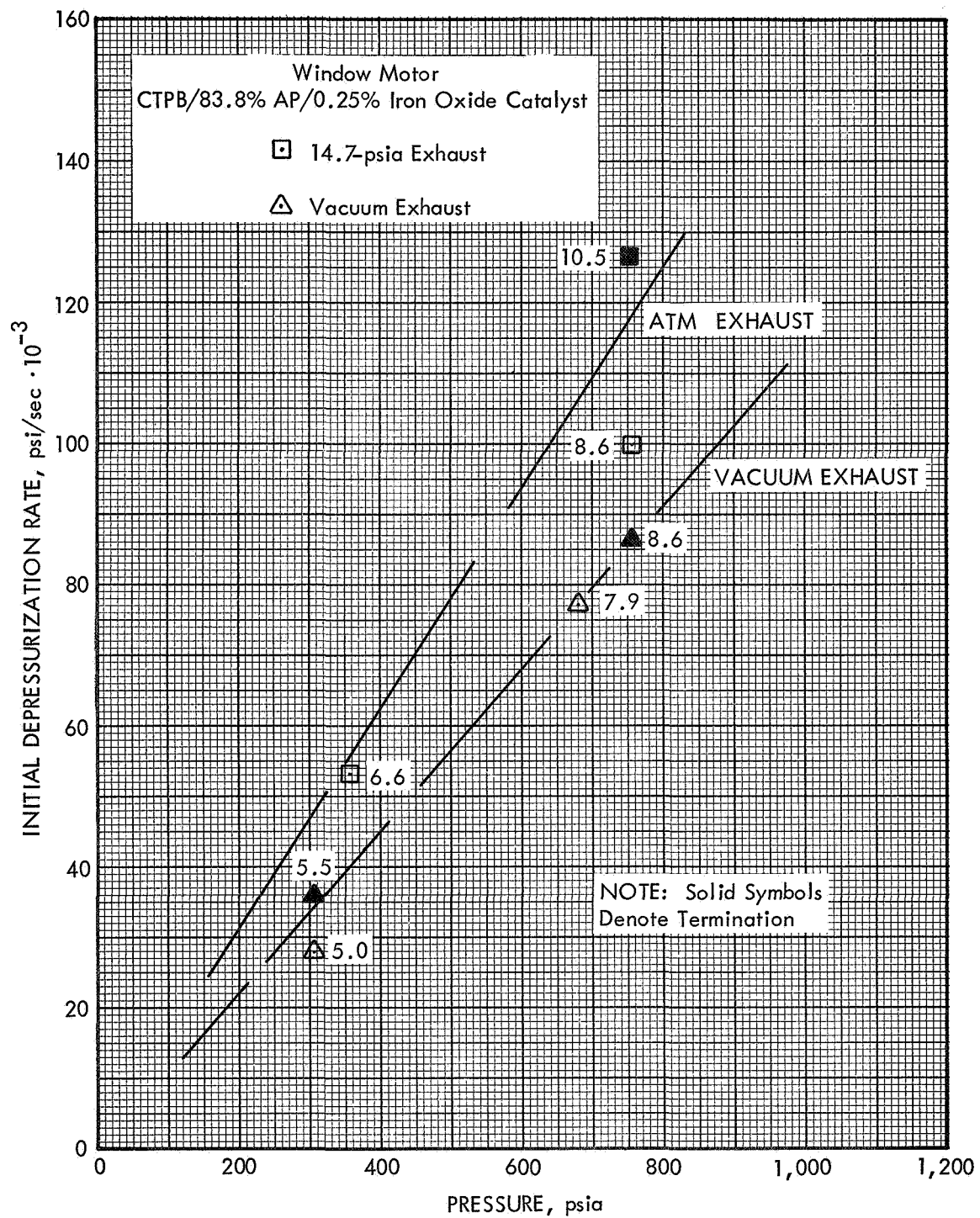


Figure 37. Combustion Extinguishment Characteristics of 0.15% Iron Oxide Catalyzed CTPB/AP Propellant (UTX 11326)

90501

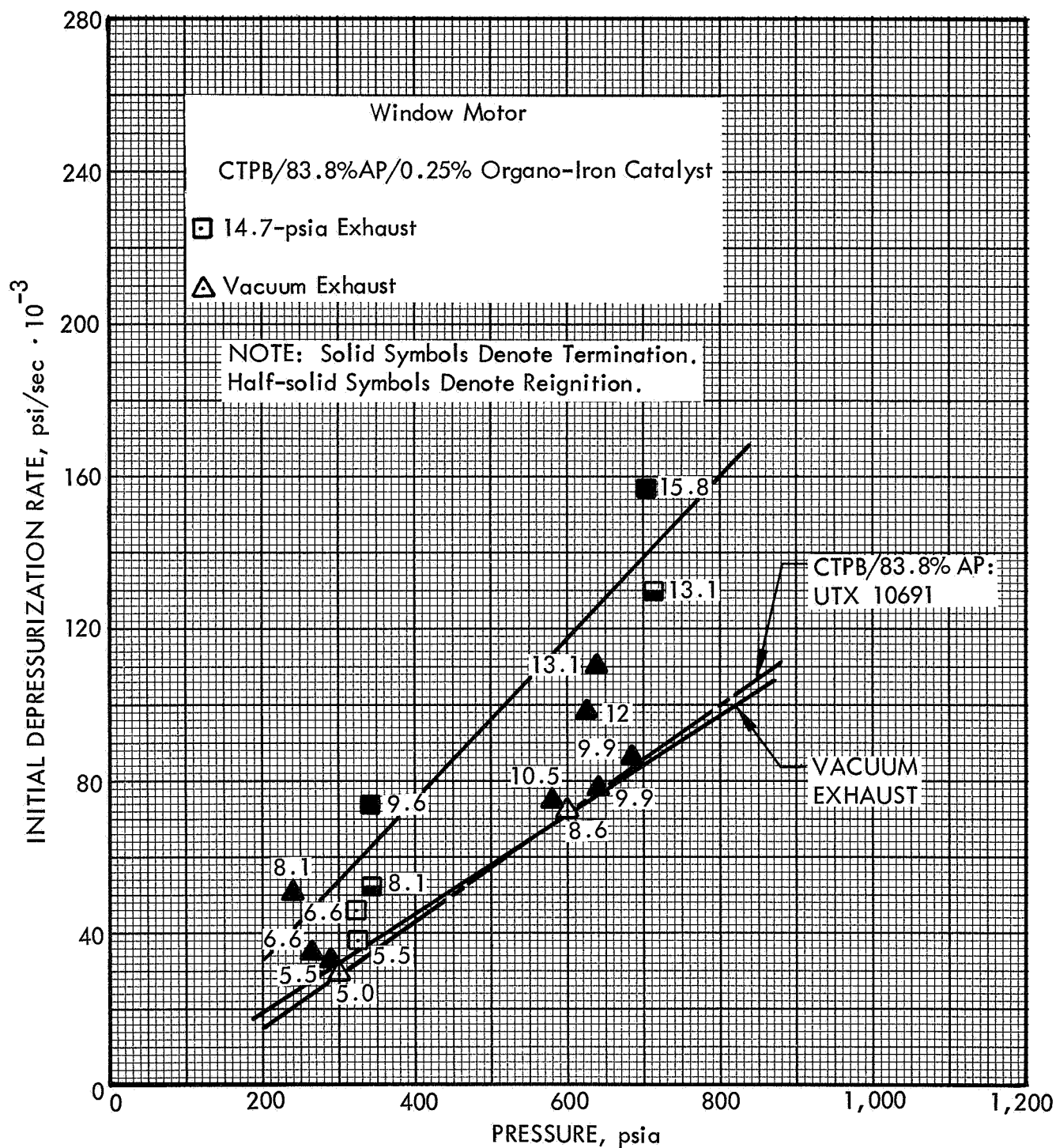


Figure 38. Combustion Extinguishment Characteristics of 0.25% Organo-Iron Catalyzed CTPB/AP Propellant (UTX 11329)

90502

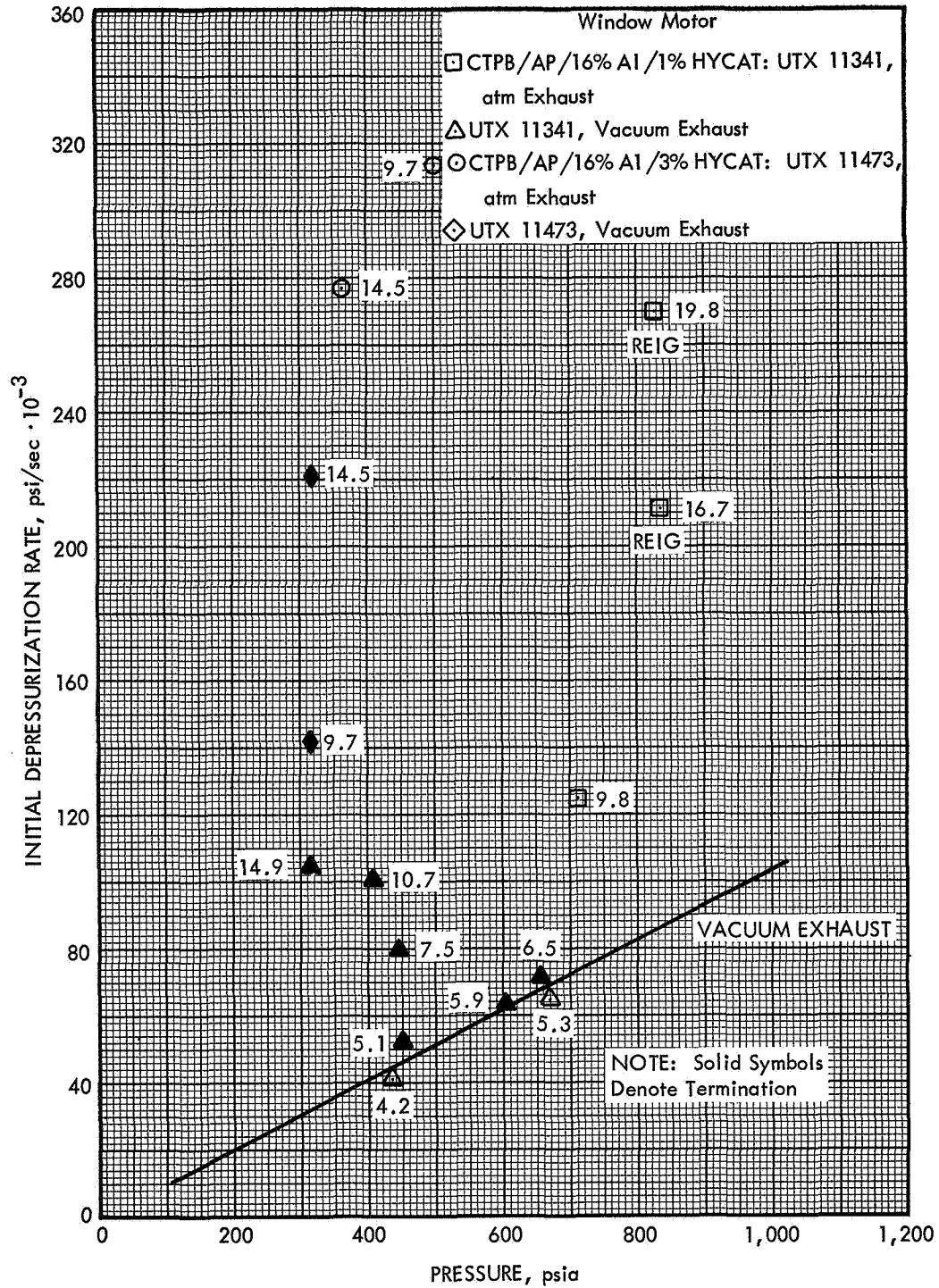


Figure 39. Combustion Extinguishment Characteristics of HYCAT Catalyzed CTPB/AP/16% Aluminum Propellants

90503

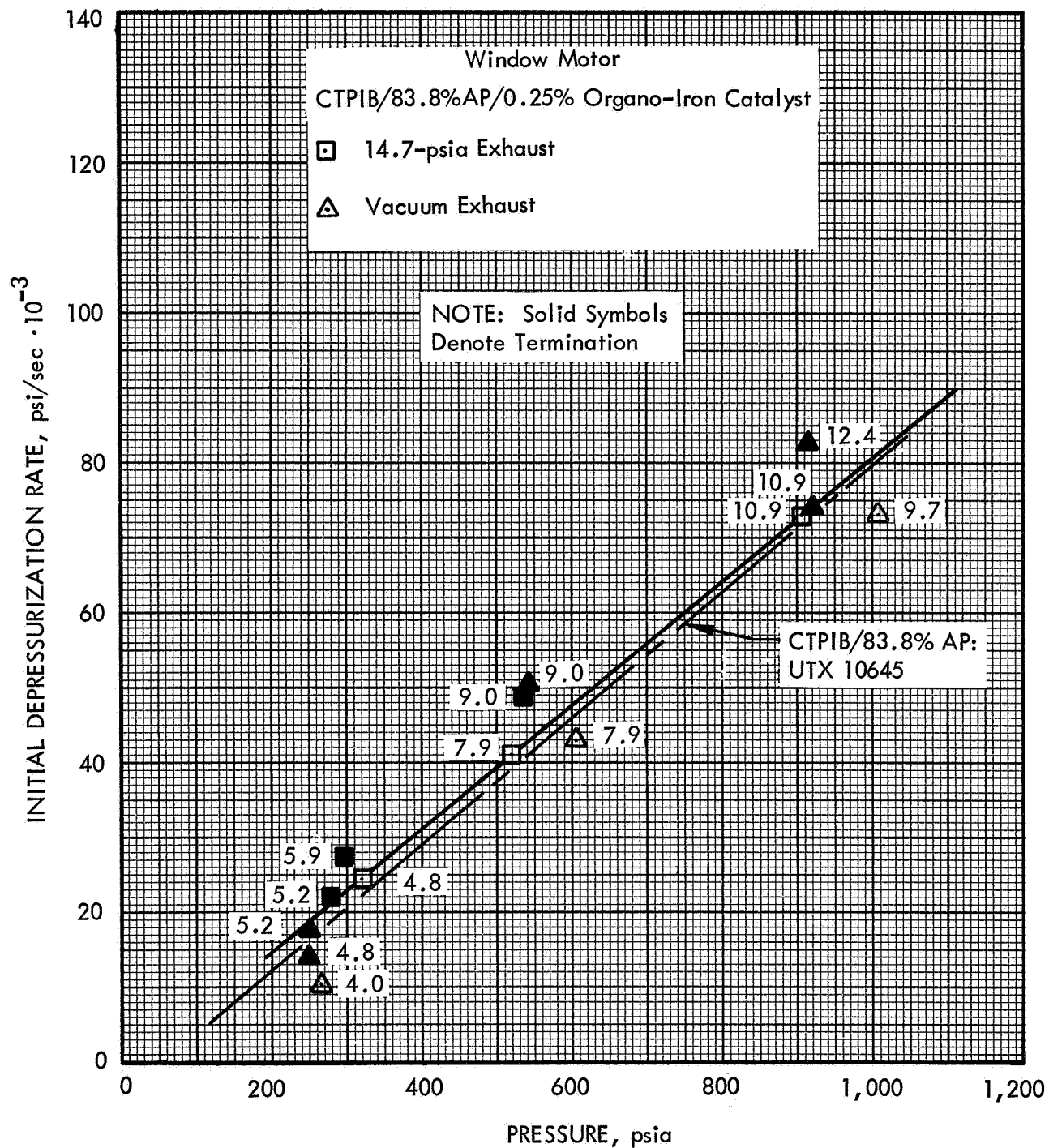


Figure 40. Combustion Extinguishment Characteristics of 0.25% Organo-Iron Catalyzed CTPIB/AP Propellant (UTX 11333)

90504

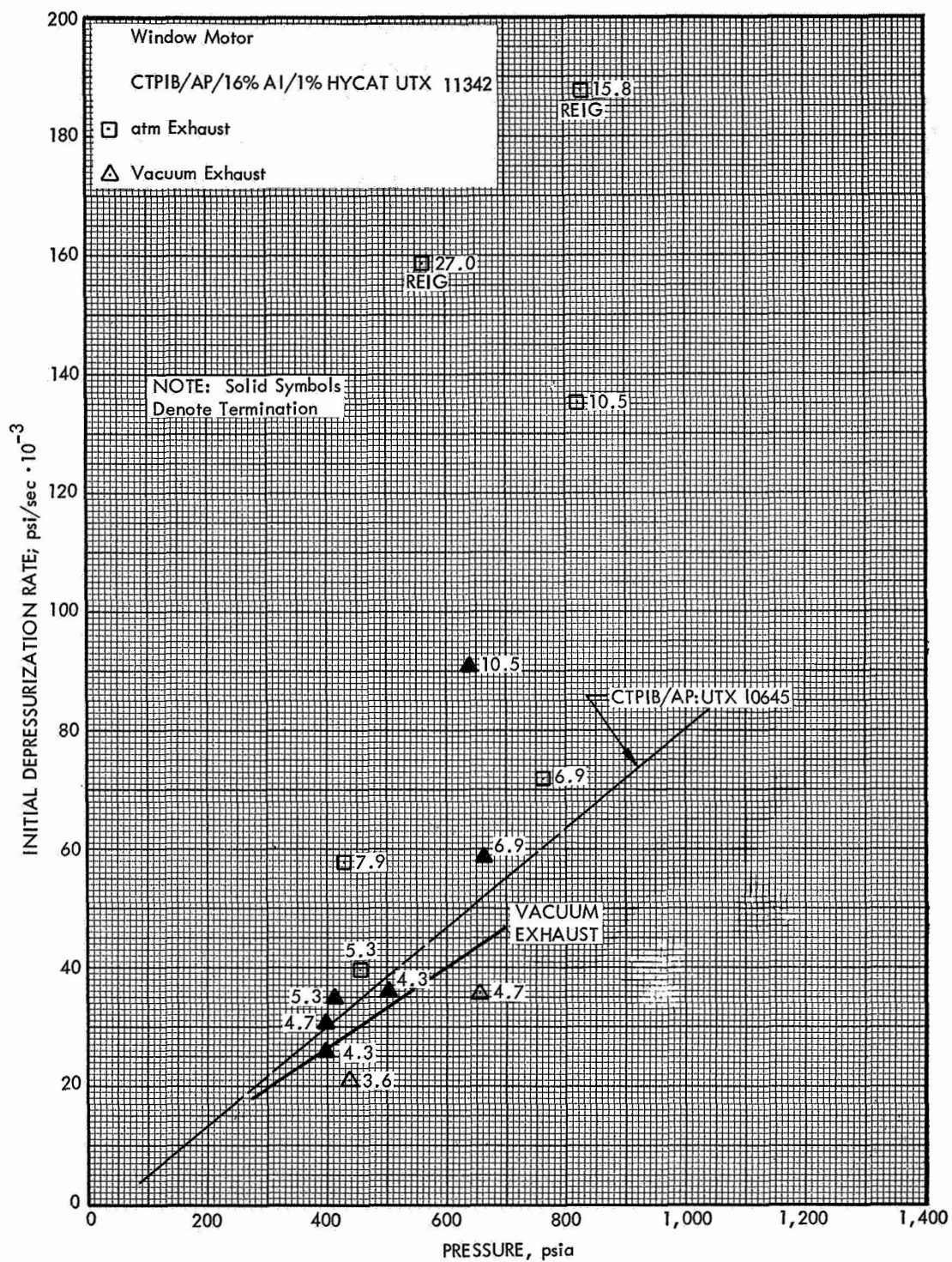


Figure 41. Combustion Extinguishment Characteristics of HYCAT Catalyzed CTPIB/AP/16% Aluminum Propellant (UTX 11342)

90505

Reignition Studies

In addition to reignition by hot, agglomerated aluminum, the most likely causes of grain reignition in any motor are radiation from hot spots in the motor, conduction of heat from hot liners, grain inhibitors or structural members within the motor cavity, and possibly combustion of hot polymeric decomposition products which are ignited when the motor is exhausted and oxygen from the atmosphere diffuses into the motor cavity. Reignition by radiation is a distinct possibility and must be considered a problem peculiar to any particular motor. If radiation is a problem, it is solely a function of the motor burn time (surface temperature of hot spots), the view factor, the material composition of the radiator (emissivity and temperature), and the ignition pressure-flux requirements of the grain.

The latter two reignition sources, conduction and combustion, are also likely to be a direct function of any given motor system and an estimate of the severity of these problems was made. During the program, several series of propellant firings were made to evaluate the influence of hot liner materials upon grain reignition. Both the window motor and the swing-nozzle motor were used for these tests, and a variety of geometries and liner types were evaluated. Charring and noncharring liners were potted at the ends of the grains, along the lengths of the grains, and parallel to but not touching the grains. The base CTPIB propellant, UTX 10645, was selected for the evaluation tests because of its potential as a \dot{P} propellant. The tests were all conducted at a nominal 400-psi motor pressure, a 1.0-sec burn time, and atmospheric exhaust. The depressurization nozzles were selected so that the developed depressurization rates would cause extinction, and an unsuccessful firing would be the result of reignition and not failure to terminate. A depressurization rate just greater than the critical depressurization rate of the particular motor and grain geometry was selected for testing. Under these conditions only two instances of grain reignition were noted.

A conclusion based on these tests is that ignition caused by combustion of hot, gaseous, liner decomposition species in air is unlikely to diffuse into the motor after termination. If such combustion occurred, all of the terminated grains would be likely to reignite. Also, considering that only two of the grains (potted liner inserts) reignited, reignition is not necessarily caused by the hot liner residue next to the terminated grain. Another likely cause of reignition would be a crack between the liner and the grain, which would be more likely to retain enough heat to cause reignition or even to be an area of nontermination. The film studies of this program and concurrent hydroquench studies being conducted at UTC have shown that a crack in the grain or void between liner and grain is a potential reignition site. Although every effort was made to prevent such voids when the liner material was cast next to the grain, it is possible that cracks or voids were created.

In the course of the program it was found that reignition of aluminized propellants has a much greater probability than reignition of nonmetallized propellants such as those described above. Reignition of the aluminized formulations occurred regularly at an exhaust pressure of 14.7 psia with depressurization rates near and sometimes greatly exceeding the critical depressurization rate. In particular, the catalyzed CTPB and CTPIB propellants with 16% aluminum consistently reignited. Although speculations upon the source of reignition can be made, additional studies are required for either quantitative or qualitative understanding.

High-Speed Film Studies

The principal objective of the high-speed film studies was to provide additional information concerning the mechanisms and conditions of combustion extinguishment. To obtain these objectives, attempts were made to increase the magnification level and to extend the film studies to higher pressure levels than were used under Contract No. NAS 1-6601. The results obtained were, in general, unrewarding as a result of a number of technical problems. The earlier film studies demonstrated that strand-type studies in nitrogen-pressurized combustion chambers are nonrepresentative of conditions in working motors. Thus, the film studies of this program were all conducted using a self-pressurized motor with attendant viewing problems. Considerable effort was expended without success in developing a lighting system capable of providing a light intensity sufficient to wash out the luminous high-pressure combustion flame but with a low radiant flux level which did not serve as a reignition source for the terminated grain surfaces. The General Electric Marc 350 lighting system used for the majority of the film tests did provide good lighting and low radiant fluxes at pressures less than 100 psi but did not permit clear viewing at higher pressures.

Attempts to realize higher magnification levels were not successful because of the small depth of field at high magnification and the problem of synchronizing the termination event so the viewed area was in focus at depressurization. After considerable effort to obtain the desired high magnification levels, the magnification was decreased so that synchronization was not a problem. A number of preliminary results were obtained using the high-speed film system at lower magnification levels. The propellant samples were ignited by means of a nichrome heater wire stuck to the grain surface with small patches of uncured CTPB propellants. It was observed that these patches charred and in some instances remained on the grain surface, serving as a hot reignition source. In one instance, complete reignition of the grain occurred 20 sec after termination because of the presence of one small piece of hot charred material. Other film tests revealed a considerable amount of charring and sloughing on the CTPB grains. The char may be a major factor in determining the termination characteristics of the CTPB formulations.

DISCUSSION AND ANALYSIS

The results presented previously provide the basis for analysis of those aspects which are most important to solid propellant extinguishment phenomena. The test results demonstrated that propellant variables, which include the binder system, the AP loading, and the catalyst and metal loadings, have a major effect on ease of extinguishment. In addition, it has been shown that the motor configuration and the exhaust pressure can have a pronounced effect upon the ease of combustion termination and the permanence of extinguishment.

Results obtained with the window motor showed that the exhaust pressure level affected the ease of extinguishment of propellants prepared using CTPB and polyurethane binder systems but did not influence the behavior of the majority of the CTPIB propellants. This indicates that combustion extinguishment of the polyurethane and CTPB propellants in the window motor must have occurred after the nozzle dechoked during depressurization to atmospheric exhaust (pressures less than 25 to 30 psia). Alternately, combustion of the CTPIB propellants must have terminated at higher pressures since the dechoking had little or no influence upon the termination process. It was also apparent that extinguishment in the swing-nozzle motor occurred at much higher pressures and depressurization rates than in either of the dual nozzle motors. The higher pressure extinguishment for the swing-nozzle motor tests is amplified by the representative data traces shown in figures 42, 43, and 44. These figures are typical of the raw data traces obtained with the window motor. Figure 42 is typical of a successful termination test, and figure 43 is typical of a test where burnout occurred. In those tests where termination was achieved in the window motor, a definite break in the pressure trace (and the light sensor trace) could generally be discerned, as shown in figure 42. This break was taken to be the point of actual combustion termination or the point at which propellant regression stopped, thus causing an abrupt change in the depressurization of the motor. The pressure at extinguishment was less for the CTPB and polyurethane propellants than for the CTPIB systems. Determination of the point of extinguishment using the swing-nozzle motor was not readily apparent because of the much greater depressurization rates and the fact that extinguishment occurred at much higher pressure levels. If the grain did not terminate, burnout occurred at a much higher pressure in the swing-nozzle motor than in the window motor; this observation reinforced the fact that extinguishment occurred at higher pressure. In order to achieve permanent extinguishment, it was necessary that the grain be terminated at a pressure above the burnout pressure. Further confirmation of the different extinguishment pressures was obtained by examination of the aluminized propellant grains extinguished in the two motors. As noted previously, the surfaces of the grains extinguished in the window motor were covered with an extensive network of sintered aluminum balls. A smaller quantity of balls was found on the grains extinguished in the swing-nozzle motor. In all probability, the extensive aluminum network on the window motor grains was formed during low-pressure deflagration. e.g., during the depressurization cycle. The lack of aluminum deposit on the swing-nozzle motor grains is indicative of combustion extinguishment at higher pressure.

An example of the type of agglomerates found on the window motor grains is shown in figure 45. Figure 45a is an electron microscopic photograph of 16% aluminized CTPIB grain (UTX 11454), taken at 100X, and shows the agglomerated aluminum balls sitting on the large AP crystals which are approximately 200μ in diameter. There is a

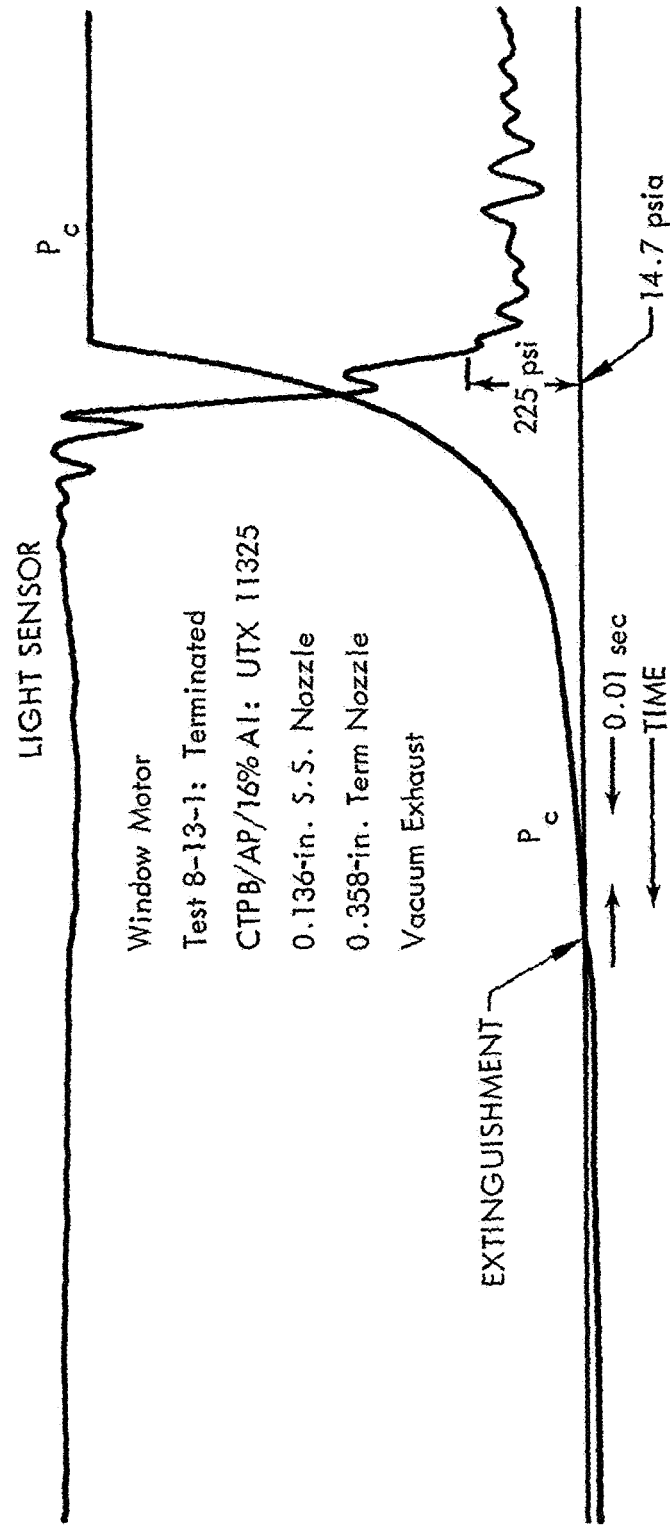


Figure 42. Window Motor Data Trace for CTPB/AP/16% Aluminum Propellant (UTX 11325) Test No. 2

90506

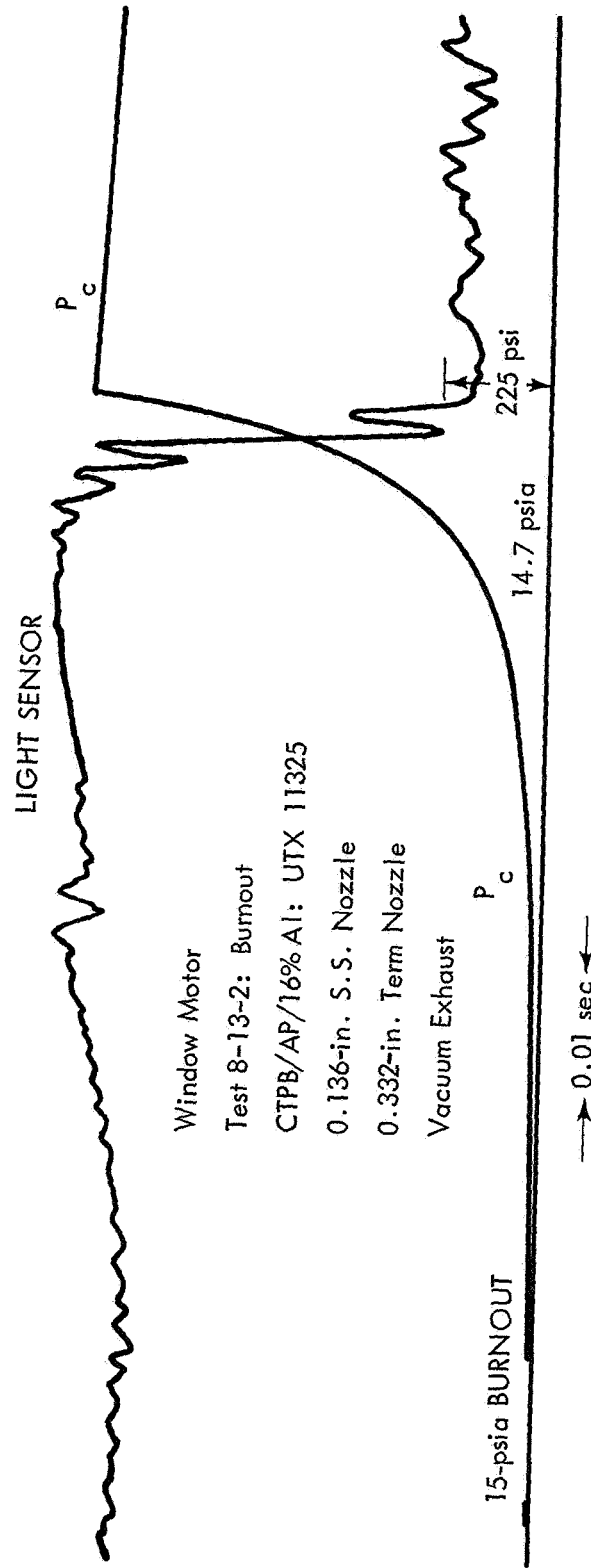


Figure 43. Window Motor Data Trace for CTPB/AP/16% Aluminum Propellant (UTX 11325)
 Test No. 2

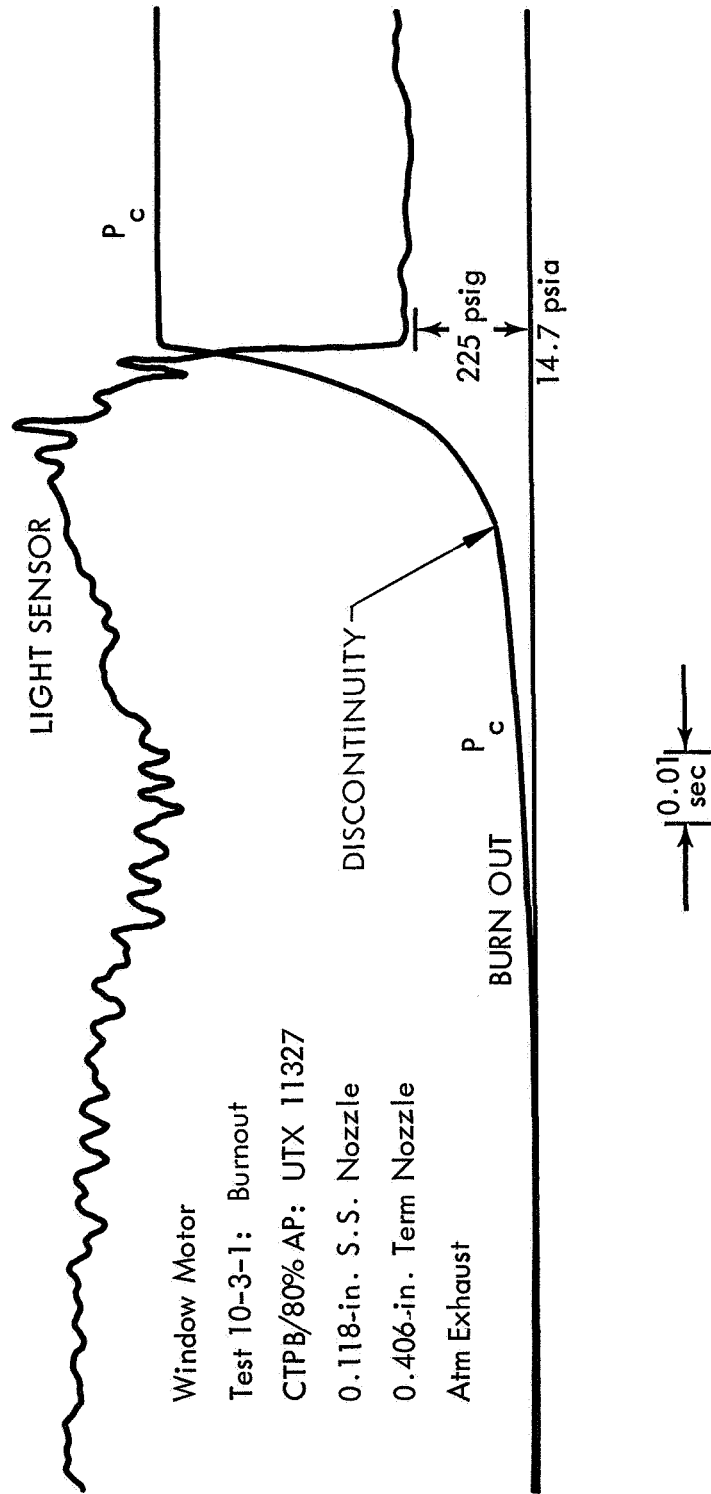
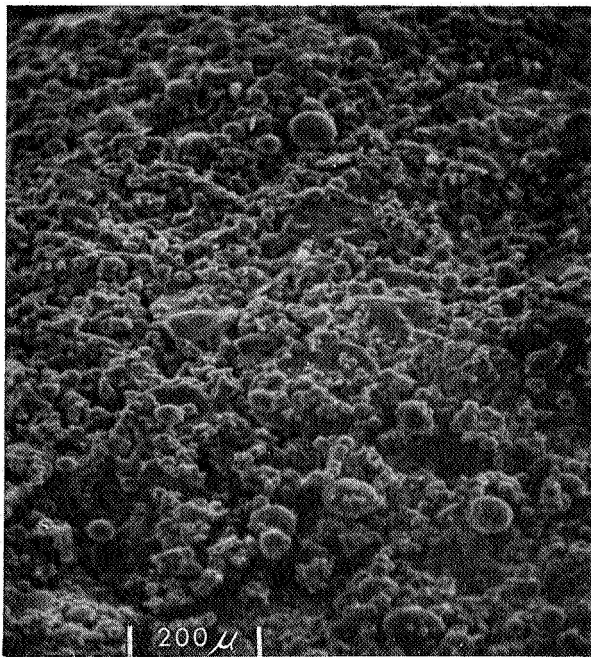
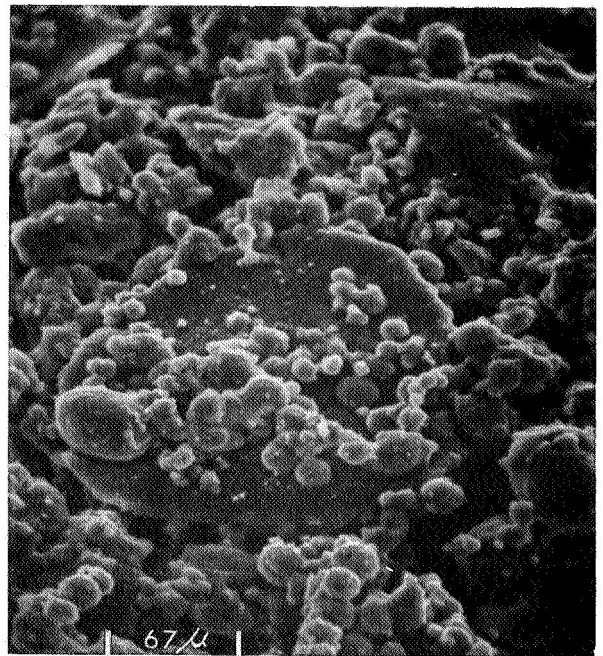


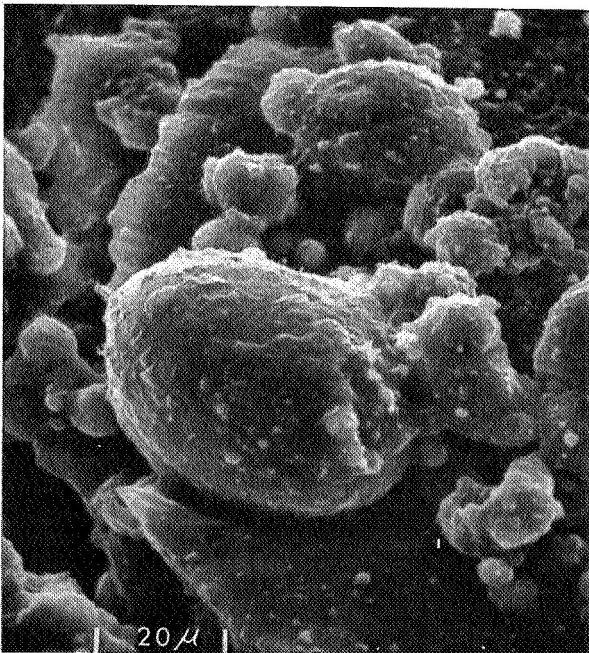
Figure 44. Window Motor Data Trace for CTPB/80% AP Propellant
 (UTX 11327)



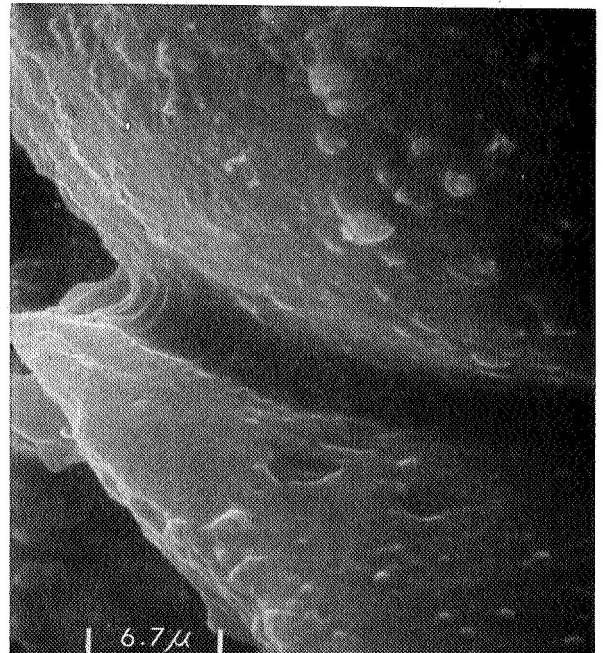
(A) 100X



(B) 300X



(C) 1000X



(D) 3000X

**Figure 45. Scanning Electron Micrographs of Terminated Propellant
Surface-CTPIB/16% Aluminum**

90509

lack of contrast between the aluminum and AP because the sample has been gold plated, giving all surfaces much the same appearance. However, earlier observation with an optical microscope showed the aluminum to be bright and shining and to be sitting on the relatively flat, transparent AP surface.

Figure 45b, taken at 300X, is an enlargement of the center of the first photo and shows a large AP crystal with a number of aluminum balls on the surface. The third and fourth photographs taken at 1000X and 3000X, respectively, show the details of a large aluminum ball sitting on the left side of the AP crystal. These photographs show that the aluminum and AP have been figuratively welded together.

In general, the experimental depressurization paths were described by a simple exponential decay function, but a number of traces did show one or more changes in slope during depressurization. The step change of the depressurization rate was also matched by a change of the light sensor signal intensity. In some instances these disturbances were possibly the result of aluminum sluffing; however, a number of tests conducted with the nonaluminized propellants showed depressurization rate discontinuities. This type of behavior was most prevalent with the 79.8% AP-loading CTPB propellant, UTX 11327. An example of this type of behavior is shown in figure 44.

Figure 46 demonstrates a type of behavior observed occasionally during tests with the swing-nozzle motor. As shown in this figure, upon depressurization the motor pressure fell to a level above the exhaust pressure and then quickly recovered to a still higher burnout pressure. In general, two or three cycles of unstable combustion were also noted during this recovery period. A similar type of behavior was observed with the window motor; however, the time scale was much longer (1 to 2 sec) and the grains generally terminated after the pressure rose and then fell for the second time.

To present the data obtained in the course of the program and to provide a means of interrelating the results derived using the different motors, the data were correlated on the basis of the depressurization paths during blowdown. The data are shown in figures 47 through 57, wherein the dashed lines represent the depressurization paths of the majority of tests performed. The depressurization rates during blowdown are plotted in logarithmic form on the ordinate, and the abscissa represents the logarithmic pressure level at any depressurization rate. The upper end on each of the dashed lines represents the initial depressurization rate and the initial or steady-state pressure. The lower end of each line represents the depressurization rate and pressure at combustion extinguishment, if extinguishment occurred. In the event the grain burned out, the lines have been plotted asymptotically to the burnout pressure. For clarity, only the pressure and depressurization rate at the point of extinguishment are represented for the majority of the tests shown. However, a number of intermediate depressurization rates and pressures are noted in some of the figures. In figure 57 several intermediate data points are noted for each of the experimental depressurization paths.

In general it was found that, if extinguishment occurred, the extinguishment depressurization paths could be adequately represented by a straight line on logarithmic coordinates. However, one of the depressurization paths depicted in figure 50 shows a step change in depressurization rate. This characteristic was often observed with the CTPB/80% AP formulation (UTX 11327).

Swing-Nozzle Motor
 Test 12-11-6: Burnout
 CTPB/AP UTX 10691
 0.413-in - dia S.S. Nozzle
 0.719-in - dia Term Nozzle
 Atm Exhaust - 15-in. Grain

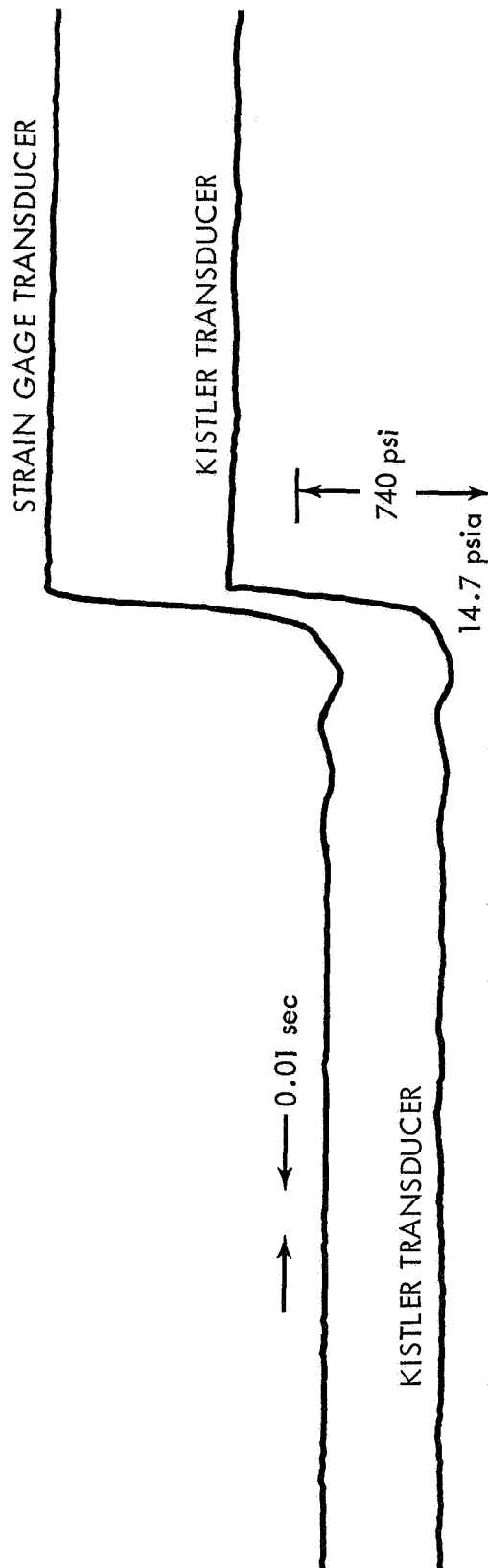


Figure 46. Swing Nozzles Motor Data Trace
 for CTPB/83.8% AP Propellant (UTC 10691)

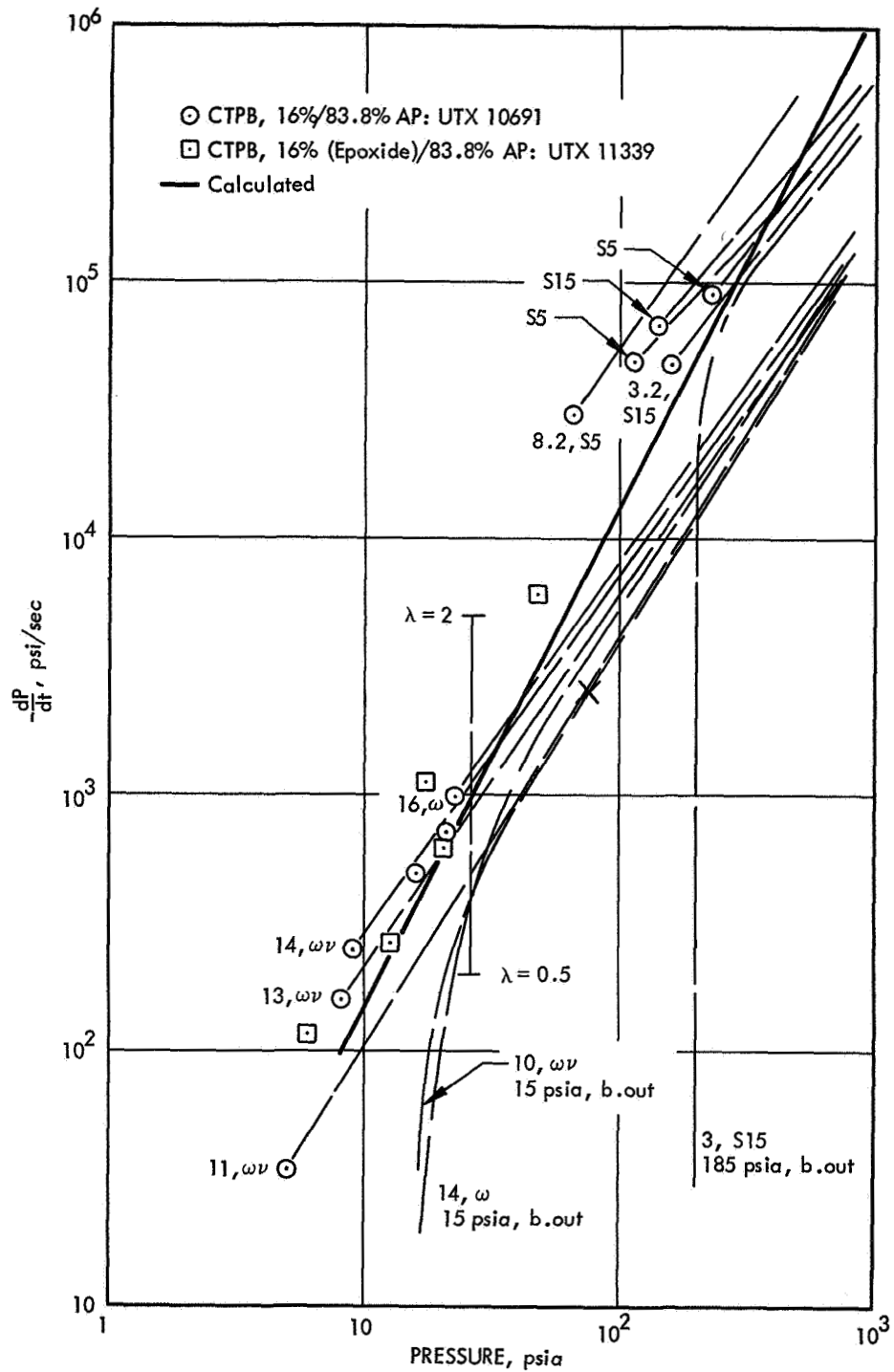


Figure 47. Comparison of Calculated and Experimental Extinguishment Requirements for CTPB/83.8% AP Propellant (UTX 10691)

90511

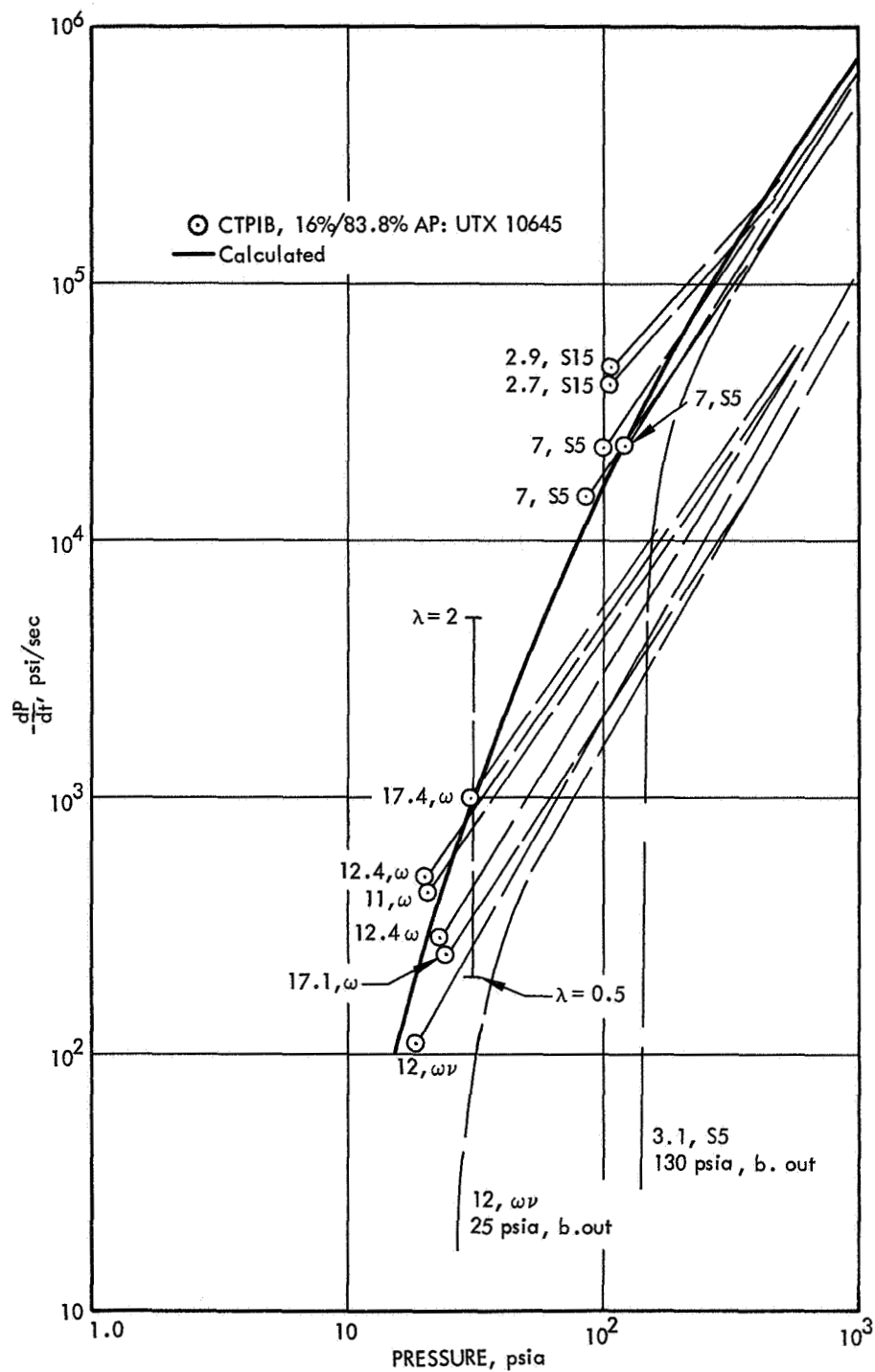


Figure 48. Comparison of Calculated and Experimental Extinguishment Requirements for CTPIB/83.8% AP Propellants (UTX 10645)

90512

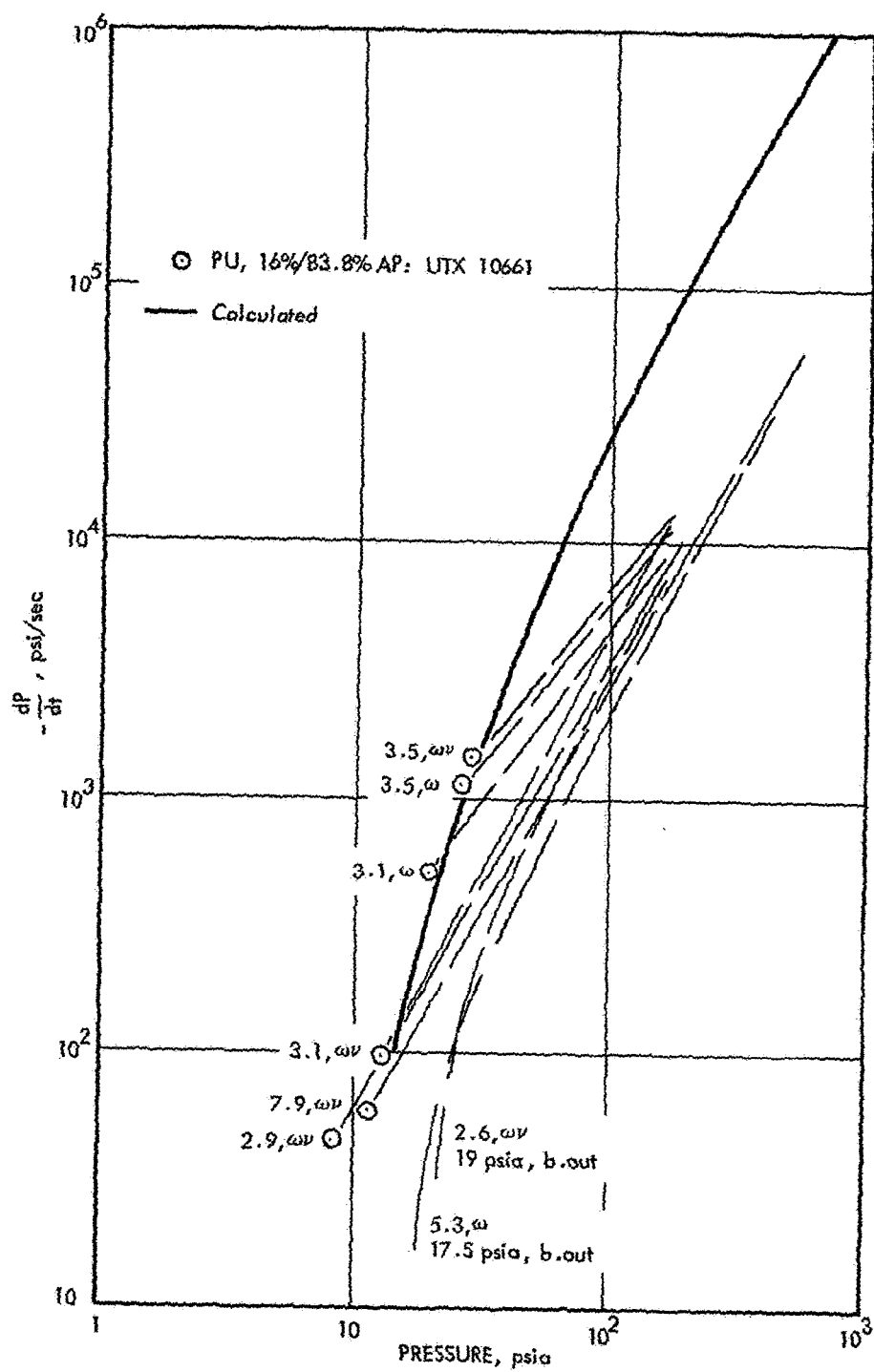


Figure 49. Comparison of Calculated and Experimental Extinguishment Requirements for PU/83.8% AP Propellant (UTX 10661)

90513

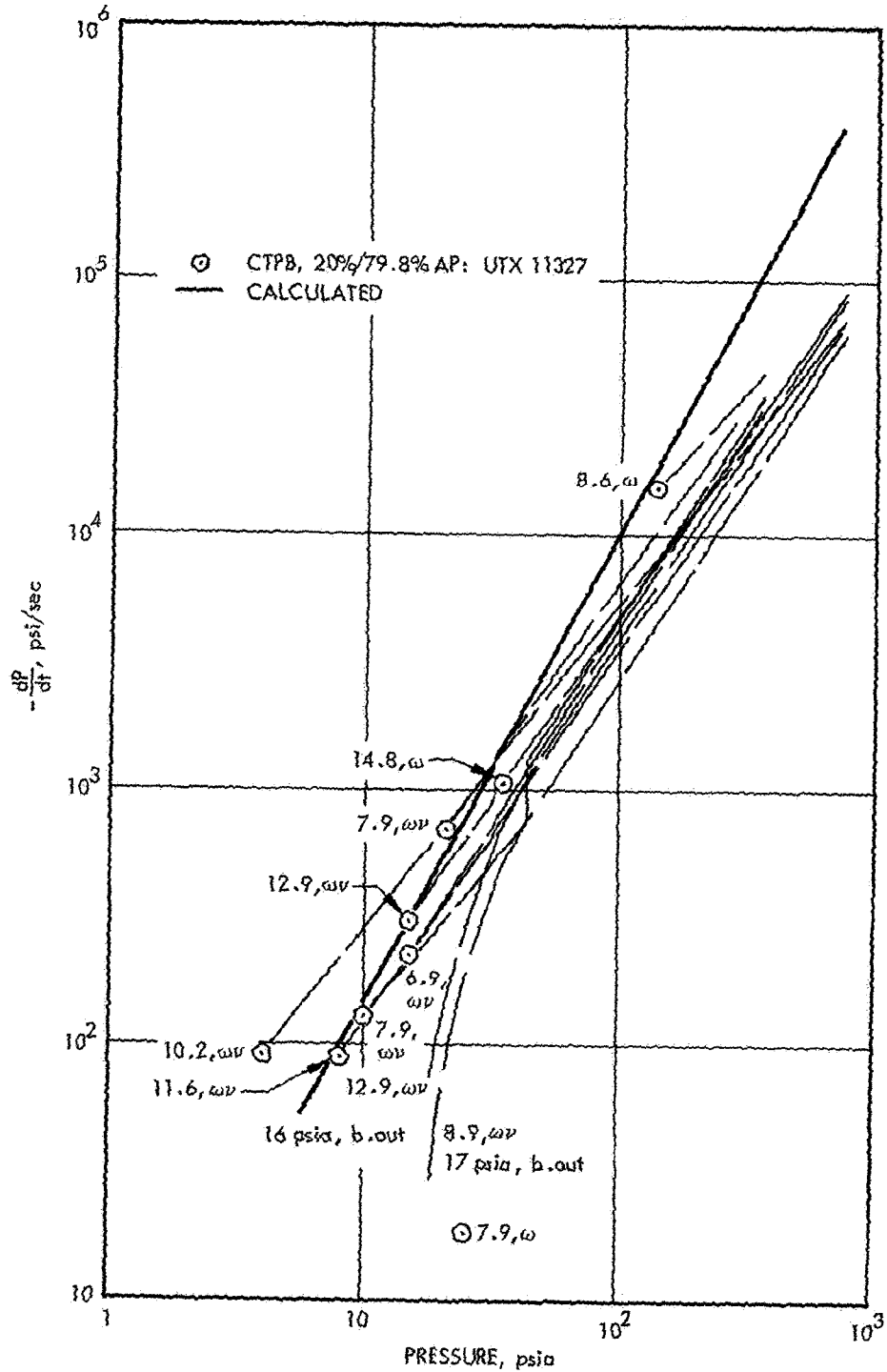


Figure 50. Comparison of Calculated and Experimental Extinguishment Requirements for CTPB/80% AP Propellant (UTX 11327)

90514

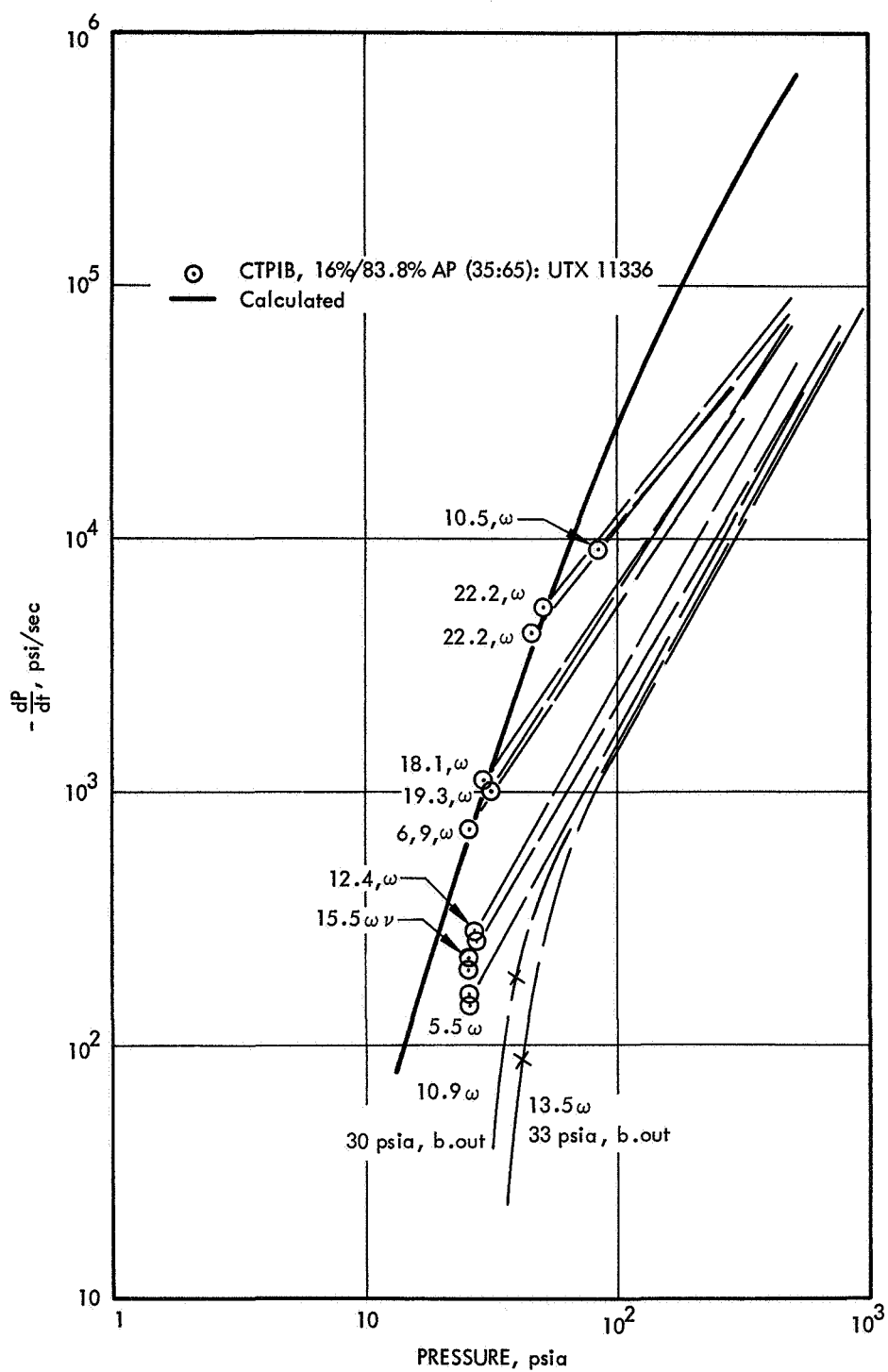


Figure 51. Comparison of Calculated and Experimental Extinguishment Requirements for CTPIB/83.8% AP (36:35) Propellant (UTX 11336)

90515

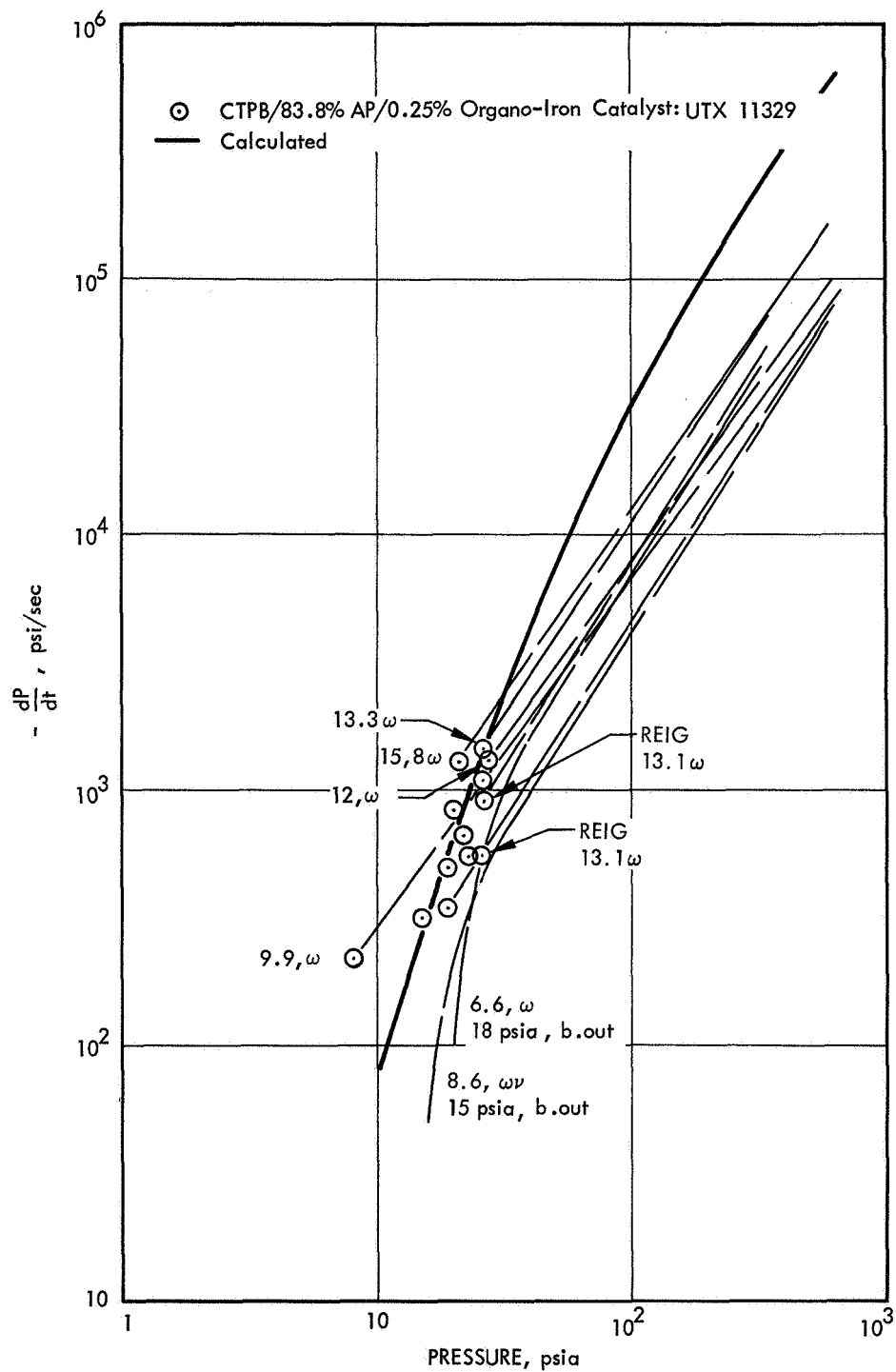


Figure 52. Comparison of Calculated and Experimental Extinguishment for CTPB/AP/0.25% Organo-Iron Propellant (UTX 11329)

90516

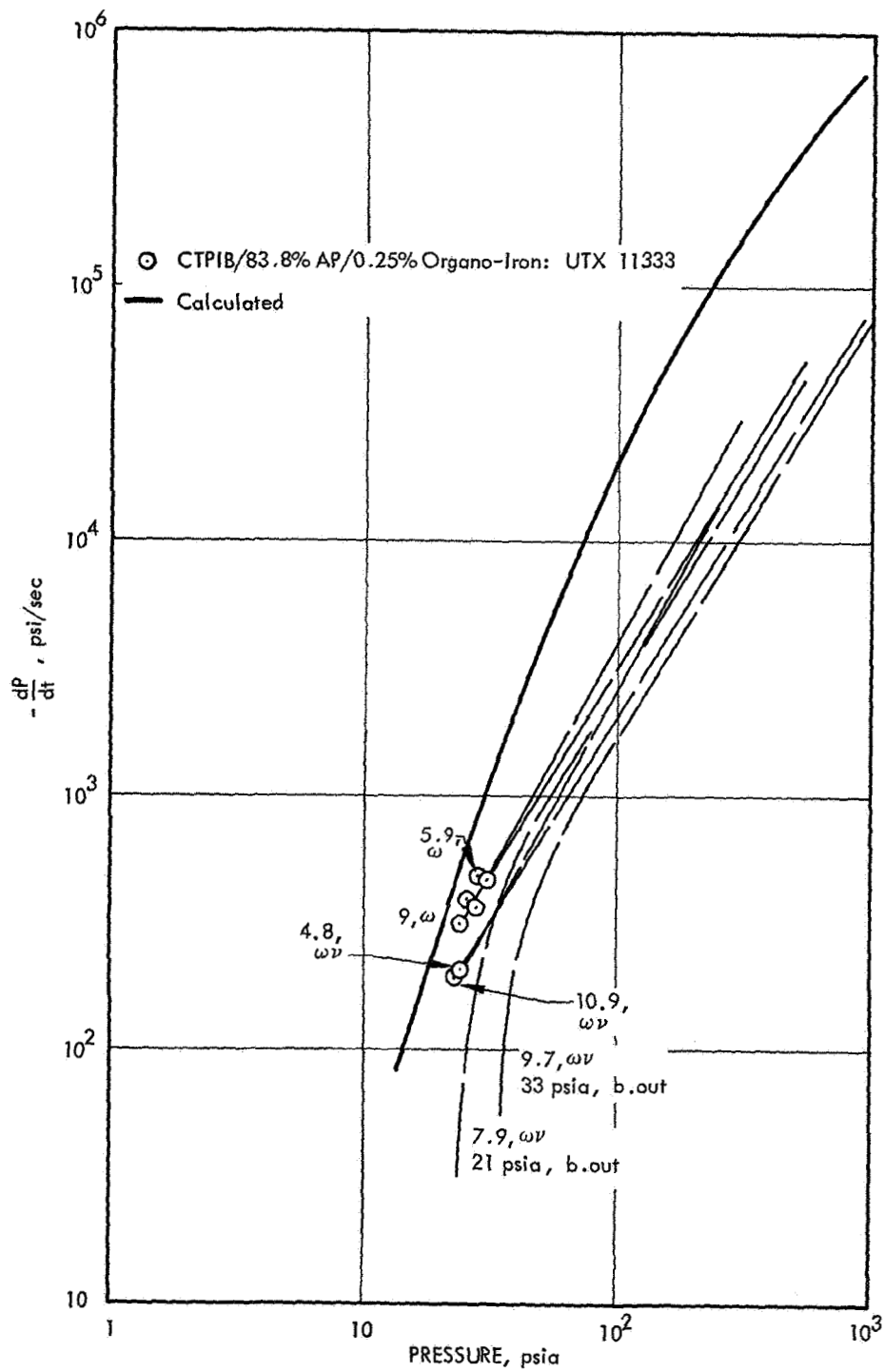


Figure 53. Comparison of Calculated and Experimental Extinguishment Requirements for CTPIB/AP/0.25% Organo-Iron Propellant

90517

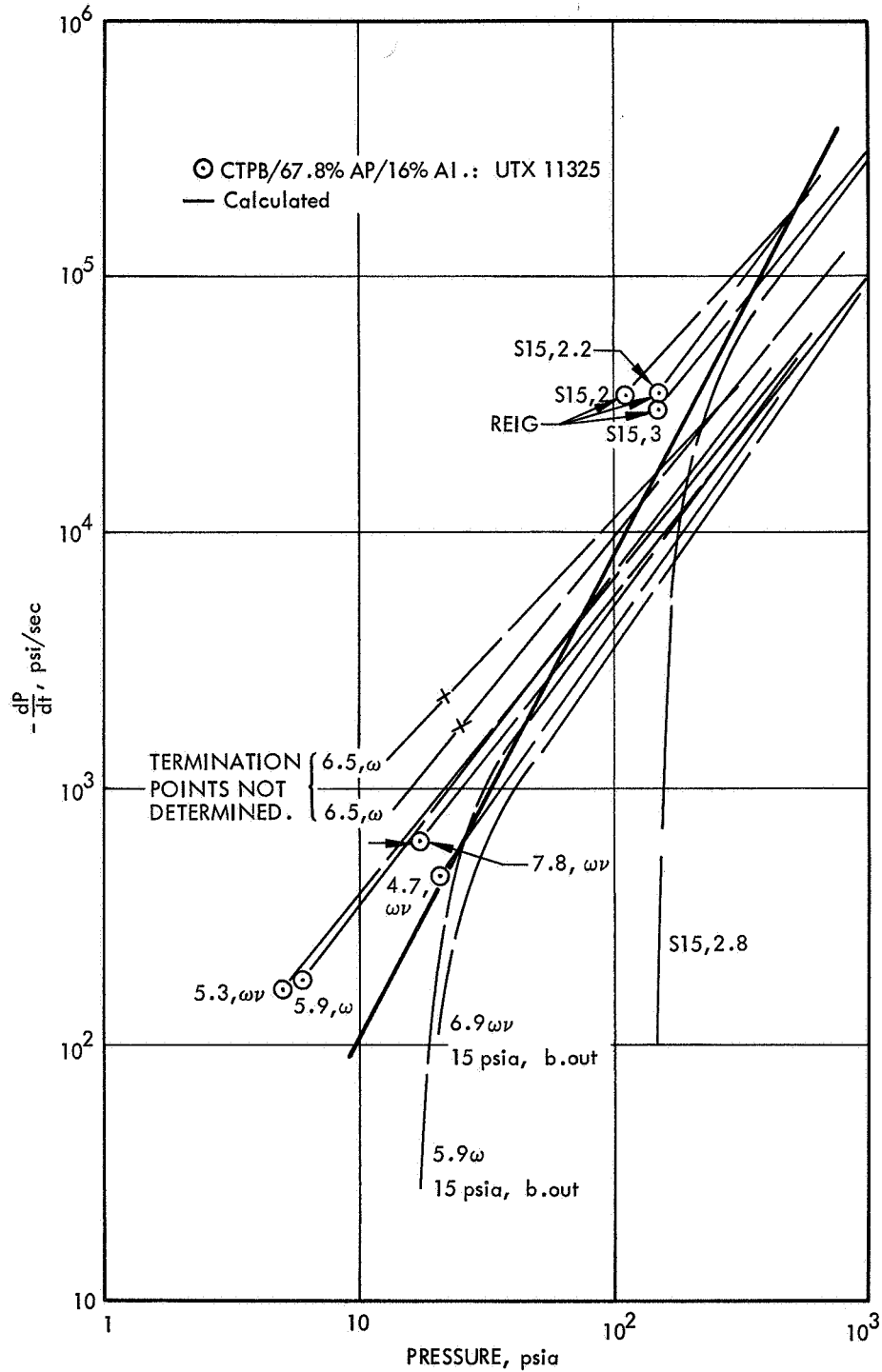


Figure 54. Comparison of Calculated and Experimental Extinguishment Requirements for CTPB/AP/16% Aluminum Propellant (UTX 11325)

90518

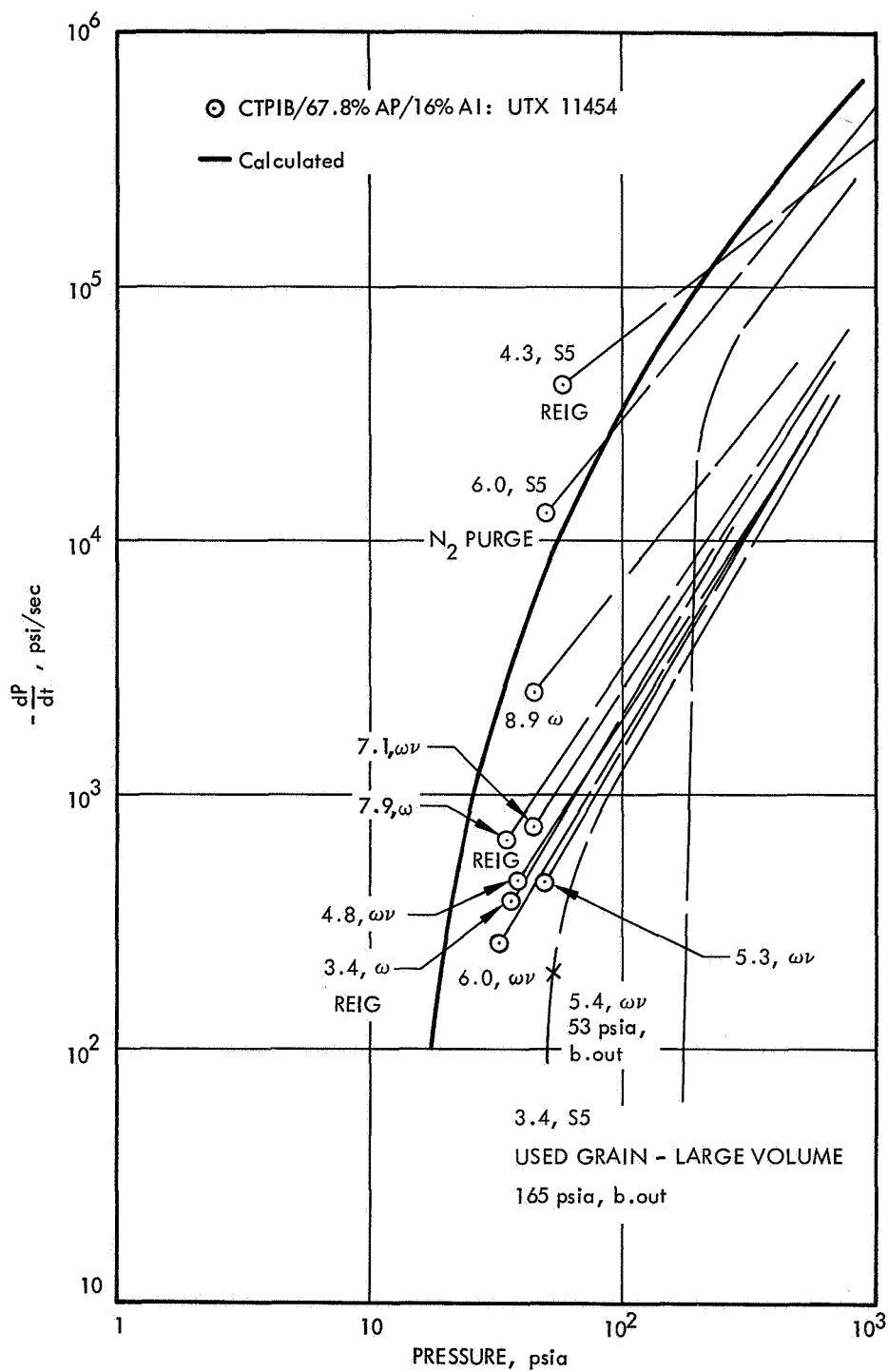


Figure 55. Comparison of Calculated Experimental Extinguishment for CTPIB/AP/16% Aluminum Propellant (UTX 11454)

90519

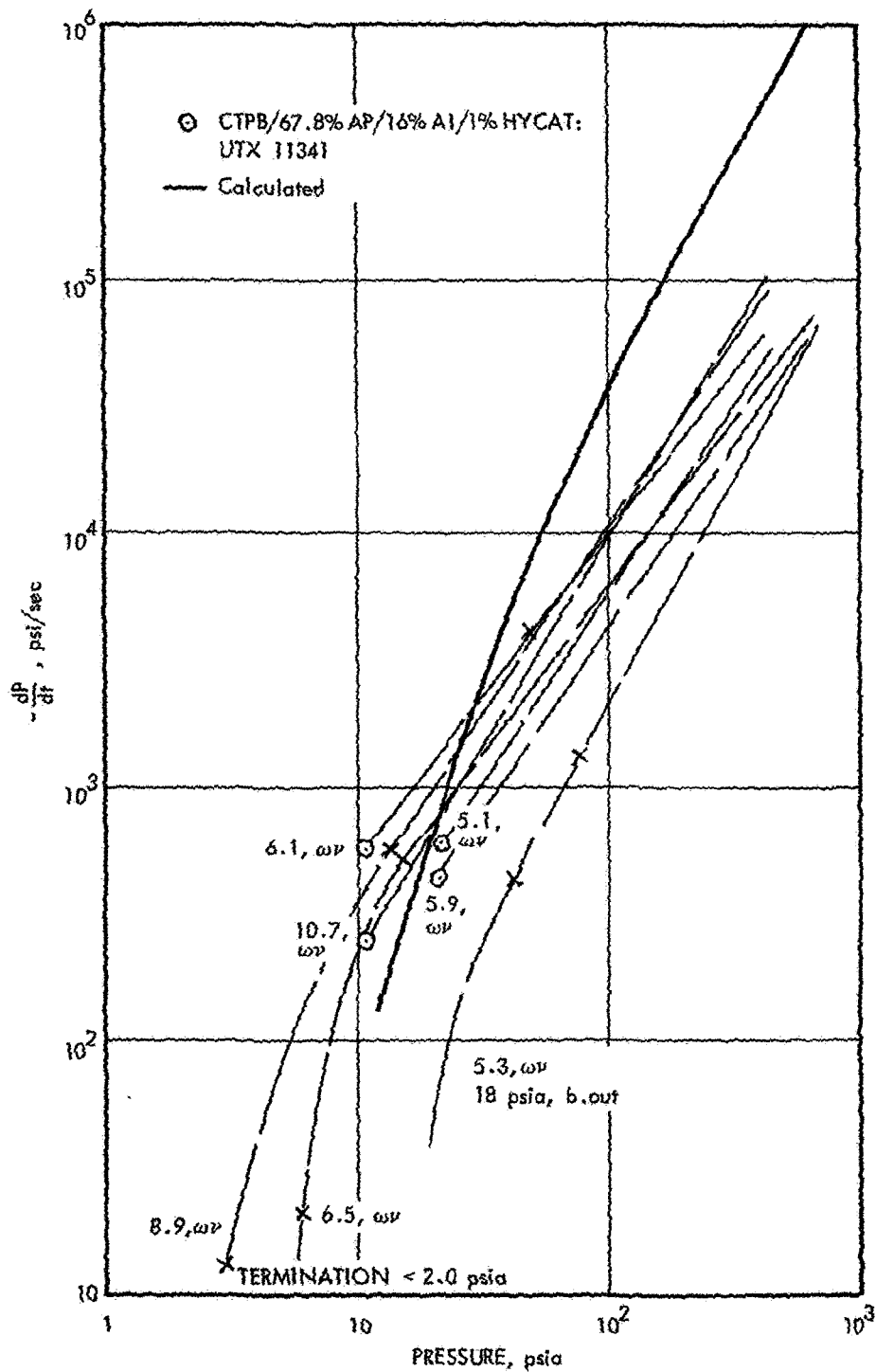


Figure 56. Comparison of Calculated and Experimental Extinguishment Requirements for CTPB/AP/16% Aluminum/1% HYCAT Propellant (UTX 11341)

90520

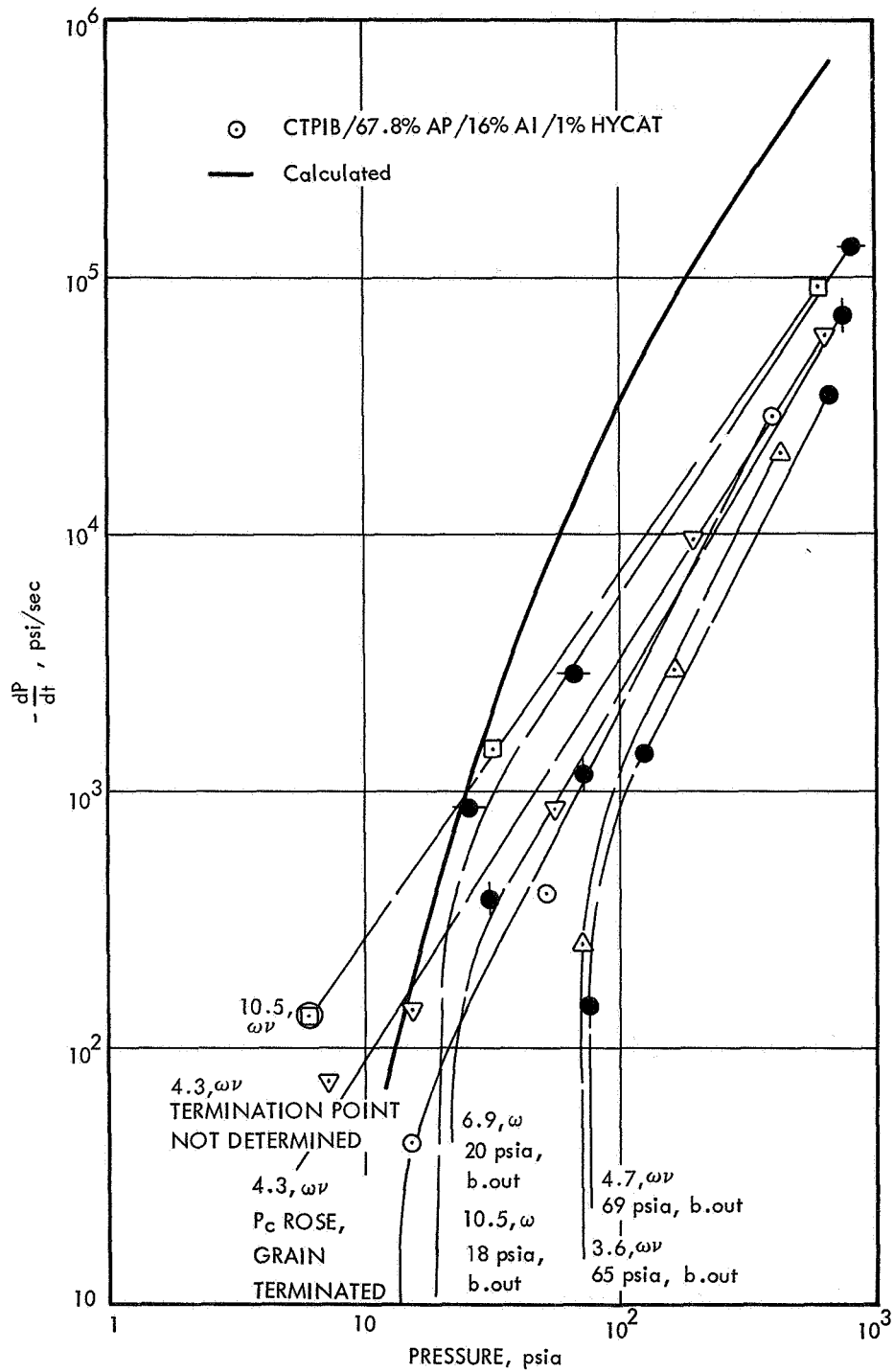


Figure 57. Comparison of Calculated and Experimental Extinguishment Requirements for CTPIB/AP/16% Aluminum/1% HYCAT Propellant (UTX 11342)

90521

The numbers beside the individual depressurization paths refer to the ratio of termination nozzle area to initial or steady-state nozzle area. The alphanumeric codes refer to the type of motor used, S5 indicates 5-in. swing-nozzle motor, S15 indicates 15-in. swing-nozzle motor, ω indicates window motor and atmospheric exhaust, and ωv indicates window motor and vacuum exhaust.

Also shown in figures 47 through 57 are the extinguishment requirements calculated by use of the Von Elbe-type model. Extinguishment is predicted when $dP/dt = \lambda \frac{Pr^2}{n\alpha}$ where λ may have a value of -0.5, -1.0, and -2.0, depending upon the particular model of combustion extinguishment. For comparison purposes the line $dP/dt = Pr^2/n\alpha$ ($\lambda = -1$) has been plotted for each of the propellants listed in figures 47 through 57. Because all burning rates could not be described by a power law expression, some of the calculated solid lines are not straight lines. For the calculated limits, n and \dot{r} were taken from the strand burning data while α , the thermal diffusivity, was taken as $2.5 \cdot 10^{-4}$ in.²/sec for the nonaluminized propellants and $3.0 \cdot 10^{-4}$ in.²/sec for the aluminized propellants.

The possible bounds of the calculated extinguishment conditions with $\lambda = -0.5$ to $\lambda = -2.0$ are shown in figure 47. These limits are greater than the errors which may result from a lack of knowledge of the thermal properties of the propellants. The most important factor in the calculated expression is the propellant burning rate at any specified pressure.

An examination of the results presented in figures 47 through 57 shows a fair agreement between the experimental and calculated extinguishment conditions. The calculated and experimental requirements were more in agreement when the window motor was used than when the swing-nozzle motor was used. However, this may be due to the greater uncertainty of the swing-nozzle motor data.

Whether the agreement between the calculated and experimental data provides experimental confirmation of the theory or is merely fortuitous is open to speculation. The possible bounds on the calculated results are quite large, as indicated in figure 50. It should also be noted that requirement for combustion extinguishment, i.e., $dP/dt = \lambda r^2 P / n\alpha$, can be obtained either from a model which considers only processes occurring in the solid phase^(4,5) or only processes occurring in the gas phase.⁽⁶⁾

There are qualitative trends in the data which can be noted from these correlations. The conditions required for experimental extinguishment of the CTPB propellants range from more severe than, to equal to the calculated conditions. Conversely, the conditions for experimental extinguishment of the CTPIB propellants are equal to, or less than the calculated requirements. Reducing the AP loading level of the CTPB propellant reduced the requirements for extinguishment of the CTPB propellant (UTX 11327) and provided better agreement with the calculated values.

Based on these trends, it is evident that the binder composition has a definite influence upon the ease of extinguishability. It is reasonable that the thermal decomposition behavior of the binder system will influence extinguishability just as it influences ignitability. Shannon⁽²²⁾ showed that these propellants, formulated with

binders which thermally degraded at lower temperatures (CTPIB), are harder to ignite at lower pressure levels than propellants formulated with more thermally stable binders (CTPB and PBAN). Also, as the endothermicity of the propellant was increased by increasing the binder level, the ignitability requirements were increased. These observations parallel the trends noted in the extinguishment data. Therefore, any simplified model of the Von Elbe type can only be of general applicability because a valid model of combustion extinguishment must be capable of including variations of binder type and loading level.

An interesting anomaly noted for the HYCAT-catalyzed propellants was the low extinguishment pressures under vacuum exhaust conditions and the propensity for these propellants to reignite at 1-atm exhaust. When the motor was exhausted into the vacuum tank, the CTPB and CTPIB propellants extinguished at lower pressures than the uncatalyzed analogs, as shown in figures 56 and 57. Examination of these grains showed a heavy layer of aluminum, which may have caused the consistent reignition observed when the motor was exhausted at 1 atm. The grains consistently reignited at 1 atm although the termination nozzles were three times the diameter of those used for extinguishment at vacuum exhaust.

Another potential problem area was revealed with the sterilizable CTPIB propellants. The sterilization process increased the termination requirements markedly but the burning rate was not affected. It is possible that the sterilization cycle resulted in loss of low-molecular-weight fragments from the binder. However, such a change would be expected to alter the burning rate behavior and the ignitability of the propellant to a greater extent than that observed.

In addition to the effects of propellant formulation and exhaust pressure level shown by these studies, a third consideration for extinguishment was found to be the motor geometry. Comparison of the results obtained from the single-grain window motor tests, the double-grain window motor tests, and the swing-nozzle motor tests showed that, as the grain surface area is increased or the motor volume decreased, the conditions required for extinguishment become more stringent. The data shown in figures 47 through 57 indicate that, for extinguishment to occur at a particular pressure, a critical depressurization rate must be achieved for that pressure. If the motor depressurization fails to achieve a critical depressurization rate at any pressure level between the initial and final pressure (new pressure corresponding to the new throat nozzle size) extinguishment will not be achieved. A simple mass balance for the motor during blowdown shows the depressurization rate to be expressed by

$$\frac{dP}{dt} = C_1 A_B \dot{r} - C_2 P A_t \quad (2)$$

where C_1 and C_2 are constants, A_B is the grain area, P is pressure, \dot{r} is the burning rate and A_t is the blowdown throat area. Depressurization requires that the second term on the righthand side of equation 2 to be greater than the first term. If the critical depressurization rate is to be achieved when the grain area is increased in a particular motor, then the termination nozzle area must also be increased to keep the difference between these two terms constant. The increase of the termination nozzle area increases the critical initial depressurization rate because the

initial depressurization rate is proportional to throat area and is not a function of the grain area. The window motor firings with a single grain and with two opposed grains demonstrated this effect; to achieve extinguishment, the diameter of the termination nozzle throat had to be increased from 0.332 in. to 0.453 in.

Because the initial depressurization rate is inversely proportional to motor volume, extinguishment requirements also are increased when the volume is reduced. An initial depressurization rate sufficient to cause extinguishment in a larger volume motor may fail to cause extinguishment in a smaller volume, smaller throat area motor. Reference to equation 3 shows that, if both the volume and throat area are reduced

$$\frac{dP}{dt}_{\text{initial}} \propto \frac{A_t}{v} \quad (3)$$

it is possible the initial depressurization may be unchanged. Reference to equation 2 shows that, to achieve extinguishment, the termination nozzle area should remain the same and the volume should be reduced, which in turn increases the initial depressurization rate. Thus, the 5-in. swing-nozzle motor, which has nearly the same grain area as the 1-lb slab motor (13.5 in.² and 11.25 in.²) but has a much smaller volume (4 in.³ and 110 in.³), required termination nozzles of nearly the same diameter (0.3-in. to 0.5-in. diameter) to achieve extinguishment. The corresponding initial depressurization rates for the swing-nozzle motor were consequently an order of magnitude greater than those obtained for the window motor.

CONCLUSIONS

The critical \dot{P} combustion-extinguishment limits of composite solid propellants have been shown to be a function of several of the formulation variables and are also determined by the motor geometry, and under some conditions the exhaust pressure level.

A number of general trends concerning the effect of formulation differences were established in the course of this program:

- (1) The substitution of aluminum for AP in either CTPB or CTPIB propellants decreased the termination requirements, although the tendency for reignition appears to be more pronounced. Tests were conducted with 4% and 16% aluminum-loaded CTPB and CTPIB propellants. The substitution of 4% aluminum for AP in both types of propellant caused a slight reduction of the critical extinguishment limits, and the substitution of 16% aluminum for AP caused a definite reduction of the critical extinguishment requirements. These effects were most noticeable under vacuum exhaust conditions. When the motors were exhausted into the atmosphere, reignition of extinguished grains often occurred, particularly with tests conducted using the swing-nozzle motor. A wide band of reignition limits was noted for the aluminized propellants tested in the swing-nozzle motor. However, it was shown that reignition could be prevented by the use of a nitrogen purge flowing through the motor immediately after depressurization. The wide reignition limits of the nonpurged motors indicate a serious potential problem for atmospherically depressurized motors.
- (2) The addition of burning rate catalysts to a propellant had little or no effect upon the extinguishment requirements in the large-volume, small-grain area motors used in this program. It is conceivable that the increased burning rates would necessitate increased termination requirements in smaller volume (or larger grain-area) motors. This area requires further study. The addition of HYCAT catalysts to the CTPB and CTPIB 16% aluminum propellants greatly increased the reignition limits of grains depressurized at atmospheric exhaust. Initial depressurization rates, an order of magnitude greater than required for extinguishment under vacuum exhaust conditions, were needed to achieve permanent extinguishment when the motors were exhausted into the atmosphere. Examination of the propellant grains terminated under vacuum conditions showed a heavy layer of agglomerated aluminum on the quenched grain surfaces.
- (3) The addition to the CTPIB system of halogens at low concentrations had little or no effect upon extinguishment behavior. Three chlorinated CTPIB propellants containing 1.2%, 3.4%, and 14.5% of chlorine (percentage of binder prepolymer which constitutes 12.55% of the propellant) were tested with the dual-nozzle window motor and were found to have nearly the same extinguishment requirements as the reference, nonchlorinated propellant.

- (4) Limited studies showed that the sterilization of nonaluminized CTPIB/AP propellants results in a marked increase of the termination requirements. This increase is not paralleled by an increase of the propellant burning rate. The cause or causes for the increase of the termination requirements were not determined.
- (5) Increasing the endothermicity of the propellant surface, either by the use of binders showing lower thermal decomposition temperature (CTPIB prepolymer) or by using higher binder loadings, results in moderate decreases of the extinguishment requirements. Propellants formulated with CTPIB prepolymer showed lower extinguishment requirements and lower burning rates than did the higher decomposition temperature CTPB propellants. DSC tests conducted with these polymers showed that the CTPIB polymer decomposed thermally at lower temperatures than the CTPB binder.

Increasing the binder content from 16% to 20% in the CTPB system caused a marked reduction of the extinguishment requirements and the propellant burning rate. These results paralleled earlier studies⁽⁷⁾ using the CTPIB binder system.

While the propellant formulation defines the extinguishment requirements in any particular motor, increasing the grain area and decreasing the motor volume increases the pressure and depressurization rate at the point of extinguishment and also increases the critical initial depressurization rate required for extinguishment. Extinguishment was shown to occur at much higher pressures (100 to 200 psi) and depressurization rates in the swing-nozzle motor as compared to the window motor.

It has been shown that the exhaust pressure level will influence extinguishment behavior if the motor geometry is such that extinguishment occurs below the dechoking pressure. Such behavior is more likely with large-volume, small-grain area motors. The permanence of extinguishment is also a function of exhaust-pressure level, particularly if the propellant contains aluminum. Unless the exhaust pressure is below the minimum ignition pressure of the propellant, reignition may occur. Permanent combustion extinguishment of aluminized systems at exhaust pressures above the minimum ignition pressure requires either depressurization rates two to three times greater than the critical rate at vacuum exhaust or requires that the motor be purged with a gaseous or liquid coolant after depressurization.

The Von Elbe type of combustion extinguishment model provides a rough guideline for motor development work. While this type of analysis fails to describe particular propellant formulation differences and the effect of exhaust pressure and reignition phenomena, it is the only model presently capable of being used for design purposes.

REFERENCES

1. Fletcher, E. A.; Paulson, R. A.; Bunde, G. W.; and Hiroki, T.: Quenching of Solid Rocket Propellants by Depressurization. WSCI Paper 66-21, presented at Western States Combustion Institute Meeting, April 1966.
2. Micheli, P. L.: A Stop-Start Study of Solid Propellant. NASA CR-66487, Final Report prepared under Contract No. NAS 1-6600 by Aerojet-General Corporation, Sacramento, California, 1967.
3. Von Elbe, G.; and McHale, E. T.: Extinguishment of Solid Propellants by Rapid Depressurization. AIAA J., Vol. 6, pp. 1417-1419, July 1968.
4. Von Elbe, G.: Theory of Solid Propellant Ignition and Response to Pressure Transients. Bulletin of the 19th ICRPG Conference, Silver Spring, Maryland, pp. 157-181, 1963.
5. Paul, B. E.; Lovine, R. L.; and Fong, L. Y.: A Ballistic Explanation of the Ignition Pressure Peak. AIAA Preprint No. 64-121, presented at the 5th AIAA Solid Propellant Rocket Conference, Palo Alto, California, January 1964.
6. Parker, K. H.; and Summerfield, M.: Response of the Burning Rate of a Solid Propellant to a Pressure Transient. AIAA Preprint No. 66-683, presented at the AIAA Propulsion Joint Specialist Conference, Colorado Springs, Colorado, June 1966.
7. Jensen, G. E.: A Stop-Start Study of Solid Propellants. NASA CR-66488, Final Report, Contract No. NAS 1-6601, United Technology Center, Sunnyvale, California, November 1967.
8. Capener, E. L.; Dickinson, L. A.; and Marxman, G. A.: Propellant Combustion Phenomenon During Rapid Depressurization. Quarterly Report No. 5, Contract No. NAS 7-389, Stanford Research Institute, Menlo Park, California, February 1967.
9. Summerfield, M.; and Merkle, G. L.: Extinguishment of Solid Propellant Flames: A Theory on a New Feedback Law. Presented at the 3rd ICRPG/AIAA Solid Propulsion Conference, Atlantic City, New Jersey, June 4-6, 1968.
10. Cantrell, R. H.: Gas Film Effects in the Linear Pyrolysis of Solids. AIAA J. 1, pp. 1544-1549, 1963.
11. Nachbar, W.; and Williams, F. A.: On the Analysis of Linear Pyrolysis Experiments. Ninth Symposium (International) on Combustion, Williams and Wilkins Co., Baltimore, Md., pp. 345-357, 1963.

12. Coates, R. L.: Linear Pyrolysis Measurements of Propellant Constituents. AIAA Preprint No. 65-55, January 1965.
13. Cheng, J. T.; Baer, A. D.; and Ryan, N. W.: Thermal Effects of Composite-Propellant Reactions. Technical Report prepared under Air Force Grants AFOSR 40-66 and 40-67, University of Utah, Salt Lake City, Utah, August 1967.
14. Madorsky, S.L.: Thermal Degradation of Organic Polymers. Interscience Publishers, New York, 1964.
15. Derr, R. L.; and Osborn, J. R.: An Experimental Investigation of the Gaseous Phase Reaction Zone in a Composite Solid Propellant. Report T.M.-67-6, JPC-438, Jet Propulsion Center, Purdue University (NASA CR-90226), September 1967.
16. Summerfield, M.; Sutherland, G. S.; Webb, M. J.; Taback, H. J.; and Hall, K. P.: Burning Mechanism of Ammonium Perchlorate Propellant, Solid Propellant Rocket Research. Vol. 1 of Progress in Astronautics and Rocketry, Academic Press, Inc., 1960, pp. 141-182.
17. Penzias, G. J.: Discussion on Paper by Watermeier, L. A.; Aungst, W. P.; and Pfaff, S. P.: Ninth Symposium (International) on Combustion. Academic Press, Inc., 1963, p. 327.
18. Waesche, R.H.W.: The Effects of Pressure and Formulation on the Emission Spectra of Solid Propellants, Proceedings of the Third ICRPG Combustion Conference. CPIA Pub. No. 138, Vol. I, Johns Hopkins University, February 1967, p. 123.
19. Madorsky, S.L.: Modern Plastics, 38, No. 6, 1961, p. 139.
20. Jellinek, H.H.G.: Degradation of Vinyl Polymers. Academic Press, Inc. New York, 1955.
21. Shannon, L. J.: Composite Solid Propellant Ignition Mechanisms. Final Report, Contract No. F44620-68-C-0053, United Technology Center, in preparation.
22. Shannon, L. J.: Composite Solid Propellant Ignition Mechanisms. AFOSR Scientific Report, AFOSR 67-1765, Contract No. AF 49(638)-1557, United Technology Center, September 1967.